University of Alberta

Dynamic Fracture Toughness Measurements in X70 & X80 Steels

by

Jason William Reinhart

A thesis submitted to the Faculty of Graduate Studies and Research in partial fulfillment of the requirements for the degree of Master of Science

in

Welding Engineering

Department of Chemical and Materials Engineering

Edmonton, Alberta

Spring 2003

Library and Archives Canada

Published Heritage Branch

395 Wellington Street
Ottawa ON K1A 0N4
Canada

Bibliothèque et Archives Canada

Direction du Patrimoine de l'édition

395, rue Wellington
Ottawa ON K1A 0N4
Canada

Your file Votre référence
ISBN: 0-612-96577-5
Our file Notre référence
ISBN: 0-612-96577-5

The author has granted a non-exclusive license allowing the Library and Archives Canada to reproduce, loan, distribute or sell copies of this thesis in microform, paper or electronic formats.

The author retains ownership of the copyright in this thesis. Neither the thesis nor substantial extracts from it may be printed or otherwise reproduced without the author's permission.

L'auteur a accordé une licence non exclusive permettant à la Bibliothèque et Archives Canada de reproduire, prêter, distribuer ou vendre des copies de cette thèse sous la forme de microfiche/film, de reproduction sur papier ou sur format électronique.

L'auteur conserve la propriété du droit d'auteur qui protège cette thèse. Ni la thèse ni des extraits substantiels de celle-ci ne doivent être imprimés ou aturement reproduits sans son autorisation.

In compliance with the Canadian Privacy Act some supporting forms may have been removed from this thesis.

While these forms may be included in the document page count, their removal does not represent any loss of content from the thesis.

Conformément à la loi canadienne sur la protection de la vie privée, quelques formulaires secondaires ont été enlevés de cette thèse.

Bien que ces formulaires aient inclus dans la pagination, il n'y aura aucun contenu manquant.

Canada

Abstract

The dynamic ductile fracture toughness of X70 and X80 pipeline materials was studied. Instrumentation of Charpy and Drop Weight Tear testers was conducted to examine the possibility of measuring propagation directly from a load-displacement trace. Tests conducted in this study showed that instrumentation that uses strain gauges for data acquisition result in energy measurement errors and therefore and alternative energy measurement technique which uses an optical encoder an linear tape was developed. This alternative technique shows promise. From the drop weight tear test load-displacement trace a region of steady state crack propagation can be measured for both the X70 and X80 materials, but side grooves must be added to Charpy specimens to induce steady state crack propagation. With the X80 material it was shown that a side groove depth of 1.0 mm does induce steady state crack propagation, but the X70 specimens require a groove depth greater than 1.5 mm, which was the maximum groove depth that could be used. Thus for the conditions tested, steady state crack propagation can be compared only between X80 Charpy and drop weight tear test specimens.

Acknowledgements

I would express sincere thanks to Dr. Barry M. Patchett for his supervision and guidance over the past few years. I have been impressed with his dynamic thought, his broad and profound knowledge and his mentoring and advising when I needed them.

His help, encouragement and stimulating suggestions have given me a great satisfaction in doing this research and I am extremely proud for the richness of having Dr. Barry M. Patchett as my supervisor.

I am thankful to my friend Krunoslav Marjanovich and his family for their endless believes and support from the very beginning of my studies.

I thank "NAMCO – Machine&Gear Works Ltd." Edmonton, for supplying and machining samples for my research.

I would particularly express my profound thanks to my family, my wife Diana, daughter Anna and sons Ivan and Matia, for patience, support, understanding, believing and never losing faith in me.

TABLE OF CONTENTS

CHAPTER 1 INTRODUCTION 1

CHAPTER 2 LITERATURE REVIEW 3

2.1 Residual Stresses 4
2.2 Transformation and Microstructure of Steel 10
2.3 Transformation and Microstructure of Weld Metal 13
2.4 Weld Zone Characteristics 13
2.5 Microstructure of Weld Metal of Carbon-Manganese Steel 19

2.6 PWHT Effects on Different Steel Properties 22
2.7 Conventional Heat Treatment of Steels 25
2.8 Tempering of Martensite 30
2.9 Tempering of Plain Carbon Steels 31
2.10 Tempering of Alloy Steels 32

2.11 PWHT – Codes and Regulations 34
2.12 Low and Medium Carbon Steels 34
2.13 Critical Thickness 35
2.14 Temperature of the Post Weld Heat Treatment 36
2.15 Minimum Holding Time at Maximum Temperature 37
2.16 Hollomon-Jaffe Parameter 38
2.17 PWHT – Code Requirements for Low Alloy Steels 39
2.18 Literature Review Summary 41

CHAPTER 3 EXPERIMENTAL PROCEDURE 45

3.1 Material 45
3.2 Welding Procedures 48
3.3 Welding Consumables 51
3.4 PWHT Procedures 52
3.5 Q&T Procedures 53
3.6 Metallurgical Examinations 54
3.7 Microhardness Testing 55

CHAPTER 4
MICROSTRUCTURE AND MICROHARDNESS EXAMINATIONS OF 1043 STEEL 58

4.1 Hardness – Mechanical Property Relationships for Steels 59
4.2 Medium Carbon 1043 Steel 60
4.3 Q&T Heat Treatment Microstructures after the 550^{0}C Tempering Temperature with Different Holding Times 64
4.4 Q&T Heat Treatment Microstructures after the 500^{0}C Tempering Temperature with Different Holding Times 66

CHAPTER 5
MICROSTRUCTURE AND MICROHARDNESS EXAMINATIONS OF 4140 STEEL 70

5.1 Low-Alloy Cr-Mo Steel 70
5.2 Q&T Heat Treatment Microstructures after the 550^{0}C Tempering Temperature for Different Holding Times 73
5.3 Q&T Heat Treatment Microstructures after the 500^{0}C Tempering Temperature for Different Holding Times 75

CHAPTER 6
MICROSTRUCTURE AND MICROHARDNESS EXAMINATIONS OF THE 1043 WELD ZONE AFTER DIFFERENT PWHTs 79

6.1 Examinations of the 1043 Weld Zone after PWHT @ 650^{0}C – 1.0 hour 79
6.2 Examinations of the 1043 Weld Zone after PWHT @ 600^{0}C – 1.0 hour 82
6.3 Examinations of the 1043 Weld Zone after PWHT @ 550^{0}C – 2.5 hours 84
6.4 Examinations of the 1043 Weld Zone after PWHT @ 550^{0}C – 4.0 hours 85
6.5 Examinations of the 1043 Weld Zone after PWHT @ 550^{0}C – 10.0 hours 87
6.6 Examinations of the 1043 Weld Zone after PWHT @ 500^{0}C– 6.0 hours 89
6.7 Examinations of the 1043 Weld Zone after PWHT @ 500^{0}C – 15.0 hours 91
6.8 Examinations of the 1043 Weld Zone after PWHT @500^{0}C – 226.0 hours 92

6.9 Discussion of PWHT Results of 1043 Weldments 94
6.10 Analysis and Comparison of 1043 Weld Zone Microstructures After Different PWHTs 99

CHAPTER 7
MICROSTRUCTURE AND MICROHARDNESS EXAMINATIONS OF THE 4140 WELD ZONE AFTER DIFFERENT PWHTs 106

7.1 Examinations of the 4140 Weld Zone after PWHT @ 650^{0}C – 1.0 hour 106
7.2 Examinations of the 4140 Weld Zone after PWHT @ 600^{0}C – 1.0 hour 109
7.3 Examinations of the 4140 Weld Zone after PWHT @ 550^{0}C – 2.5 hours 110
7.4 Examinations of the 4140 Weld Zone after PWHT @ 550^{0}C – 4.0 hours 112
7.5 Examinations of the 4140 Weld Zone after PWHT @ 550^{0}C – 10.0 hours 114
7.6 Examinations of the 4140 Weld Zone after PWHT @ 500^{0}C – 6.0 hours 115
7.7 Examinations of the 4140 Weld Zone after PWHT @ 500^{0}C – 15.0 hours 117
7.8 Examinations of the 4140 Weld Zone after PWHT @ 500^{0}C – 226.0 hours 119
7.9 Discussion of PWHT results of 4140 Weldments 121
7.10 Analysis and Comparison of 4140 Weld Zone Microstructures After different PWHTs 126
7.11 PWHTs-Diffusion Coefficient 133

CHAPTER 8
CONCLUSIONS AND RECOMMENDATIONS 141

8.1 Conclusions 141
8.2 Recommendations 145

REFERENCES 147

List of Tables

Table 1 Critical Thickness for PWHT Required by Different Codes.....35

Table 2 Summary of Code Requirements for PWHT Temperature for C and C-Mn Steels.....36

Table 3 Summary of Code requirements for low alloy steels 40

Table 3.1 Chemical Compositions of 4140 and 1043 Steels.....46

Table 3.2 Properties of 1043 Steel – Normalized Condition (900^0C-Air Cooled).....47

Table 3.3 Properties of 4140 Steel.....48

Table 3.4 Welding Parameters for 1043 and 4140 Steels.....51

Table 3.5 As-Welded Properties of E 48018-1 and E 11018 – M Filler Materials..... 52

Table 3.6 PWHT Principal Parameters.....54

Table 3.7 Temperature – Time Parameters for Q&T Treatments 55

Table 4.1 Microhardness Results of 1043 As-Received 1043 Steel.....61

Table 4.2 Microhardness Results of 1043 Steel after Q&T at 860^0C/650^0C – 1.0 hr.....62

Table 4.3 Microhardness Values of 1043 steel after Q&T at 860^0C/600^0C – 1.0 hour.....64

Table 4.4 Hardness Measurements after Q&T at 550^0C for Different Holding Times.....66

Table 4.5 Hardness Measurements after Q&T at 500^{0}C for Different Holding Times 68

Table 5.1 Hardness Values of 4140 Steel As-Received 71

Table 5.2 Hardness Values after Q&T at 860^{0}C/650^{0}C – 1.0 hr 72

Table 5.3 Hardness Values after Q&T at 860^{0}C/600^{0}C – 1.0 hr 72

Table 5.4 Hardness Measurements after Q&T at 550^{0}C for Different Holding Times 75

Table 5.5 Hardness Measurements after Q&T at 500^{0}C for Different Holding Times 77

Table 6.1 Hardness Measurement Results of 1043 Weld Zone after PWHT@ 650^{0}C/1.0 hr 80

Table 6.2 Hardness Measurement Results of 1043 Weld Zone after PWHT @ 600^{0}C/1.0 hr 83

Table 6.3 Hardness Measurement Results of 1043 Weld Zone after PWHT @ 550^{0}C/2.5 hrs 85

Table 6.4 Hardness Measurement Results of 1043 Weld Zone after PWHT @ 550^{0}C/4.0 hrs 86

Table 6.5 Hardness Measurement Results of 1043 Weld Zone after PWHT @ 550^{0}C/10.0 hrs 87

Table 6.6 Hardness Measurement Results of 1043 Weld Zone after PWHT @ 500^{0}C/6.0 hrs 89

Table 6.7 Hardness Measurement Results of 1043 Weld Zone after PWHT @ 500^{0}C/15.0 hrs 92

Table 6.8 Hardness Measurement Results after PWHT @ 500^{0}C/226.0 hrs 93

Table 7.1 Hardness Measurement Results of 4140 Weld Zone after PWHT @ 650^{0}C/1.0 hr 107

Table 7.2 Hardness Measurement Results of 4140 Weld Zone after PWHT @ 600^0C/1.0 hr 109

Table 7.3 Hardness Measurement Results of 4140 Weld Zone after PWHT @ 550^0C/2.5 hrs 111

Table 7.4 Hardness Measurement Results of 4140 Weld Zone after PWHT @ 550^0C/4.0 hrs 112

Table 7.5 Hardness Measurement Results of 4140 Weld Zone after PWHT @ 550^0C/10.0 hrs 114

Table 7.6 Hardness Measurement Results of 4140 Weld Zone after PWHT @ 500^0C/6.0 hrs 116

Table 7.7 Hardness Measurement Results of 4140 Weld Zone after PWHT @ 500^0C/15.0 hrs 117

Table 7.8 Hardness Measurement Results of 4140 Weld Zone after PWHT @ 500^0C/226.0 hrs 119

List of Figures

Figure1.0 The Maximum Residual Stress Before and After PWHT With Different Soaking Temperature [Olabi, 1996].....5

Figure 1.1 The Maximum Residual Stress Before and After PWHT With Different Heating Rates [Olabi, 1996] 6

Figure 1.2 The Maximum Residual Stress Before and After PWHT With Different Time Durations [Olabi, 1996].....7

Figure 1.3 The Maximum Residual Stress Before and After PWHT With Different Cooling Rates [Olabi, 1996] 8

Figure 2.1 The Metastable System Fe-Fe3C [Lancaster, 1993] 11

Figure 2.2 Metallurgical Designations in Heat Affected Zone [Patchett, 2000].....13

Figure 2.3 HAZ of a Single Pass Weld [Easterling, 1983].....16

Figure 2.4 Shematic Illustration of the Effect of Multi-Pass Welding On the Microstructure of the HAZ [Shiga, 1990].....18

Figure 2.5 Typical Microstructural Constituents of Weld Metals Associated with Carbon-Manganese Steels [Dolby, 1983] 21

Figure 2.6 Shematic Presentation of Ductility, Toughness, and Brittleness [Liscic, 1997].....26

Figure 2.7 Stress-Strain Diagram of a Steel after Different Heat Treatments [Liscic, 1997] 27

Figure 2.8 Hardening and Tempering Diagram of DIN 20CrMo2 Steel [Liscic, 1997] 28

Figure 2.9 Microstructure of DIN 34CrNiMo6 after Hardening and Tempering. Tempered Fine-Grained Martensite Magnification 500x [Liscic, 1997] 29

Figure 2.10 Operation and Phases in the Process of Hardening and Tempering [Liscic, 1997] 30

Figure 2.11 Isothermal Transformation Diagram of 4140 Steel [ASM, 1977] 33

Figure 2.12 Time/Temperature Parameter Relationships [Hrivnak, 1985] 39

Figure 2.13 Heat Treatment Times for Various Codes [Fidler, 1984] 41

Figure 2.14 Relationship between Convenient and Post Weld Heat Treatment [Zulic, 2003] 43

Figure 3.1 Schematic Presentation of the Specimen 50

Figure 3.2 Location of Microhardness Testing of the Weld Zone 57

Figure 4.1 BM Microstructures of 1043 Steel As-Delivered (Left-398x: Right-800x) 61

Figure 4.2 Microstructures of 1043 Steel after Q&T Heat Treatment: T_A=860^{0}C/0.5 hr – T_T=650^{0}C/1.0 hr (398x and 800x) 62

Figure 4.3 Microstructures of 1043 Steel after Q&T Heat Treatment: T_A=860^{0}C/0.5 hr – T_T=600^{0}C/1.0 hr (398x and 800x) 63

Figure 4.4 Microstructures of 1043 Steel after Q&T Heat Treatment: T_A=860^{0}C/0.5 hr – T_T=550^{0}C/2.5 hrs (398x and 800x) 65

Figure 4.5 Microstructures of 1043 Steel after Q&T Heat Treatment: T_A=860^{0}C/0.5 hr – T_T=550^{0}C/4.0 hrs (398x and 800x) 65

Figure 4.6 Microstructures of 1043 Steel after Q&T Heat Treatment: T_A=860^{0}C/0.5 hr – T_T=550^{0}C/10.0 hrs (398x and 800x) 65

Figure 4.7 Microstructures of 1043 Steel after Q&T Heat Treatment: T_A=860^{0}C/0.5 hr – T_T=500^{0}C/6.0 hrs (398x and 800x) 67

Figure 4.8 Microstructures of 1043 Steel after Q&T Heat Treatment: T_A=860^{0}C/0.5 hr – T_T=500^{0}C/15.0 hrs (398x and 800x) 67

Figure 4.9 Microstructures of 1043 Steel after Q&T Heat Treatment: T_A=860^{0}C/0.5 hr – T_T=500^{0}C/226 hrs (398x and 800x).....67

Figure 4.10 Hardness Profile of 1043 steel after Different Q&T Treatments 69

Figure 5.1 Microstructures of 4140 Steel As Received (Left 398x – Right 800x).....70

Figure 5.2 Microstructure of 4140 Steel after Q&T Treatment T_A=860^{0}C/0.5 hr – T_T=650^{0}C/1.0 hr (398x and 800x).....71

Figure 5.3 Microstructures of 4140 Steel after Q&T Heat Treatment: T_A=860^{0}C/0.5 hr – T_T=600^{0}C/1.0 hr (398x and 800x).....72

Figure 5.4 Microstructures of 4140 Steel after Q&T Heat Treatment: T_A=860^{0}C/0.5 hr – T_T=550^{0}C/2.5 hrs (398x and 800x).....74

Figure 5.5 Microstructures of 4140 Steel after Q&T Heat Treatment: T_A=860^{0}C/0.5 hr – T_T=550^{0}C/4.0 hrs (398x and 800x).....74

Figure 5.6 Microstructures of 4140 Steel after Q&T Heat Treatment: T_A=860^{0}C/0.5 hr – T_T=550^{0}C/10.0 hrs (398x and 800x).....74

Figure 5.7 Microstructures of 4140 Steel after Q&T Heat Treatment: T_A=860^{0}C/0.5 hr – T_T=500^{0}C/6.0 hrs (398x and 800x).....76

Figure 5.8 Microstructures of 4140 Steel after Q&T Heat Treatment: T_A=860^{0}C/0.5 hr – T_T=500^{0}C/15.0 hrs (398x and 800x).....76

Figure 5.9 Microstructures of 4140 Steel after Q&T Heat Treatment: T_A=860^{0}C/0.5 hr – T_T=500^{0}C/226 hrs (398x and 800x).....76

Figure 5.10 Hardness Profile of the 4140 Steel after Different Q&T Treatments.....78

Figure 6.1 Microstructures of the 1043 Weld Zone after PWHT @ 650^{0}C-1.0 hr (127x) a)-WM b)-HAZ c)-BM 80

Figure 6.2 Hardness Profile of 1043 Weldment after PWHT @ 650^{0}C – 1.0 hr 81

Figure 6.3 Microstructures of the 1043 Weld Zone after PWHT
@ 600^{0}C-1.0 hr (127x) a)-WM b)-HAZ c)-BM 82

Figure 6.4 Hardness Profile of 1043 Weldment after PWHT
@ 600^{0}C – 1.0 hr 82

Figure 6.5 Microstructures of the 1043 Weld Zone after PWHT
@550^{0}C-2.5 hrs (127x) a)-WM b)-HAZ c)-BM 84

Figure 6.6 Hardness Profile of 1043 Weldment after PWHT
@ 550^{0}C – 2.5 hrs.....84

Figure 6.7 Microstructures of the 1043 Weld Zone after PWHT
@ 550^{0}C-4.0 hrs (127x) a)-WM b)-HAZ c)-BM.....86

Figure 6.8 Hardness Profile of 1043 Weldment after PWHT
@ 550^{0}C – 4.0 hrs.....86

Figure 6.9 Microstructures of the 1043 Weld Zone after PWHT
@ 550^{0}C-10.0 hrs (127x) a)-WM b)-HAZ c)-BM 88

Figure 6.10 Hardness Profile of 1043 Weldment after PWHT
@ 550^{0}C – 10.0 hrs.....88

Figure 6.11 Microstructures of the 1043 Weld Zone after PWHT
@ 500^{0}C-6.0 hrs (127x) a)-WM b)-HAZ c)-BM 90

Figure 6.12 Hardness Profile of 1043 Weldment after PWHT
@ 500^{0}C – 6.0 hrs.....90

Figure 6.13 Microstructures of 1043 Weld Zone after PWHT
@ 500^{0}C-15.0 hrs (127x) a)-WM b)-HAZ c)-BM 91

Figure 6.14 Hardness Profile of 1043 Weldment after PWHT
@ 500^{0}C – 15.0 hrs.....91

Figure 6.15 Microstructures of the 1043 Weld Zone after PWHT
@ 500^{0}C-226.0 hrs (127x) a)-WM b)-HAZ c)-BM.....93

Figure 6.16 Hardness Profile of 1043 Weldment after PWHT
@ 500^{0}C – 226 hrs.....93

Figure 6.17 Hardness Profile of the 1043 Weldments after different PWHTs....94

Figure 6.18 Microstructures of the WM of 1043 Weld Zone after Different PWHTs (127x)....100

Figure 6.19 Microstructures of the HAZ of 1043 Weld Zone after Different PWHTs (127x)....101

Figure 6.20 Microstructures of the BM of 1043 Weld Zone after Different PWHTs (127x)....102

Figure 7.1 Microstructures of 4140 Weld Zone after PWHT @ 650^{0}C/1.0 hr (127x) a)-WM b)-HAZ c)-BM....107

Figure 7.2 Hardness Profile of the 4140 Weldment after PWHT @ 650^{0}C – 1.0 hr....107

Figure 7.3 Microstructures of 4140 Weld Zone after PWHT @ 600^{0}C-1.0 hr (127x) a)-WM b)-HAZ c)-BM....109

Figure 7.4 Hardness Profile of the 4140 Weldment after PWHT @ 600^{0}C – 1.0 hr....110

Figure 7.5 Microstructures of 4140 Weld Zone after PWHT @ 550^{0}C-2.5 hrs (127x) a)-WM b)-HAZ c)-BM....111

Figure 7.6 Hardness Profile of the Weldment after PWHT @ 550^{0}C – 2.5 hrs....111

Figure 7.7 Microstructures of 4140 Weld Zone after PWHT @ 550^{0}C-4.0 hrs (127x) a)-WM b)-HAZ c)-BM....113

Figure 7.8 Hardness Profile of the 4140 Weldment after PWHT @ 550^{0}C – 4.0 hrs....113

Figure 7.9 Microstructures of 4140 Weld Zone after PWHT @ 550^{0}C-10.0 hrs (127x) a)-WM b)-HAZ c)-BM....114

Figure 7.10 Hardness Profile of the 4140 Weldment after PWHT @ 550^{0}C – 10.0 hrs....115

Figure 7.11Microstructures of 4140 Weld Zone after PWHT
@ 500^{0}C-6.0 hrs (127x) a)-WM b)-HAZ c)-BM 116

Figure 7.12 Hardness Profile of the 4140 Weldment after PWHT
@ 500^{0}C – 6.0 hrs.....116

Figure 7.13 Microstructures of 4140 Weld Zone after PWHT
@ 500^{0}C-15.0 hrs (127x) a)-WM b)-HAZ c)-BM 118

Figure 7.14 Hardness Profile of the 4140 Weldment after PWHT
@ 500^{0}C – 15.0 hrs.....118

Figure 7.15 Microstructures of 4140 Weld Zone after PWHT
@ 500^{0}C-226.0 hrs (127x) a)-WM b)-HAZ c)-BM.....120

Figure 7.16 Hardness Profile of the 4140 Weldment after PWHT
@ 500^{0}C – 226.0 hrs.....120

Figure 7.17 Hardness Profile of the 4140 Weldments after
Different PWHTs.....121

Figure 7.18 Hardness Profile of the 4140 BM after different Q&T and
PWHTs.....125

Figure 7.19 Microstructures of the WM of 4140 Weld Zone
after Different PWHTs (127).....127

Figure 7.20 Microstructures of the HAZ of 4140 Weld Zone
after Different PWHTs (127x).....128

Figure 7.21 Microstructures of the BM of 4140 Weld Zone
after Different PWHTs (127x).....129

Figure 7.22 HAZ Microstructures with Highest Hardness Values (800x) 132

Figure 7.23 BM Microstructures of 4140 Steel with Increased Hardness
Values (800x).....133

Figure 7.24 Relationship among Tempering Parameters.....139

CHAPTER 1

INTRODUCTION

It is a well established practice to submit – whenever technically and economically desirable or required– a welded construction to a post weld heat treatment (PWHT) aimed at reducing residual stresses resulting from manufacturing, particularly from welding.

It is accepted that, when achieved in the best conditions, such treatments are generally useful, and sometimes mandatory.

It appears more and more important that such treatments exert metallurgical changes that are generally favorable and their importance may be even more significant than the relaxation of residual stresses [IIW, 1987].

The PWHT is mostly regulated by Codes and Standards in many countries around the world. The examination of Codes and Standards reveal a wide variety of points of view, but it appears that the only agreement about PWHT is that it is mandatory in the case of equipment undergoing risk of stress corrosion, or risk of brittle fracture or fatigue failure.

The differences among codes are based on four essential criteria:

- the allowable maximum thickness without the need for PWHT
- the heat treatment temperature

- the minimum holding time at maximum temperature
- the maximum heating and cooling rates, the maximum loading and minimum unloading temperature.

The objective of this project is to analyze the PWHT of a medium carbon 1043 steel and a low alloy 4140 steel at temperatures lower than those prescribed by Codes and Standards and to asses the application of the Hollomon-Jaffe parameter for lower tempering temperatures. Also, the common heat treatments – austenitization and quenching with tempering at lower tempering temperatures were performed to examine microstructural and hardness changes of the 1043 and 4140 steels.

A literature review of the PWHTs of C, C-Mn, and Cr-Mo steels is presented in Chapter 2. The experimental procedures used in the study are outlined in Chapter 3. The microstructure and hardness examinations after different quenching and tempering parameters of 1043 steel are presented in Chapter 4. Chapter 5 concerns the effects of different Q&T heat treatments for 4140 steel. Microstructure and microhardness examinations of the 1043 steel weld zones after different PWHT's are present in Chapter 6 and the same examinations for the 4140 weld zones are presented in Chapter 7. Chapter 8 presents conclusions found with regard to performing different PWHTs at lower temperatures in both steels and recommendations for future work.

CHAPTER 2

LITERATURE REVIEW

Post Weld Heat Treatment (PWHT) is used on welded components to reduce the tendency for catastrophic failure by its effect on microstructure, residual stress or a combination of both [Smith and Garwood, 1992].

PWHT is a process performed by heating a welded structure to a temperature below the lower critical temperature A_{C1} and cooling at a suitable rate with the prime purpose of relieving residual stresses resulting from fabrication and to improve metallurgical properties, i.e., improve toughness levels, reduce hardness levels and maintain adequate weld metal strength. Residual stress caused by welding eventually affects the performance of welded structures in various ways, such as brittle fracture, buckling deformation, fatigue failure and stress corrosion cracking [Mochizukia and Toyoda, 2001]. The stress present after welding is reduced by a creep process in which the elastic strain is converted to plastic strain. Consequently, it is necessary to heat the component to a temperature where creep takes place and it follows that the greater the creep resistance of the material the higher must be the temperature of stress relief [Murray, 1967].

The application of PWHT also results in lowering of hydrogen content and obtaining excellent properties for room temperature strength, creep strength and fracture toughness. But overdoing PWHT, such as higher temperature and longer holding times than needed by the weld, causes a decrease in conventional strength and creep

strength and the deterioration of toughness through the coarsening of precipitates and grain size and in some cases through the growth of a decarburization zone in the heat-affected- zone (HAZ) and weld metal (WM) [Shiga et al., 1996].

The influence of PWHT on the properties of weld joints depends greatly on the chemical compositions of both steels and weld metals and it is therefore very important to understand the change in properties after PWHT [Shiga et al., 1996].

2.1. Residual Stresses

Welding is used to bond a structure by heating and melting locally. Accordingly, when the welded zone goes through heating and cooling under restraint transformation and residual stresses are generated by thermal expansion and contraction [Murakawa, 1997].

In welding, under the effect of a sharp and localized thermal transient the base metal undergoes a complex pattern of thermal expansions and shrinkages. This significantly affects properties of metallurgical and mechanical origins and gives rise to residual stresses. These stresses are located in the welded joint and in its vicinity. Generally they reach a level close to the yield strength of the metal. Under conditions of multi-axial loading, residual stresses can result in brittle fracture and early fatigue failure of a welded joint. The residual stresses may cause cracking and other flaws. High tensile residual stresses in the weld zone can cause fracture under certain conditions.

It has been observed that after the application of PWHT the residual stresses for low carbon 1020 steel are reduced to different levels depending on the heat treatment

scheme. It was also observed [Olabi, 1996] that after the application of PWHT with soaking temperature of 450^0C the maximum value of the residual stress is reduced to about 200 MPa. After the application of PWHT with soaking temperature of 550^0C the maximum value of the residual stress is dropped to about 95 MPa near the welding line. After the application of PWHT with soaking temperature of 650^0C the residual stresses are almost totally relieved with maximum value less than 10 MPa [Olabi and Hashmi, 1966].

Olabi also noticed that the residual stress decreases as the distance from the welding line increases. Fig. 1.0 shows a comparison diagram between the maximum residual stress across the specimen axis before and after PWHT with different soaking temperature.

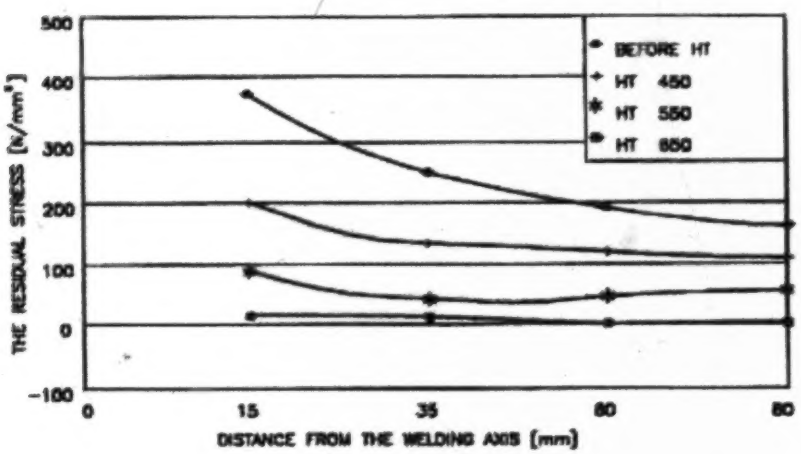

Fig. 1.0. –Maximum residual stress before and after PWHT with different soaking temperature – 2.0 hrs holding time [Olabi and Hashmi, 1996]

It can be seen from figure 1.1 that after application of PWHT with different heating rates of 50, 100, and 400^0C/h the maximum value of the residual stress is reduced from 360 MPa to the range of 180 to 205 MPa. It can be also noticed from these results that there is no significant difference in the reduction of the residual stress value after the application of these different schemes of heat treatments. The maximum value of the residual stress is decreased only slightly by decreasing the heating rate.

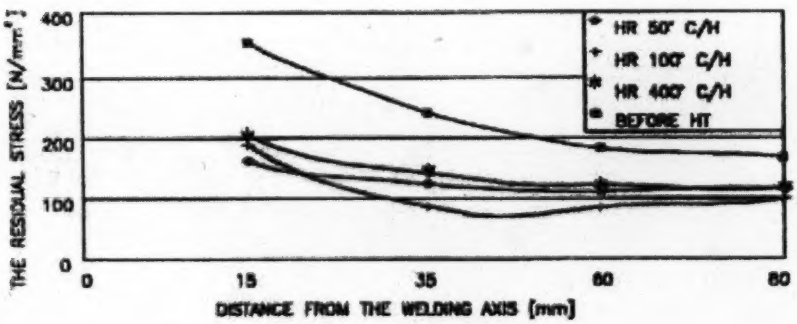

Fig. 1.1. – Maximum residual stress before and after PWHT with different heating rate [Olabi and Hishami, 1996]

However, the maximum value of the residual stress is decreased to different levels after the applications of different schemes of heat treatments which varied in the time durations [Olabi and Hishami, 1996].

It has been noticed that the maximum value of the residual stress significantly decreased after application of PWHT with a longer time duration.

It can be seen from Fig. 1.2. that the maximum value of the residual stress is reduced to about 110 MPa after application of PWHT with a time duration of 10 hours. The

maximum value of the residual stress is around 200 MPa by applying PWHT with time duration of 0.5 of 2 hours.

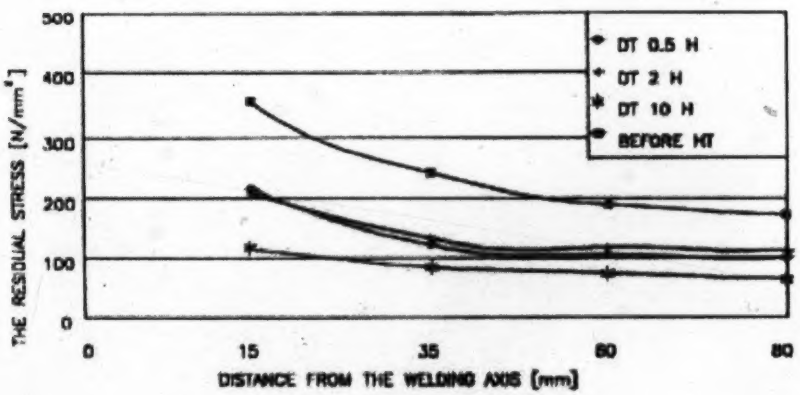

Fig. 1.2. – Maximum residual stress before and after PWHT with different time durations [Olabi and Hishami, 1996]

It is evident from Fig. 1.3. that after the application of PWHT with different cooling rates the maximum value of the residual stress is decreased to different levels ranging from 170 MPa after PWHT with cooling rate of 10^0C/h to 210 MPa after PWHT with cooling rate of 125^0C/h. These results point out that the maximum value of the residual stresses can be decreased significantly by applying PWHT with a lower cooling rate.

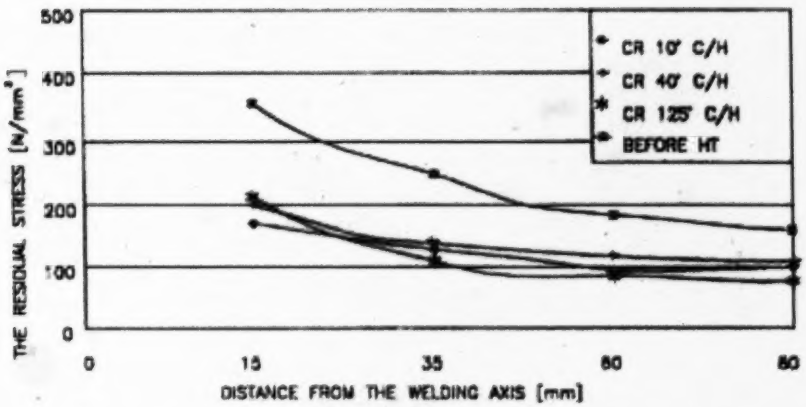

Fig. 1.3. – Maximum residual stress before and after PWHT with different cooling rates [Olabi and Hishami, 1996]

Many researchers have discussed the effect of welding residual stresses on the properties of welds. As it has been demonstrated welds usually have residual stresses at the level of the yield strength of the base material, many Codes or Standards assume this point for the design of welded structures. Because residual stresses are linked to thermal cycles and metallurgical transformation in HAZ as well as in the weld metal, few researchers have nevertheless demonstrated that residual stresses can be lower than expected [Mabelly and Bourges, 2001]. The effect of metallurgical transformation on weld residual stresses in application to E690 steel grade (Superelso 702) has demonstrated that when the weld was sufficiently alloyed to have martensite or lower bainite in the weld metal, residual stresses were lower. Mabelly and Bourges then demonstrated that properties of high-strength steels, especially when sufficiently alloyed, are to be higher then expected because the residual stresses are much lower than the assumed level.

Effects of preheating at 20^0, 200^0 and 400^0C on residual stresses in mild steel welds were also demonstrated as beneficial [Benson and Watson, 1955]. This investigation found that preheating resulted in progressive reduction in residual stress, which amounted to about 50% after preheating at 400^0C, which is very high preheat. If the preheating temperature is limited for practical reasons to about 400^0C, this treatment cannot be regarded as a substitute for the usual stress-relief treatment at about 600^0 – 650^0C after welding, which is known to result in substantially complete stress relief. The real value of preheating to minimize stresses is that it enables heavy rigid welds to be made without cracking before they reach the stress-relieving stage.

A study was conducted to decide whether the number of passes in welds of constant dimensions has any practical influence on the residual stresses and strain energy through the thickness of the welds [Bratt and Barme, 1966]. It has been demonstrated (for 20 mm plates welded with 10 and 15 passes and the same groove dimensions) that the general trend for the longitudinal residual stresses appears to be a compressive stress at the top surface. With increasing depth this compressive stress is reduced and becomes zero about midway between top and bottom of the welds.

In the lower portion of all welds investigated, a tensile residual stress prevailed. These tensile stresses appeared to be 3 times higher in the 10 pass welds than in the 15 pass welds. At the bottom surfaces the compound stresses were compressive in all specimens.

In the transverse direction the residual stresses were compressive throughout the weld thickness, and fairly evenly distributed, except at the top, where there is an increase in magnitude of the stress. Contrary to expectations compressive stresses appear to

prevail on the top and bottom surface of the welds. This may have a beneficial effect on the fatigue strength of the welds [Bratt, 1966].

The variation of the residual stress through the thickness normally is negligible in plates with thickness less than about 25 mm, but may be considerable in thick plates [Bjorhovde et al., 1972].

Although residual stresses can have many different origins they are all the result of misfit. These misfits can be between different parts, different phases, or different regions within the same part. Furthermore, their origin can be mechanical or thermal, or can arise from a transformation [Withers and Bhadeshia, 2001].

2.2 Transformation and Microstructure of Steel

Although the subject of residual stress has been well studied, comparatively little attention has been given to the metallurgical effects that are inseparable from residual stresses, yet these effects can hardly be a less important factor in the behavior of structures than residual stresses themselves [Boyd, 1961].

Metallurgical effects are defined as those changes which occur in the nature of a metal, and which affect its mechanical properties. Such effects include work hardening, strain-ageing, quench-ageing, grain growth and refinement, allotropic transformation and so on. Such changes need not necessarily imply any changes in microstructure detectable by the optical microscope [Boyd, 1961].

The basic metallurgy for welding always considers that there is the rapid heat input and high energy density involved in welding, causing very different thermal effects

than do conventional heat treatments. Very rapid heating cycles (fractions of a second to a few seconds), high peak temperatures (in excess of the melting temperature) and relatively rapid cooling rates to ambient temperature (fractions of a second to many minutes) are all involved [Patchett, 2000].

Regardless of the primary phase structure, carbon and low-alloy steels, such as 1043 and 4140, transform to austenite at a temperature not far from the solidification point, and finally to ferrite plus carbide in some form. The equilibrium structure of iron-carbon alloys is shown in Fig. 2.1 [Lancaster, 1993].

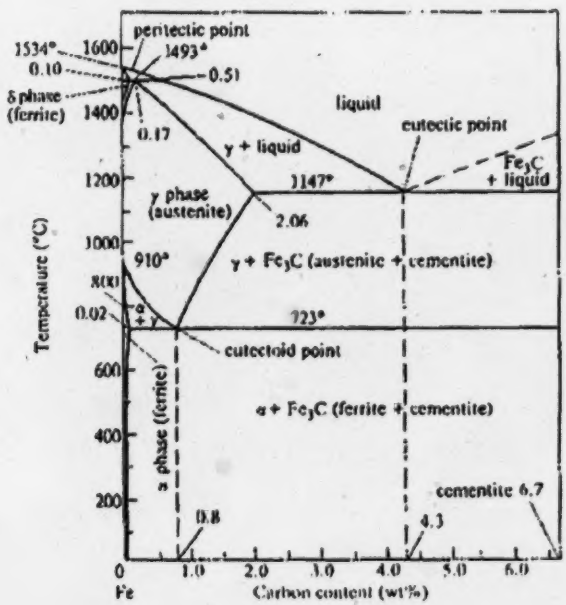

Fig.2.1. – The metastable system Fe-Fe_3C [Lancaster, 1993]

At a temperature where the steel falls within the region designed "γ phase", the steel is austenitic. On slow cooling, transformation starts when the temperature falls to the

point on the lower boundary of this region corresponding to the carbon content of the steel – the upper critical temperature. Ferrite containing a small amount of carbon in solid solution is precipitated, leaving austenite grains that become smaller and are progressively enriched in carbon as the temperature falls. At 723^0C (the lower critical temperature), the residual austenite, which now contains about 0.8% carbon, transforms into pearlite – a laminated eutectoid mixture of ferrite and cementite (Fe_3C) [Lancaster, 1993].

Rapid cooling depresses the temperature at which γ to α change takes place.

As the transformation temperature falls, the distance over which carbon atoms can diffuse is reduced, and there is a tendency to form structures involving progressively shorter movements of atoms. Whereas on slow cooling carbon can segregate into separate individual grains of austenite, with more rapid cooling carbides precipitate around or within the ferrite, which now appears in the form of needles or plates rather than equiaxed grains, a structure known as bainite.

At even more rapid rates of cooling, the transformation is depressed to a temperature at which martensite is formed. This transformation product is produced by a shear movement of the austenite lattice, the carbon being retained in solid solution in a distorted body-centred cubic lattice. Generally speaking, the transformation product is harder and more brittle the lower the transformation temperature and (particularly for martensite) the higher the carbon content [Lancaster, 1993].

2.3 Transformation and Microstructure of Weld Metal

2.4 Weld Zone Characteristics

As a result of welding, a unique area of varying properties and microstructures is created in the vicinity of the weld. During welding, a transformable metal is exposed to every temperature from ambient to melting under rapid heating conditions, is held at a peak temperature for a short time, and is then cooled at rates between fast and exceptionally fast. This experience is entirely different from conventional heat treatments which feature slow heating rates, isothermal peak temperatures held for long and controlled periods of time, followed by controlled cooling rates (quenches) and possible isothermal follow-up heat treatments such as stress relief and tempering. Responses of weld zone to thermal cycles are therefore more complex metallurgically than would be expected from heat treatment knowledge. The metallurgically important zones produced in a single pass weld in a transformable metal, for example a hardenable alloy steel, are shown in Fig. 2.2.

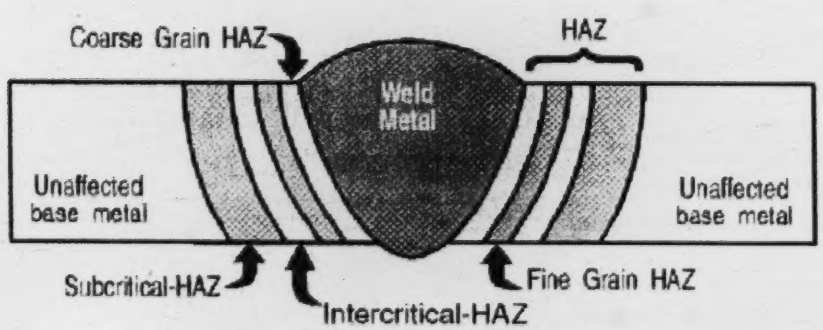

Fig. 2.2 – Metallurgical designations in heat affected zone [Patchett, 2000]

The *unaffected* base metal is defined at temperature below the lower critical temperature, i.e. the temperature above which austenite starts to form or A_1, which is about 720^0C (1330^0F) in C-Mn steels. In alloy steels, the following equations can be used to estimate transformation temperatures in ^{0}C:

Transformation on Slow Cooling

Ar_3=868-396%C-68.1%Mn-36,1%Ni-20.7%Cu-24.8%Cr+24.6%Si or

Ar_3=868-396%C-58.7%Mn-50%Ni-35%Cu+24.6%Si+190%V

Close inspection of the unaffected zone reveals that carbides are somewhat broken up and spheroidized before the lower critical temperature is reached, so that the visible HAZ starts at temperature about 50^0C (120^0F) below the critical temperature [Patchett, 2000].

The next zone is the intercritical zone, where the temperature is between the temperature where austenite starts to form, A_1, and the higher A_3, where all ferrite + carbide is gone and only fine grain austenite remains. For eutectoid steel, this temperature 'range' is a single temperature, the A_3. In the intercritical zone, the austenite formed is often close to the eutectoid composition, so it is quite hardenable and may form martensite on cooling.

The fine grained HAZ is just above the upper critical temperature (A_3) and extends to peak temperature regions up to 100^0C (210^0F) above it. The fine austenite grain size reduces hardenability in this range, although some carbon gradients from carbide dissolution still exist because of lack of time for diffusion, especially in banded microstructures.

In the coarse grained HAZ, grain growth of the austenite takes place right up to the fusion line temperature (>1450^{0}C or 2640^{0}F). Austenite composition is more homogenous than it is in the fine grain zone, but gradients still exist. Coarse initial microstructures, for example hot rolled rather than normalized steel, slow down carbides dissolution and diffusion, exacerbating gradient removal and increasing local hardenability. Higher heat inputs promote diffusion, but also cause larger grains. Large austenite grain size increases hardenability for a given composition, increasing the chance of forming martensite for a given cooling rate. Martensite is hard, strong and brittle and is susceptible to Hydrogen Assisted Cracking (HAC), also called Cold Cracking [Patchett, 2000].

A schematic diagram of the HAZ in a single pass weld is shown in Fig. 2.3.

The varied microstructure in the HAZ, involving varying grain size, two inhomogeneous phases and a mixed phase region have complicated responses to the cooling rates following welding. Most welding cooling rates are relatively fast, inducing a quench in conventional heat treatment terms. When austenite survives to low temperatures due to high hardenability, transformation to low temperature products (bainite or martensite) will occur. In alloy steels, the temperatures at which martensite and bainite start to form under isothermal conditions can be estimated by:

1. Martensite Ms(^{0}C)=561-474%C-33%Mo-17%Ni-17%Cr-21%Mo
2. Bainite Bs(^{0}C)=830-270%C-90%Mn-37%Ni-70%Cr-83%Mo

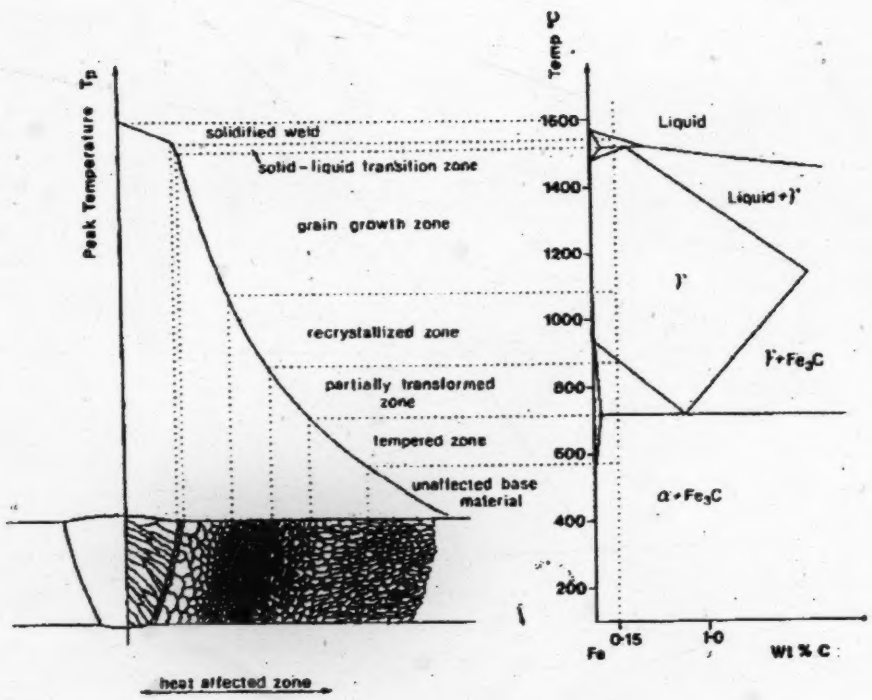

Fig. 2.3 – HAZ of a Single Pass Weld [Easterling, 1983]

In continuous cooling circumstances, these temperatures are depressed. Therefore the coarse grain zone and some of the fine grain and intercitical zones may form brittle martensite or bainite, reducing toughness. Tempering with a postweld heat treatment is necessary to restore toughness in those areas [Patchett, 2000].

There is a well-defined gradient of microstructure in the heat-affected zone, as a function of the distance from the fusion line. There are four specific regions: coarse grained, fine grained, partially transformed and a tempered region [Honeycombe and Bhadeshia, 1995].

In multipass welds in transformable alloys, the above effects are complicated by overlapping of the thermal cycles in a given area, causing reheating and cooling on an already varied microstructure. The effects of multipass welding on the microstructure of the HAZ are shown in Fig. 2.4.

For point B, the CGHAZ is improved by the tempering and recrystallization effects of the second thermal cycle. For C and E, the structure is deteriorated by the second thermal cycle. At point C, the formation of martensite austenite (MA) constituents can occur on the austenite grain boundary by reheating into the two-phase region. These MA constituents become local brittle zones (LBZ) in the weld zone, which reduce the toughness of the HAZ [Shiga, 1990].

To improve the toughness in multi-pass welds, it is therefore beneficial to reduce the volume of MA constituents present. This can be achieved through careful weld procedure control and by reducing the levels of elements that promote the formation of MA.

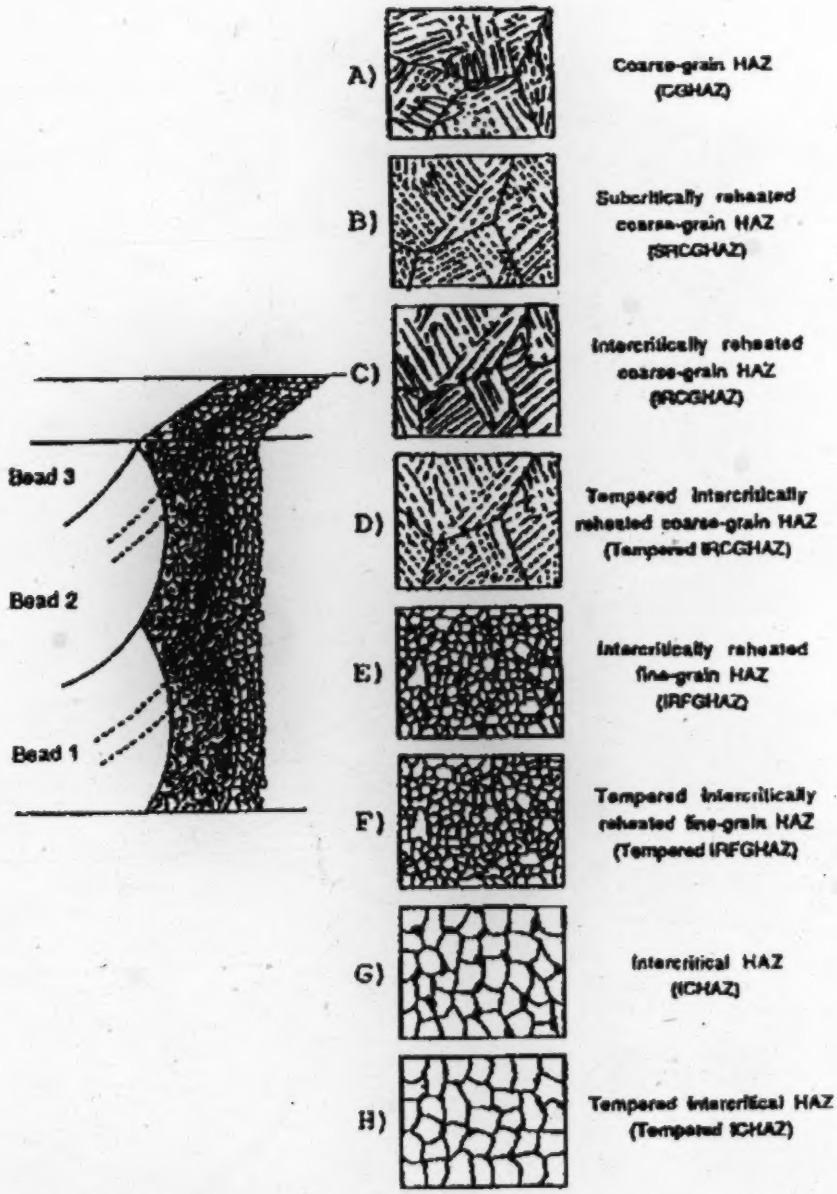

Fig 2.4 – Schematic Illustration of the Effect of Multi-Pass Welding on the Microstructure of the HAZ [Shiga, 1990]

2.5 Microstructure of Weld Metal of Carbon-Manganese Steel

The character of the weld metal microstructure depends in the first place on alloy content. In Cr-Mo low-alloy steel, for example, the weld metal transforms uniformly to martensite and bainite. It will then normally be given a postweld heat treatment, which has the effect of tempering and stress-relieving the joint as a whole.

In carbon, carbon-manganese and microalloyed steel, however, the microstructure and weld metal properties are much affected by details of weld procedure and composition. Factors that affect the microstructure of this type of weld metal include cooling rate, composition, the presence of non-metallic nuclei and plastic strain.

Cooling rates for weld metal are generally such that diffusion is limited. The overall grain size depends upon heat input rate and composition, the finer structures corresponding with low rates of heat input. Improved productivity, however, is achieved through high heat inputs rates, and much research effort is devoted to achieving a combination of fine grain structure with high heat input by control of composition.

Non-metallics are important in that they may act as nuclei for transformation products; such nuclei may range from relatively coarse inclusions to the micrometre-sized particles. Plastic strain occurs during cooling of the weld and may have an effect on the weld metal properties.

The major microconstituents of carbon-manganese steel weld metal are shown in Fig. 2.5 using nomenclature proposed by Abson, Duncan and Pargeter (1988) [Lancaster, 1993].

Essentially these structures are a mixture of primary (grain boundary and polygonal) ferrite, here designated PF(G) and PF(I), and Widmanstätten ferrite. The latter may take the form of side plates, which are nucleated at the austenite grain boundaries and form the lamellar structures marked FS(A) in Figures 2.1.4. a and b. Alternatively the interior of the grain may transform wholly or in part to a fine acicular ferrite, as shown in Fig. 2.1.4. c and d. In some instances, ferrite-carbide aggregates more similar to equilibrium forms may appear, as in Fig. 2.5 e.

Good notch ductility of the fused zone of carbon-manganese steel is generally associated with a high portion of acicular ferrite, whilst lamellar structures such as FS(A) and coarse grain boundary ferrite are, from this point of view, undesirable.

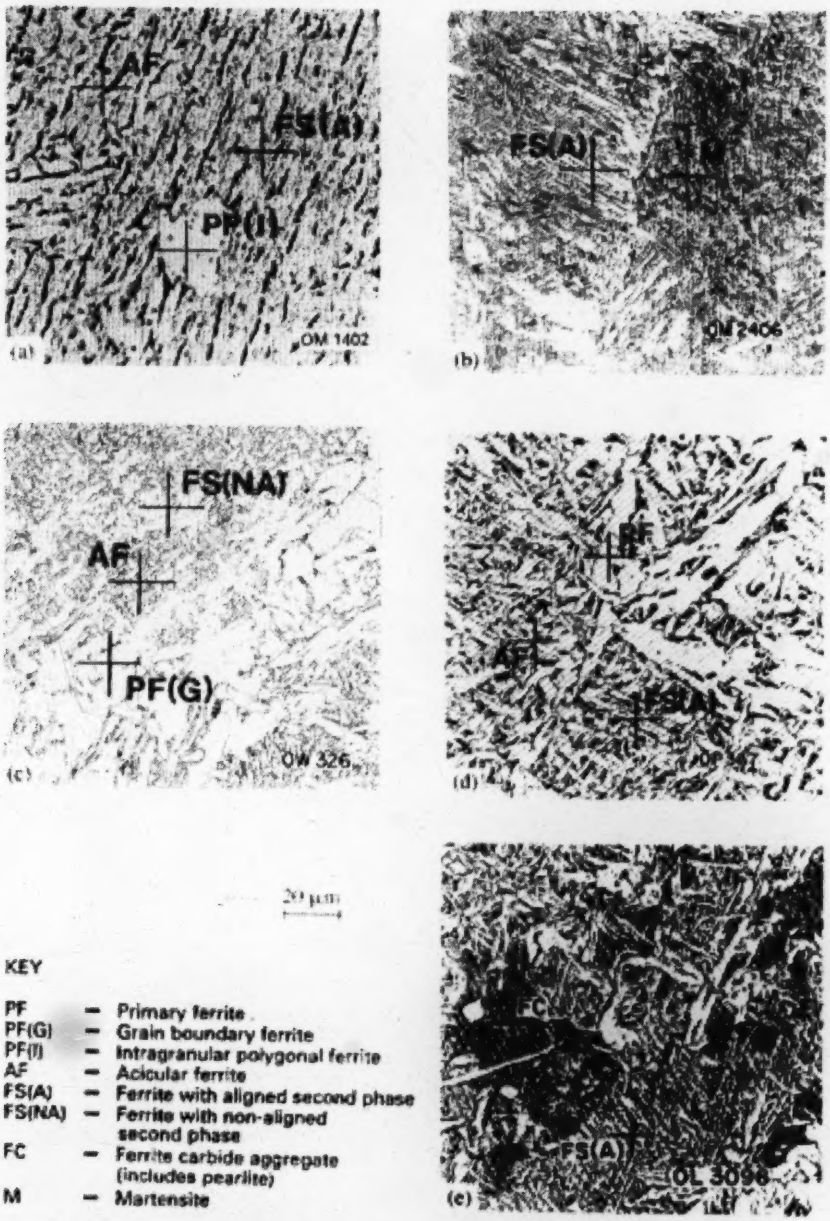

Fig. 2.5 - Typical microstructural constituents of weld metals associated with carbon-manganese steels (x500). (From Dolby, 1983)

2.6 - PWHT Effects on Different Steel Properties

Numerous works about effects of PWHT on steel properties have been reported. The effect of PWHT temperature on Charpy toughness and heat affected zone hardness properties of 4130 and 4140 steels has shown that no relationship existed between HAZ toughness properties for each of the steel grades examined in the PWHT condition [Still, 1997].

In electron beam welded SAE 4130 steel plates, PWHT reduced residual stresses by decreasing of crystal defects (vacancies and dislocations) and the change of microstructure in the weldments from coarse lath martensite to tempered martensite [Huang et al., 1997].

The microstructural stability and elemental redistribution in dissimilar weldments between 9Cr – 1Mo and 2.25Cr – 1Mo ferritic steels, during various post-weld heat treatments (PWHTs) at 1023 K (750^0C) for various times, resulted in the formation of a soft zone in the low Cr side and a carbide rich hard zone adjoining the soft zone in the high Cr side of the weldment. The width of these zones and their hardness are influenced by the time of exposure at elevated temperature and the change in the width and the hardness of soft as well as hard zones slows down considerably after 15 h at 1023 K (750^0C) [Sudha et al, 2002].

The stress relief cracking response of conventional 2.25Cr-1Mo and HCM2S steels has shown that HCM2S alloy is more susceptible to stress-relief cracking than 2.25Cr-1Mo over the range of weld thermal simulations and tempering schedules. HCM2S experienced brittle intergranular failure along prior austenite grain boundaries under each set of test conditions. The 2.25Cr-1Mo steel also failed intergranularly along prior austenite grain boundaries, but exhibited significant macroductility. Increasing the post-weld heat treatment temperature increased the ductility for 2.25Cr-1Mo steel, but had no significant effect on HCM2S. The as quenched hardness of the CGHAZ produced at each energy input for 2.25Cr-1Mo steel was ~ 450 HKN and for HCM2S was ~ 400 HKN. This difference in as-quenched hardness was attributed to the higher carbon content of the 2.25Cr-1Mo steel. The hardness of the CGHAZ after tempering decreased to ~ 300 HKN for 2.25Cr-1Mo steel, but remained the same as the as-quenched hardness of the CGHAZ for HCM2S. With the tempering temperatures and times used in this study, ε-carbide and Fe3C are expected to precipitate in 2.25Cr-1Mo steel. The precipitation of cementite from the supersaturated matrix is the mechanism that results in softening of the CGHAZ. In HCM2S, VC is expected to form which retards softening and ultimately leads to the higher SRC susceptibility [Nawrocki et al., 1998].

The effect of the long stress relieving treatments given to reactor pressure vessels on the tensile, Charpy impact, creep and stress rupture properties of reactor quality, low-carbon, high-manganese steels has been investigated. The result reported show that a prolonged stress relieving treatment, similar to that given *in situ* stress relief of large

vessels can have a significant effect on mechanical properties. On the mild steel plate and weld metals investigated a prolonged stress relieving treatment of 600^0C and above can give a marked deterioration in tensile, impact and creep properties. Such a marked change in tensile properties is not found with a short-term stress relief, as would occur in conventional practice, i.e., 1 hr at 600^0C per 1 in. of thickness. There is seldom any metallographic change on stress relief, which can be associated with this marked change in mechanical properties [Watkins et al., 1963].

Temper embrittlement has been observed in the heat affected zones of Cr – Mo steels in temperatures around 775 K (500^0C) when welded constructions were used in service and around 950 K when welded constructions were stress relieved. The data of temper embrittlement in HAZ of 2.25Cr – 1Mo and 1.25Cr – 0.5Mo steels have been published as IIW documents since 1992. Those data are revised and summarized in the present document. Temper embrittlement was examined systematically according to type, nature and cause of embrittlement and the following results were obtained: the first to fifth types of temper embrittlement were found in HAZ specimens of both steels. SR-treatment will be effective for suppressing the first to fourth types of temper embrittlement of 2.25 – 1Mo steels. The temperature range for SR of the latter steel is close to that of the fifth type of embrittlement; the fifth type will occur when the SR treatment is too long. The causes of the first to fifth types of embrittlement were discussed from the viewpoint of precipitation of carbide and segregation of impurity elements.

Carbide phases (cementite, chromium carbide, molybdenum carbide) will induce temper embrittlement through (i) hardening the ferrite matrix reducing its ductility, (ii) providing the crack-initiation site in the ferrite grain or the grain boundaries. The fracture can be also induced by the segregation of impurity elements in the grain boundary of prior-austenite. The segregation of phosphorus, nitrogen, chromium, molybdenum and carbon was detected on the fracture surface. Phosphorus and nitrogen will weaken the grain boundary to cause intergranular fracture, their action will be intensified by chromium, molybdenum and carbon [Tamaki, 1999].

2.7 Conventional Heat Treatment of Steels

The traditional route to high strength in steels is by quenching to form martensite which is subsequently reheated or *tempered* at an intermediate temperature, increasing the toughness of the steel without too great loss in strength. This combined heat treatment, consisting of hardening plus tempering, is performed at temperatures between 450 and 680^{0}C for structural steels where the maximum toughness at a specified strength level is achieved [Liscic, 1997]. The aim of hardening and tempering structural steels will be better understood if one has a clear notion of the difference between toughness and ductility.

Ductility is the property denoting the deformability of a material and is measured in a tensile test as elongation (A in %) and reduction of area (Z in %). It is a one-dimensional property.

Toughness of a material, however, is a two-dimensional property because it is an integral (or product) of strength and ductility, as schematically shown in Figure 2.6 [Liscic, 1997].

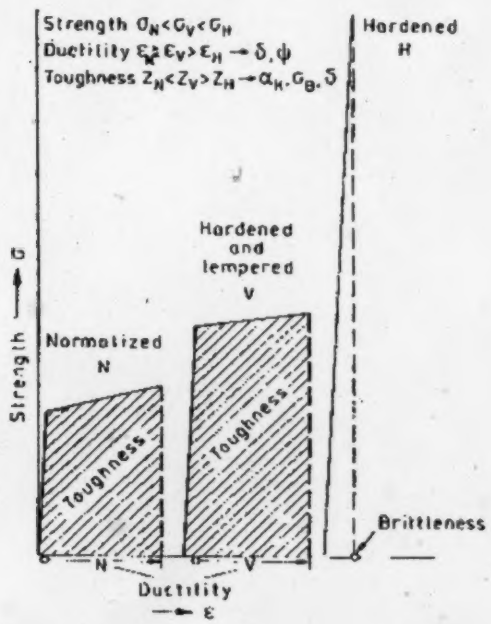

Fig. 2.6 – Schematic presentation of ductility, toughness, and brittleness [Liscic, 1997]

As Figure 2.6 shows, a normalized steel (N) having the same ductility as a hardened and tempered steel (V) will have lower toughness because of its lower strength level. The aim of the hardening and tempering process can also be explained by means of the stress-strain diagram schematically shown in Fig. 2.7.

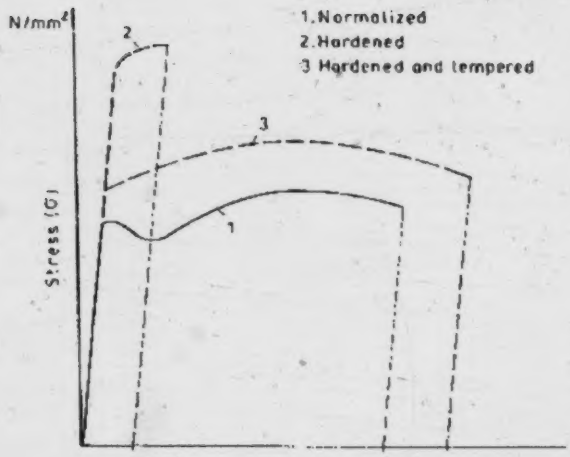

Fig.2.7 – Stress-strain diagram of a steel after different heat treatments [Liscic, 1997]

As hardened, a steel has high yield strength but low ductility, and a small area below the stress-strain curve (curve 2) indicates low toughness. As-hardened and tempered (curve 3) steel has higher yield strength than in its normalized condition but also much higher ductility than in its hardened conditions. The greatest area below the stress-strain curve indicates a substantial increase in toughness compared to either normalized or hardened conditions

For certain steel grades, the relation between mechanical properties and the tempering temperature can be read from a diagram as shown in Figure 2.8 for the steel DIN 20 CrNiMo 2 (0.15%C, 0.20%Si, 0.88Mn, 0.53%Cr, 0.50%Mo, 0.86%Si).

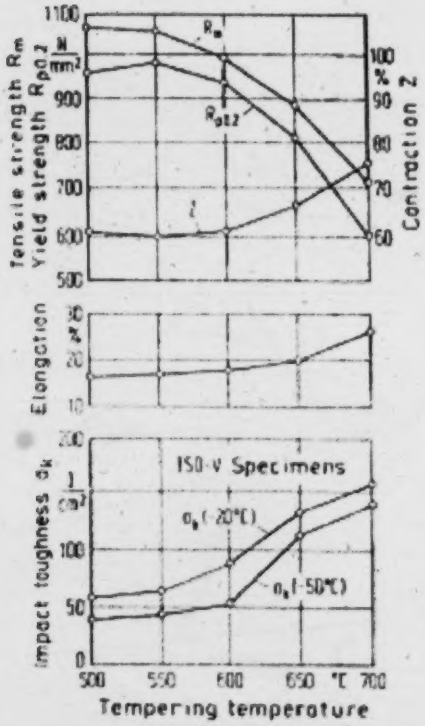

Fig. 2.8 – Hardening and tempering diagram of DIN 20CrNiMo2 steel [Liscic, 1997]

It can be clearly seen from the lower part of this diagram how the impact toughness increases when the steel is tempered at a temperature above 550^0C (1022^0F). Such diagrams enable precise optimization of the strength level and toughness by selection of the proper tempering temperature.

There are also diagrams for practically every steel grade from which the tempering temperature may be determined if the ultimate tensile strength or yield strength required after tempering is known.

The properties of a hardened and tempered steel correlate to a high degree with the microstructure after hardening and tempering. Maximum toughness values are obtained when tempering a structure that after quenching consists of fine-grained martensite (having a grain size of ASTM $\geq$ 6) as can be seen in Figure 2.9 [Liscic, 1997].

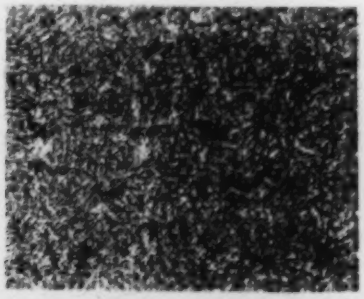

Fig.2.9 – Microstructure of DIN 34CrNiMo6 steel after hardening and tempering. Tempered fine-grained martensite. Magnification 500x [Liscic, 1997]

The process of hardening and tempering has been divided into operations of austenitization (A), quenching (Q), and tempering (T) as shown in Fig. 2.10.

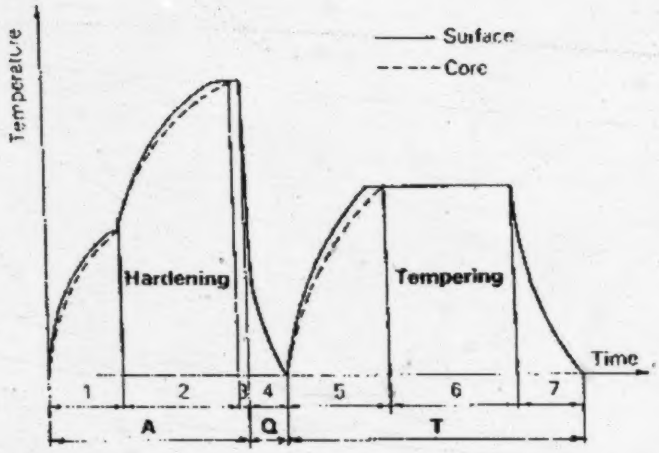

Fig. 2.10 – Operations and phases in the process of hardening and tempering [Liscic, 1997]

Within the austenitization operation, the phases are (1) preheating, (2) heating to austenitization temperature with workpiece equalization at that temperature, and (3) homogenization of the structure.

Within tempering, the phases are (5) heating to the tempering temperature and temperature equalization, (6) soaking at tempering temperature, and (7) cooling down from the tempering temperature [Liscic, 1997].

2.8 Tempering of Martensite

Martensite is a very strong phase, but it is normally very brittle so it is necessary to modify the mechanical properties by heat treatment (tempering) in the range 150 – 700^{0}C. Essentially, martensite is a highly supersaturated solid solution of carbon in

iron which, during tempering, rejects carbon in the form of finely divided carbide phases. The end result of tempering is a fine dispersion of carbides in an α-iron matrix which often bears little structural similarity to the original as-quenched martensite. It should be born in mind that, in many steels, the martensite reaction does not reach completion on quenching, resulting in varying amounts of retained austenite which does not remain stable during the tempering process [Honeycombe, 1995].

2.9 Tempering of Plain Carbon Steels

The as-quenched martensite possesses a complex structure where the laths are heavily dislocated to an extent that individual dislocations are very difficult to observe in thin-foil electron micrographs. On reheating as-quenched martensite, the tempering takes place in four distinct but overlapping stages:

Stage 1, up to 250^0C – precipitation of ε-iron carbide; partial loss of tetragonality in martensite

Stage 2, between 200 and 300^0C – decomposition of retained austenite

Stage 3, between 200 and 350^0C – replacement of ε-iron carbide by cementite; martensite loses tetragonality

Stage 4, above 350^0C – cementite coarsens and spheroidizes; recrystalization of ferrite [Honeycombe, 1995].

From the PWHT point of view, the stage 4 is particularly interesting due to the similarity of tempering temperatures between them. In the stage 4, the cementite

particles undergo a coarsening process and essentially lose their crystallographic morphology, becoming spheroidized. The coarsening commences between 300 and 400^0C, while spheroidization takes place increasingly up to 700^0C. At the higher end of this range of temperature the martensite lath boundaries are replaced by more equi-axed ferrite grain boundaries by a process which is best described as recrystallization. The final result is an equi-axed array of ferrite grains with coarse spheridized particles of Fe_3C, partly, but not exclusively, in the grain boundaries.

Plain carbon steels with less than 0.25 wt% C are not normally quenched and tempered, but in the range 0.25-0.55 wt% C heat treatment is often used to upgrade mechanical properties. The usual tempering temperature is between 300 and 600^0C allowing the development of tensile strengths between1700 and 800 MN m^{-2}, the toughness increasing as the tensile strength decreases [Honeycombe, 1995].

2.10 Tempering of Alloy Steels

The addition of alloying elements to steel has a substantial effect on the kinetics of the $\gamma \rightarrow \alpha$ transformation, and also of the pearlite reaction. Most commons alloying elements move the TTT curves (Figure 2.11 for 4140 steel analyzed in this research [ASM, 1977]) to longer times, with the result that it is much easier to "miss" the nose of the curve during quenching. This essentially gives higher hardenability, since martensite structures can be achieved at slower cooling rates and, in practical terms, thicker specimens can be made fully martensitic. Alloying elements have also shown to have a substantial effect in depressing the Ms temperature.

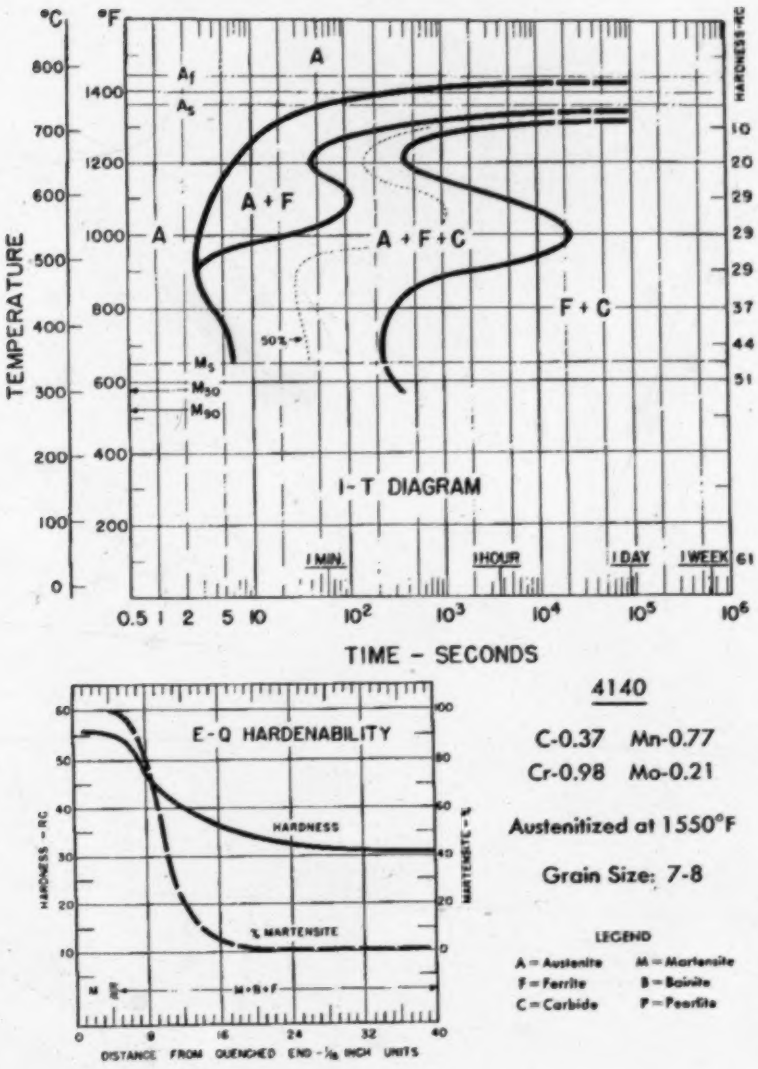

Fig. 2.11 – Isothermal Transformation Diagram of 4140 steel [ASM, 1977]

When a steel containing chromium is tempered, two chromium carbides are very often encountered: Cr_7C_6 and $Cr_{23}C_6$. The normal carbide sequence during tempering is

$$\text{Matrix} \rightarrow (FeCr)_3C \rightarrow Cr_7C_3 \rightarrow Cr_{23}C_6$$

While this sequence occur in higher chromium steels, bellow about 7 wt% Cr, $Cr_{23}C_6$ is absent unless other metals such as molybdenum are present. Chromium is weaker carbide former than vanadium, which is illustrated by the fact that Cr_7C_3 does not normally occur until the chromium content of the steel exceeds 1 wt% at a carbon level of about 0.2 wt% [Honeycombe, 1995].

2.11 PWHT – Codes and Regulations

2.12 Low and Medium Carbon Steels

Although the examination of the fields of application foreseen by the codes reveals a wide variety of points of view about PWHT, it appears rather clearly that the stress relief heat treatments are mandatory in the case of equipment undergoing risk of stress corrosion, or risk of brittle fracture or fatigue failure in hydrotest or service conditions.

The difference among codes requiring PWHT of low and medium carbon steels can be compared in terms of four essential criteria of comparison:

1. – The allowable maximum thickness without heat treatment.
2. - The heat treatment temperature.
3. - The minimum holding time at maximum temperature.

4. – The maximum heating and cooling rates, the maximum loading and minimum unloading temperature.

2.13 Critical Thickness

The thickness is a determinant factor in the prescription of the codes for the PWHT application. Bellow a certain thickness, the treatment may be omitted, whereas it is mandatory above a certain limit.

Steels	ASME VIII/2	BS 5500	AD HP 7 Rc<370	AD HP 7 630>Rc>370	ISO DIS 2694	KBN F11-001	Rules NL	NF 32-105 Rm<560 MPa	NF 32-105 Rm<700 MPa	DIN 17155	IIS Rec
C and C Mn	32 38	35 40	30 38 50	30	30 38 50	20	32	40	30	30	35
0.35 Mo	16	20	30-38-50	30	30-38-50	30	32	-	-	-	20
0.5 Mo	16	20	30-38-50	30	20	30	0	-	-	-	20
1Cr-0.5Mo	16	0	-	-	15	15	0	-	-	-	0
2.25Cr-1Mo	0	0	-	-	0	0	0	-	-	-	0
CrMoV	-	0	-	-	0	0	0	-	-	-	15

Table 1. – Critical thickness (mm) for PWHT required by different codes [IIW, 1987]

A comparison of different codes reveals a wide dispersion in the determination of that limit thickness, whatever the steel type may be.

The C and C-Mn steels may not be subjected to PWHT when the thickness is lower than a value, according to the codes, from 20 up to 50 mm.

The Mo, Cr-Mo, Cr-Mo-V low alloy steels are also subject to prescriptions very differently according to the codes. In general, the maximum limit thickness is reduced gradually as the alloying content of the steel increases.

2.14 Temperature of the Post Weld Heat Treatment

The holding temperature is considered as the leading factor to obtain a good stress relief as well as the driving factor concerning the metallurgical effects of the PWHT. By comparative examination of the codes, it can be observed that these ones are characterized by the largest scatter in temperature to be reached.

The C and C-Mn steels can be heat treated in temperature range from 530 to 650^{0}C as shown in Table 2.

CODE	COUNTRY	T ^{0}C
CODAP 80 F2	F	530-580
DIS 2694	ISO	560-600
BS 5500	UK	580-620
ASME VIII	USA	593
AD M DIN	GER	600-650
+ SEW 089	RFA	530-580
JIS B 8243	J	600
RULES	NL	600
NBN 629	B	580-620
CODE	Ex Yu	<560
CS 420284	Cs	600-650
OP – 02CS - 66	USSR	630-660
Doc X-861-77	IIS	540-580

Table 2. – Summary of code requirements for PWHT temperature for C and C-Mn steels [IIW, 1987]

The holding temperature between 530 and 580^{0}C is recommended by:

AD Merkblatt according to SEW089 for steel with yield strength lower than 370 MPa, and for fine grained steels with thicknesses above 30mm;

CODAP 80-F-2 for the C-Mn steels and by the DIN 17155 for STE 460 steels.

The Dutch code imposes a minimum of 600^{0}C, so does the Japanese code for P1, P2 and P3 steels according to the standard JIS B 8243.

The American code ASME Section VIII recommends, for the steel P1 and thickness of 30 mm and above (40 mm if there is a preheat above 95^{0}C), a temperature of 593^{0}C. The highest temperatures are recommended by former Soviet codes 0P 02CS-66 and RTM-1S-73 of 630^0-660^{0}C and 650^0-680^{0}C respectively.

Cr-Mo and Cr-M0-V low alloy steels are in general heat treated after welding, essentially to improve the toughness of the fused metal and of the heat affected zones. The examination of some codes shows, here again, fairly large discordance, but these vanish when the Cr content increases (3% Cr or 5%Cr). For example, ASME code Section VIII recommends 593^{0}C for 1/2Cr-1/2Mo, 1Cr-1/2Mo and 1 1/4Cr-1/2Mo-Si steels and 675^{0}C for 2 1/4Cr-1Mo and 3Cr-1Mo steels.

2.15 Minimum Holding Time at Maximum Temperature

For C or C-Mn steel, it can be observed that several codes (CODAP, AD Merkblatt DIN and SEW etc) agree to adopt a duration of 2 min/mm in a thickness range between the minimum thickness requiring PWHT and up to 60mm. For the lowest

time, the codes often impose a minimum holding time of 20 to 60 min when the treatment is necessary. Above 60 mm, some codes reduce proportionally values (2.5 min/mm), but admit the possibility to integrate the heat-up and cool-down operations.

2.16 Hollomon-Jaffe parameter

The maximum temperature and holding time at this temperature are principal variables in carrying out a PWHT. The parameter that includes the effect of temperature and the effect of holding time was given by Hollomon and Jaffe:

$$Hp = T\,(20 + \log t) \times 10^{-3}$$

where: T = temperature of heat treatment (^{0}K)

t = holding time (hr)

This relation is graphically illustrated for temperatures from 450 to 700^{0}C in Fig. 2.12.

From the diagram below, the 6min holding at 700^{0}C has the same effect as 15-min holding at 675^{0}C or 60 hr holding at 575^{0}C or 1000 hr holding at 525^{0}C.

[Hrivnak, 1985]

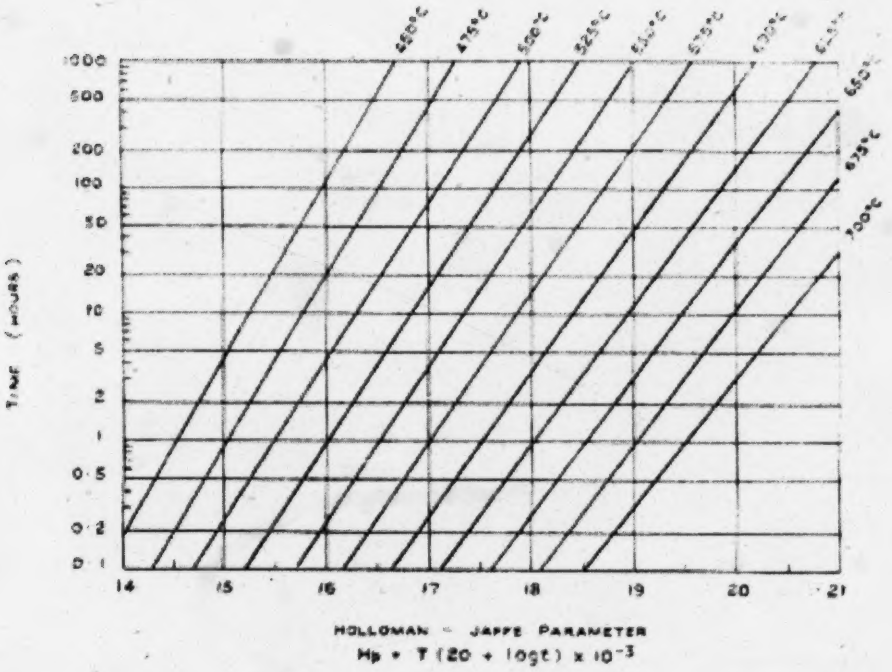

Fig. 2.12 – Time/Temperature parameter relationships [Hrivnak, 1985]

2.17 PWHT – Code requirements for low alloy steels

The Cr-Mo and Cr-Mo-V steels in the normalized and tempered conditions are used extensively for pipes for carrying high temperature high-pressure steam operating very often under creep conditions. For pipes with wall thickness greater than 25mm, various codes require a mandatory post weld heat treatment and requirements by some codes can be seen in the Fig. 2.13.

Code	Heating rate	Soak temperature and time	Cooling rate
BS 2633	Not exceeding 100°C/hr or 6250/t °C/hr whichever is lower	680-720 °C 2.5 min per mm Subject to a minimum of 180 min	Not exceeding 100°C/hr
BS 5500	Not exceeding 220°C/hr for thickness up to 25 mm Not exceeding 550°/t °C/hr or 55°C/hr whichever is greater, for thicknesses above 25 mm	680-720 °C 2.5 min per mm Subject to a minimum of 180 min	Not exceeding 275°C/hr for thicknesses up to 25 mm Not exceeding 657/t °C/hr or 55°C/hr whichever is the grater, for thicknesses above 25 mm to 400°C.Cool in still air from 400°C
CEGB 23583 & 23584 GDCD61	Not exceeding 100°C/hr or 6250/t °C/hr, whichever is the smaller	670-720 °C 4-8 min per mm Subject to a minimum of 180 min 680°C (minimum)	50°C/hr to 400°C. Followed by natural cooling with lagging in place
ASME VIII*	Not exceeding 55°C/hr or 5588/t °C/hr, whichever is the greater	2.4 min per min for thicknesses less than 125 mm minimum 15 min# (300+0.6 t – 125) min for t>125 mm	55°C/hr or 5588/t °C/hr whichever is the greater

t = thickness of pipe, mm
* ASME data are for 2 ¼ Cr 1Mo steel. 1/2Cr 1/2Mo 1/4V is not catered but is assumed to be similar
# the requirement of ASME III (the nuclear code) is similar but the minimum time required is 30 min

Table 3 – Summary of code requirements for PWHT of low alloy steels [IIW, 1987]

All four standards require essentially the same soak temperature but the time at temperature for a specific thickness varies markedly, as shown in Fig. 2.14.

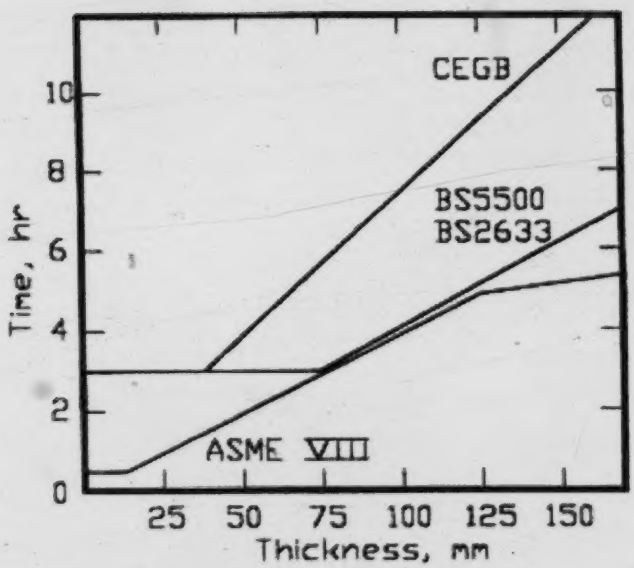

Fig. 2.13 – Heat treatment times for various codes [Fidler, 1984]

For example, a pipe weld of 25 mm wall thickness requires 3hr soaking according to both the British Standard and CEGB Standard (Central Electricity Generating Board), but only 1 hr according to ASME VIII. A weld of 100mm thickness would require 8hr soaking according to CEGB StandardGDCD61, 4.16hr according to BS 5500 and 2663, and 4hr according to ASME VIII [Fidler, 1984].

2.18 Literature Review Summary

It is well known that the PWHT reduces the amount of residual stresses and alters metallurgical characteristics of the weld zone. Most codes do not explicitly state the

purpose of the PWHT, although the ASME pressure vessel codes mention the need to increase fracture toughness, but it is known to lower residual stresses and to improve the weld metal fracture toughness which are both desirable effects. However, the extent to which these effects occur is not known, and in particular the codes do not give any guidance as to what level of residual stresses may be expected after any PWHT cycle. It is easier to quantify the degree of tempering during PWHT but, clearly, it is really difficult to quantify the degree of stress relief because the as-welded residual stress field is unknown. Due to this, the codes attempt to overcome this deficiency by specifying a time for PWHT that will give and acceptable low probability of failure during the lifetime of the weld. But further confusion is caused by the inconsistencies among the various codes about the time at PWHT temperature.

In defining an optimum PWHT it is necessary to choose the temperature and time of PWHT to achieve reduction of residual stresses and adequate tempering of the welded structure.

The definition of principal variables of temperature and time of PWHT can be additionally complicated when welding quenched and tempered steels such as 1043 and 4140 steels. This situation is present in the Fig. 2.15.

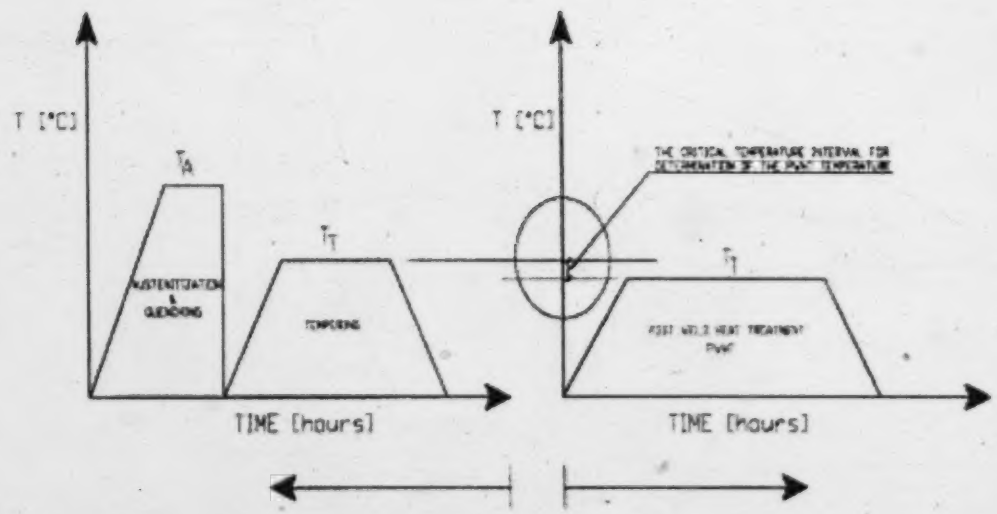

Fig. 2.14 - Relationship between convenient and post weld heat treatment [Zulic, 2003]

The temperature of tempering during a conventional heat treatment must be known in defining the adequate temperature of PWHT and this temperature of PWHT should be at least 20^0C lower. This consideration has been very often overlooked or neglected.

Even if the common heat treatment tempering temperature is known, which is usually from 600^0C to 650^0C for 4140 steel, all codes require the PWHT at higher temperatures at which many steel properties will deteriorate.

In defining the temperature of PWHT, as well as other optimum variables, there may be present some conflicting factors, which have to be taken into consideration. Generally, PWHTs at temperatures above 600^0C have been regulated by many Codes and Standards regardless on some disagreements among them. Very little is known about PWHTs below these temperatures and this project is aimed to investigate possible temperature-time relationship in obtaining desirable results after performing PWHTs at lower temperatures.

CHAPTER 3

EXPERIMENTAL PROCEDURE

3.1. Material

Two grades of steel were used in this investigation: a medium carbon 1043 normalized steel and a low alloy chromium-molybdenum 4140 heat treated steel. These steels have similar carbon content but different alloying content that affects both hardenability and weldability.

The samples for performing convenient heat treatments, welding and subsequent PWHT were cut from the steel bar of 180 mm in diameter to the thickness of 15 mm. Both steels were chemically analyzed and results are given in Table 3.1.

Element	Test result (wt%) 4140	Test Result (wt%) 1043
Carbon (C)	0.38	0.48
Manganese (Mn)	0.85	0.82
Phosphorous (P)	0.010	0.011
Sulphur (S)	0.014	0.011
Silicon (Si)	0.29	0.25
Nickel (Ni)	0.20	0.13
Chromium (Cr)	1.05	0.072
Molybdenum (Mo)	0.22	0.004
Copper (Cu)	0.15	0.16
Vanadium (V)	0.003	<0.001
Niobium (Nb)	0.001	<0.001
Titanium (Ti)	0.003	0.010
Aluminum (Al)	0.038	0.030
Boron (B)	<0.0002	<0.0002
Cobalt (Co)	0.010	0.007
Tungsten (W)	<0.003	<0.003
Calcium (Ca)	0.0024	0.0012
Arsenic (As)	<0.005	<0.001
Tin (Sn)	<0.02	<0.002
Iron (Fe)	Balance	Balance

Table 3.1. - Chemical compositions of 4140 and 1043 steels

The properties of 1043 steel are shown in Table 3.2.

Physical Properties	Metric	English	Comments
Density	7.87 g/cc	0.284 lb/in³	Typical for steels.
		Mechanical Properties	
Hardness, Brinell	201	201	
Hardness, Knoop	223	223	Converted from Brinell hardness.
Hardness, Rockwell B	93	93	Converted from Brinell hardness.
Hardness, Rockwell C	13	13	Converted from Brinell hardness. Value below normal HRC range, for comparison purposes only.
Hardness, Vickers	211	211	Converted from Brinell hardness.
Tensile Strength, Ultimate	689 MPa	99900 psi	
Tensile Strength, Yield	386 MPa	56000 psi	
Elongation at Break	21.7 %	21.7 %	in 50 mm
Reduction of Area	41.6 %	41.6 %	
Modulus of Elasticity	200 GPa	29000 ksi	Typical for steel
Bulk Modulus	140 GPa	20300 ksi	Typical for steel
Izod Impact	31 J	22.9 ft-lb	as rolled, 27 J at normalized at 900°C, 18 J at annealed at 790°C
Shear Modulus	80 GPa	11600 ksi	Typical for steels.

Table 3.2. – Properties of 1043 steel – normalized condition (900°C – air cooled) [MatWeb, 2003]

The 1043 medium carbon steel is much stronger than low carbon or mild steel. Its hardness and higher tensile strength can be increased by heat treatment and the amount of improvement depends on the carbon content of the steel. Application for this steel includes farm equipment, engine components, gears and structural fixtures.

The properties of 4140 low alloy steel are given in Table 3.3.

Physical Properties	Metric	English	Comments
Density	7.85 g/cc	0.284 lb/in³	
		Mechanical Properties	
Hardness, Brinell	277	277	
Hardness, Knoop	302	302	Converted from Brinell hardness.
Hardness, Rockwell B	99	99	Converted from Brinell hardness.
Hardness, Rockwell C	28	28	Converted from Brinell hardness.
Hardness, Vickers	292	292	Converted from Brinell hardness.
Tensile Strength, Ultimate	883 MPa	128000 psi	
Tensile Strength, Yield	685 MPa	99400 psi	
Elongation at Break	19.2 %	19.2 %	
Reduction of Area	60.4 %	60.4 %	
Modulus of Elasticity	205 GPa	29700 ksi	Typical for steel
Bulk Modulus	140 GPa	20300 ksi	Typical for steels.
Machinability	65 %	65 %	Based on AISI 1212 as 100% machinability.
Shear Modulus	80 GPa	11600 ksi	Typical for steels.

Table 3.3. - Properties of 4140 steel [MatWeb, 2003]

Chromium-Molybdenum (Cr-Mo) steels are popular engineering grades used in steam piping and gas and oil processing. At elevated temperature in service, Cr provides oxidation resistance and Mo provides secondary hardening for creep resistance. The 4140 steel is normally heat treated to obtain desired grain size and required mechanical properties characterized by an excellent combination of strength and toughness. This steel has been also very often used for making so called "HPG" gears (High Power Gears) in a way that this steel is hardened and tempered to give tensile strength $\sigma_m \approx 1000\text{-}1250\ N/mm^2$ with additional induction hardening of teeth with the method tooth by tooth to obtain hardness of HRc 54 – 60.

3.2. Welding Procedures

The shielded metal arc welding (SMAW) process was selected for welding both 1043 and 4140 steels. The sample and welding preparation are shown in Figure 3.1.

The SMAW welds were made using a Hobart R-600-S constant current power source. Since both grades of steel are heat treatable due to their chemical composition, the knowledge of welding technology is a prerequisite to obtain the engineering benefits of these steels in welded construction.

Eight samples of 1043 steel and eight samples of 4140 steel that were welded with ten passes using the same welding parameters and the same preheat temperature. The

interpass temperature did not exceed 300^0C during welding controlled by tempil sticks.

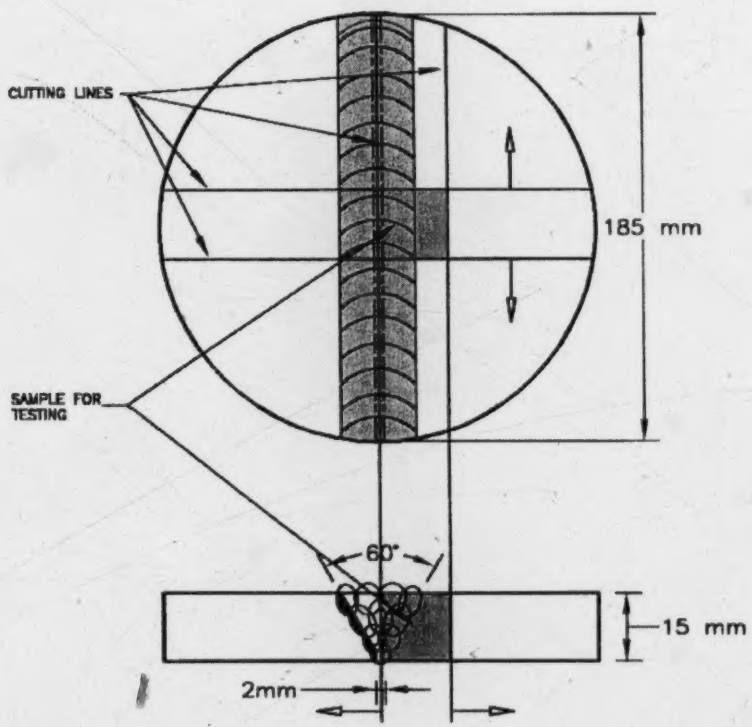

Fig. 3.1. – Schematic presentation of the specimen

The 1043 steel is weldable by all of the welding methods. However its higher carbon content and its consequently high carbon equivalent (CE) of CE=0.69 requires applying preheat and post weld heat treatment particularly for thicker and complex design of welded structures.

The 4140 steel additionally alloyed with Cr and Mo has CE=0.84 and is hardenable even under quite slow cooling rates and is sensitive to Hydrogen Assisted Cracking (HAC) in the both the weld and HAZ. Preheats recommended are therefore fairly high with PWHT after welding.

Welding settings for 1043 and 4140 steels are given in Table 3.4.

SMAW process	1043 steel	4140 steel
Current	130 Amps	130 Amps
Voltage	24 V	24 V
Tp	200^0C	200^0C
Welding Speed	180-200 mm/min	180-200 mm/min
Electrical Characteristics	DCEP	DCEP

Table 3.4. – Welding parameters for 1043 and 4140 steels

According to the welding parameters, welding was carried out by introducing low heat input into the weld zone of about 1.3 kJ/mm which favorites a narrow HAZ.

Generally, all welding procedures were performed under the conditions as much similar as the welding procedures in the industry.

3.3. Welding Consumables

Filler materials for welding 1043 and 4140 steel by the SMAW process were chosen on the basis of matching yield strength (YS) values of the base materials. The two electrodes used were E 48018-1 for welding 1043 steel and E 11018-M for 4140 steel.

Both electrodes were baked at 400^0C/min 1.5 hrs prior to welding.

Specifications for each of the consumables are given in Table 3.5.

Electrode	E 48018-1	E 83018 – M
Tensile Strength	70 ksi 480 MPa	110 ksi 760 MPa
Yield Strength	57 ksi 390 Mpa	98-110 ksi 680-760 MPa
Elongation %	22	20
C %	0.12	0.10
Mn %	0.60	1.30
Si %	0.40	0.60
P %	0.03	0.030
S %	0.03	0.030
Ni %	-	1.25-2.50
Cr %	-	0.40
Mo %	0.40-0.65	0.25-0.50
V %	-	0.05

Table 3.5. – As-welded properties of E 48018-1 and E 83018 – M filler materials

3.4. PWHT Procedures

All post weld heat treatments were performed immediately after welding in the furnace "LINDBERG/BLUE" model name: BOX FURNACE, V=240 V, A=19 A, P=4.5 kW, Tmax=1200^{0}C.

Heating rate from the welding temperature to the tempering temperature was approximately 300^{0}C/hr, while all samples were furnace-cooled after PWHTs with approximate cooling rate of 200^{0}C/hr.

The principal variables, such as the tempering temperature and the holding time at this temperature; were chosen approximately according to ASME Section VIII (lower PWHT temperatures are permitted only for P-No 1 Gr. Nos 1 and 2 materials) and withdrawn British Standard 1500 which did not state applicable steel grades. PWHTs were also carried out in accordance with some of today's relevant codes. Particular PWHTs were done based on the Hollomon-Jaffe parameter calculations. The PWHT parameters applied to 1043 and 4140 steels are given in Table 3.6.

	1043 steel	4140 steel
Most Codes	650^0C – 1.0 hr	650^0C – 1.0 hr
Most Codes	600^0C – 1.0 hr	600^0C – 1.0 hr
~ BS 1590	550^0C – 2.5 hrs	550^0C – 2.5 hrs
~ ASME VIII	550^0C – 4.0 hrs	550^0C – 4.0 hrs
Hollomon-Jaffe Parameter	550^0C – 10.0 hrs	550^0C – 10.0 hrs
~ BS 1590	500^0C – 6.0 hrs	500^0C – 6.0 hrs
~ ASME VIII	500^0C –15.0 hrs	500^0C – 15.0 hrs
Hollomon-Jaffe Parameter	500^0C – 226.0 hrs	500^0C – 226.0 hrs

Table 3.6. – PWHT principal parameters

3.5. Q&T Procedures

The convenient heat treatments (quenching and tempering) of 1043 and 4140 steels were carried out using the same furnaces described in section 3.4 above. The samples, eight for each specified Q&T treatment, were small cubes 15x15x15 mm. The standard procedure was:

-heating to the austenitization zone

-soaking in this zone

-quenching in oil

-tempering at different tempering temperatures.

Heat treatment procedures are given in Table 3.7.

Steel Grade	Austenitization T_A (^{0}C)	Holding Time (hr)	Tempering T_T (^{0}C)	Tempering time (hr)
1043 - 4140	860	0.5	650	1.0
1043 - 4140	860	0.5	600	1.0
1043 - 4140	860	0.5	550	2.5
1043 - 4140	860	0.5	550	4.0
1043 - 4140	860	0.5	550	10.0
1043 - 4140	860	0.5	500	6.0
1043 - 4140	860	0.5	500	15.0
1043 - 4140	860	0.5	500	226.0

Table 3.7. – Temperature-Time parameters for Q&T treatments

3.6. Metallurgical Examinations

All of 1043 and 4140 welded and post weld heat-treated plates were cut as shown in Fig. 3.1. to prepare samples for microstructural and microhardness testings. Samples for microstructure analysis were mounted in 1.25" bakelite molds using a manual hot press. A pressure of 3000 psi (20.7 MPa) was applied until the temperature reached 60^{0}C and then a pressure of 6000 psi (41.4 MPa) until the temperature reached 140^{0}C. The samples were then cooled down to the room temperature and then ground and polished. Firstly, all samples were ground with 240-320- 400 and 600 grit SiC paper, and then roughly polished with 6 μm diamond paste

on a nylon cloth. Fine polishing was done with 1 μm diamond paste on a nylon cloth and final polishing with 0.05 μm alumina on a short napped cloth. Cleaning of samples between each steep was performed with water followed by a 10% ethanol rinse to prevent oxidation of the metal surface. Finally, all samples were etched with a 2% Nital solution and examined using a "Carl Ziess" Ultraphot 3 optical microscope.

3.7. Microhardness Testing

The Vickers method was chosen for all microhardness measurements in accordance with ASTM E 384-89. Measurements were done by a Shimadzu Microhardness Tester with the Dataletty 150 data processor. The applied load was 500 g for 15 sec. Hardness measurements were taken from the regions in the weld zone schematically shown in the Fig. 3.2.

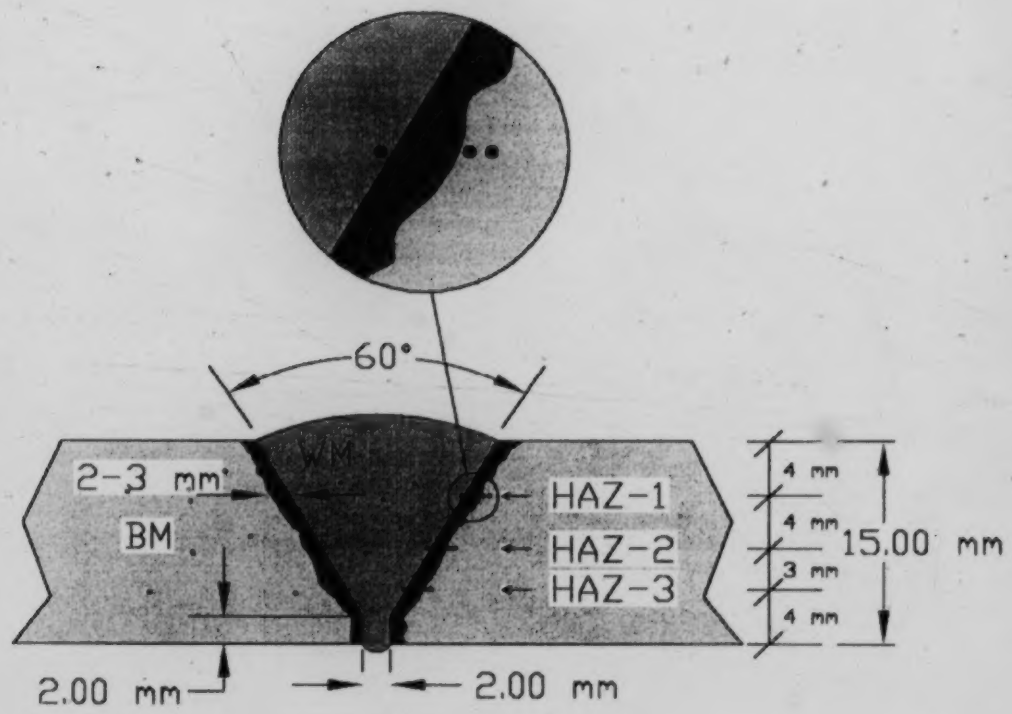

Fig. 3.2. – Locations of microhardness testing of the weld zone

As can be seen, the microhardness was measured at three regions in the welding zone, the WM, HAZ and BM. This is done to asses the influence of successive thermal cycle on the HAZ in multipass welds. The HAZ in the weld zone is always particularly interesting so three hardness measurements HAZ-1, HAZ-2 and HAZ-3 were done in this zone,where the depth surface to each of the HAZ surveys is ¼ (HAZ-1), ½ (HAZ-2) and ¾ (HAZ-3) from the plate thickness. The HAZ width

varied from 2.0 to 3.0 mm. Hardness testing started from the WM, then across the HAZ to the BM and the aim was to get the results from the all regions in the weld zone.

CHAPTER 4

Microstructure and Microhardness Examinations of 1043 steel

The primary effect of different tempering temperature – time parameters on medium carbon 1043 steel microstructures and microhardness results are analyzed in this chapter.

Firstly, microstructural and hardness examinations of 1043 steel were done in the as-received condition to compare the microstructures before and after different heat treatment regimes.

Secondly, the microstructure and microhardness examinations of this steel were performed after different Q&T treatments where the tempering temperature after quenching was the same as temperature of the PWHT that was employed below.

Thirdly, the microstructure and hardness analysis were done after different PWHT temperature-time parameters with particular attention to the weld metal, heat affected zone and base metal microstructures.

4.1. – Hardness – Mechanical Property Relationships for Steels

There have been some investigations aimed at establishing a method for predicting the ultimate tensile strength of a material from Brinell-type hardness tests. The prediction of the ultimate tensile strength Su (Rm) is based on a consistent relationship between Su and a material's hardness coefficient, Kd. A simple experimental procedure for determining Kd from indentation-hardness test data is presented. The relationship between Su and Kd id found to be 1/3 for all cubic metals [Datsko et al, 2001].

Also, based on the computer simulation of heat treatment transformation processes, the mechanical properties can be estimated by using the following formulas:

$$Rm = 3.412HV - 64.3$$

where Rm is the ultimate tensile strength in MPa, and HV is the Vickers hardness. [Szilvassy et al, 1995]. For the calculation of the yield point R (MPa), elongation A_{50} (%) in 50 mm (2 in.), reduction in area Z (%), and Charpy value KU (Joules), the equations below were suggested [Szilvassy et al, 1995]:

$$R = (117\text{-}0.0007y_m)\,Rm + 3.72y_m - 484$$

$$A_{50} = 40 - (0.03 \rightarrow 0.0001y_m)\,Rm$$

$$Z = 100 - (0.06 - 0.00024y_m)\,Rm$$

$$KU = 296 - (0.285 - 0.00098y_m)\,Rm$$

where y_m is the volume fraction of martensite in %.

These equations are valid for low-alloy, case hardened, and quenched and tempered steels with the following compositional range: 0.15-0.55%C, 0.17-0.4%Si, 0.5-1.3%Mn, 0.1-2%Cr, 0.02-0.3Mo, 0.05 to 16%Ni, 0.01-0.2%V, and 0.05-0.4%Cu. ASTM E 140 - 97^{C2} standard, revised in April 2000, gives us standard hardness conversion tables for metals among Brinell hardness, Vickers hardness, Rockwell hardness, Rockwell superficial hardness, Knoop hardness and Scleroscope hardness.

4.2. Medium Carbon 1043 Steel

The as-received microstructure of the grade 1043 steel at two different magnifications is shown in Figure 4.1

Fig.4.1. - BM microstructures of 1043 steel
As Delivered (left-400x: right- 800x)

The microstructure of the as-received 1043 steel consists of polygonal ferrite (white) and pearlite (dark and lamellar). Hardness values of as-received 1043 steel are given in Table 4.1.

	Hardness HV 1043 steel	+/-	Avg.
As received	149 – 146 – 142 – 152 – 156 - 153	10	150

Table 4.1. – Microhardness results of 1043 as-received 1043 steel

Q&T heat treatments of 1043 were performed according to the Table 3.7.

The resulting microstructure after the quenching and tempering at 650^0C is shown in Fig. 4.2.

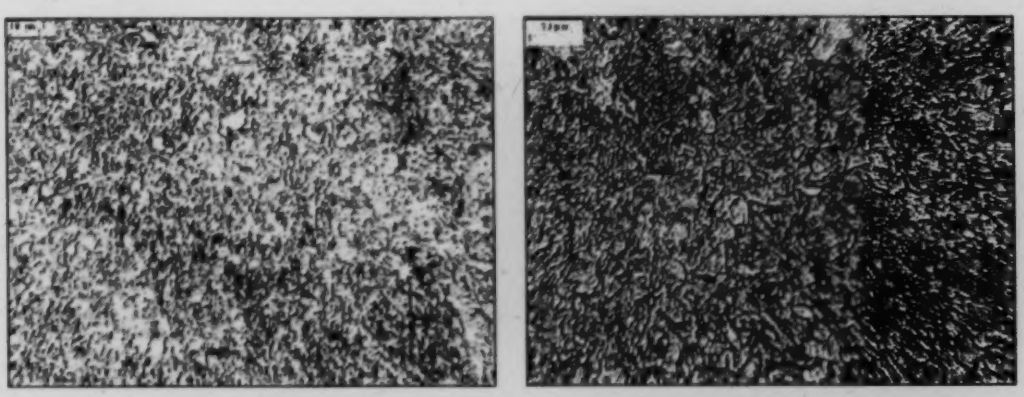

Fig. 4.2. – Microstructure of 1043 steel after Q&T heat treatment: T_A=860^{0}C/0.5 hr -T_T=650^{0}C/1.0 hr (400x and 800x)

The hardness measurements after this heat treatment are present in Table 4.2.

	Hardness HV 1043 steel	+/-	Avg.
Q&T condition	233 – 229 – 236 – 221 - 229	15	229

Table 4.2. – Microhardness results of 1043 steel after Q&T at 860^0/650^{0}C-1.0 hr

This microstructure consists of tempered martensite (dark areas) and ferrite (white, light areas). Tempered martensite is not as hard as just-quenched martensite but it is much tougher and fine grained.

Quenched martensite forms during quenching from face centered cubic austenite to the body centered form of iron without precipitation of cementite and the carbon is retained in the iron crystal structure. This structure is stretched slightly so it is no longer cubic. Martensite is ferrite supersaturated with carbon with its hardness value from 580 – 670 HV.
As quenched, martensite is brittle with significant amount of internal stresses.
By tempering - heating just-quenched martensite to temperature below the eutectoid for a specified time, the martensite becomes very strong but with much better ductility and toughness, which is the result of producing small uniformly dispersed cementite in ferrite. Increased cementite particle size results in softer, more ductile, material.

The average microhardness values after Q&T heat treatment of 229 HV compared to 150 HV after annealing clearly show all benefits obtained by quenching and tempering of 1043 steel. This hardness of 229 HV is associated with the presence of tempered martensite. It can be suggested that the 1043 steel with its chemical composition be used in a Q&T condition.

The next Q&T heat treatment parameters were different in ways that only tempering temperature after quenching was lower; 600^0C instead of 650^0C. The microstructure after this heat treatment is shown in Fig. 4.3.

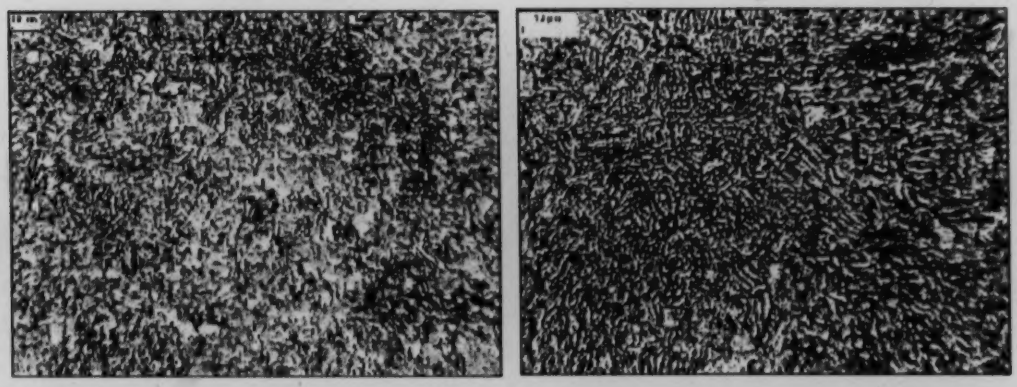

Fig. 4.3. – Microstructures of 1043 steel after Q&T heat treatment: T_A=860°C/0.5 hr – T_T=600°C/1.0 hr (400x and 800x)

The microhardness values measured after these Q&T parameters are given in Table 4.3.

	Hardness HV 1043 steel	+/-	Avg.
Q&T Condition	240 – 239 – 246 – 235 – 239 – 248 - 248	15	241

Table 4.3. – Microhardness values of 1043 steel after Q&T at 860°/600°C-1.0 hr

By examination of microstructures and hardness values after tempering at 650°C and 600°C, it can be seen differences in the grain size (bigger grain size at 650°C) as well as the % of ferrite regions which are more present in the microstructure tempered at 650°C, which is relatively close to the eutectoid temperature. Consequently, hardness values are lower by about 5% and these differences can be associated with the fact

that increased cementite particle size and less C in the matrix result in softer and more ductile (lower hardness level) microstructures. Generally, larger particles are produced at higher tempering temperature.

Both tempering temperatures are the most common in Q&T heat treatment processes.

4.3. Q&T Heat Treatment Microstructures after the 550^{0}C Tempering Temperature with Different Holding Times

At a tempering temperature of 550^{0}C three different holding times of 2.5, 4.0 and 10.0 hrs were performed and microstructures obtained after each heat treatment are shown in Fig. 4.4., Fig. 4.5., and Fig. 4.6.

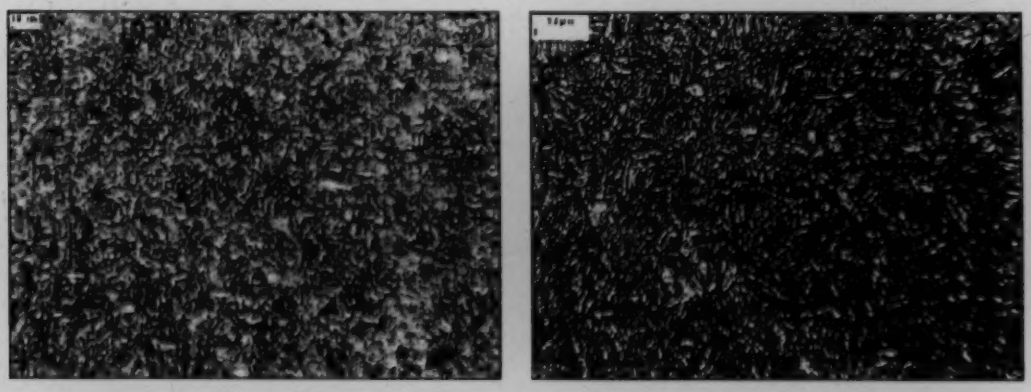

Fig. 4.4. –Microstructures of 1043 steel after Q&T heat treatment: T_A=860^{0}C/0.5 hr – T_T=550^{0}C/2.5 hrs (400x and 800x)

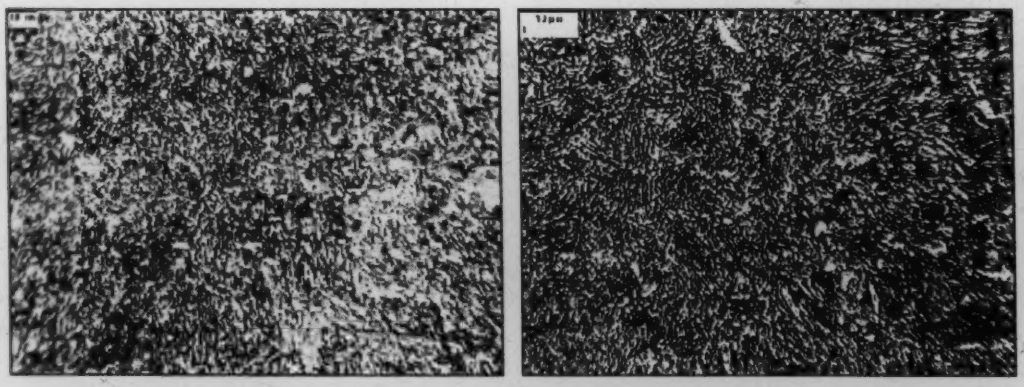

Fig. 4.5. – Microstructures of 1043 steel after Q&T heat treatment: T_A=860^{0}C/0.5 hr – T_T=550^{0}C/4.0 hrs (400x and 800x)

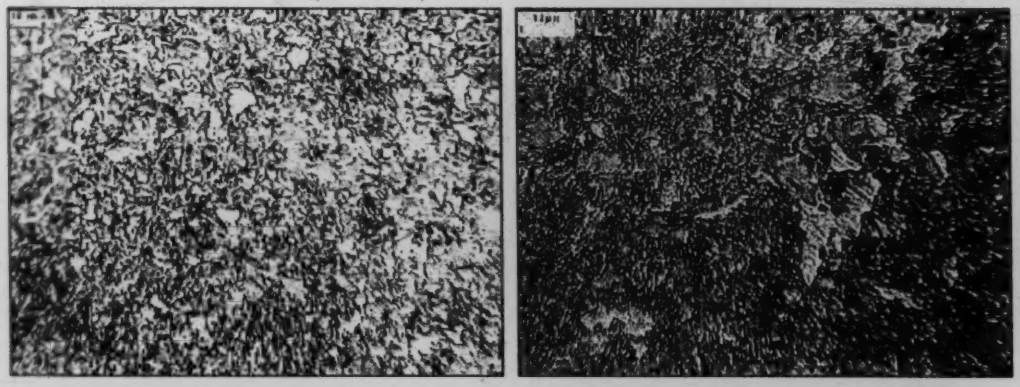

Fig. 4.6. - Microstructures of 1043 steel after Q&T treatment: T_A=860^{0}C/0.5 hr – T_T=550^{0}C/10.0 hrs (400x and 800x)

The hardness measurement values are given in Table 4.4.

Tempering Parameters	**Hardness HV** 1043 steel	+/-	Avg
T_T= 550^{0}C/ 2.5 hrs	372 – 352 – 381 – 361 – 348 - 354	33	361
T_T= 550^{0}C/ 4.0 hrs	254 – 276 – 262 – 261 – 252 - 266	24	262
T_T = 550^{0}C/ 10.0 hrs	211 – 207 – 229 – 220 – 213 - 215	22	216

Table 4.4. – Hardness measurements after Q&T at 550^{0}C for different holding times

Microstructure examination illustrates obvious differences among these microstructures tempered at the same temperature but for the different tempering times. The difference in hardness values after the shortest tempering times and the longest one is about 40%. Both microstructure and hardness results indicate that the tempering time of 2.5 hrs was not enough to complete the tempering process of quenched martensite.

On the contrary, the tempering time of 10.0 hrs resulted in an increase of the grain size and lowered the hardness to the level of 216 HV, which corresponds to the hardness of the annealed condition.

If the microstructures and hardness values attained after 600^0C or 650^0C, as the most used and representative ones, then the most similar result to these is obtained after tempering at 550^0C for 4.0 hrs producing slightly higher hardness of 262 HV or 8-15%.

4.4.Q&T Heat Treatment Microstructures after the 500^0C Tempering Temperature with Different Holding Times

Tempered microstructures resulted after three different holding times at 500^0C are shown in Fig.4.7., Fig. 4.8. and Fig. 4.9.

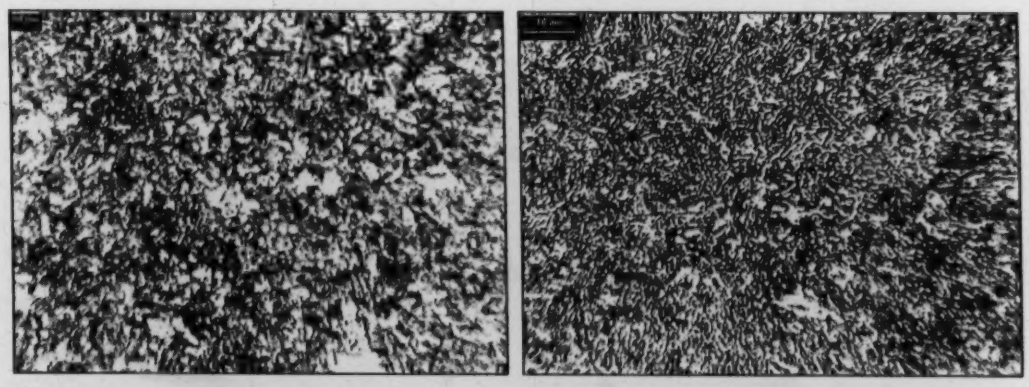

Fig. 4.7. – Microstructures of 1043 steel after Q&T treatment: T_A=860^{0}C/0.5 hr – T_T=500^{0}C/6.0 hrs (400x and 800x)

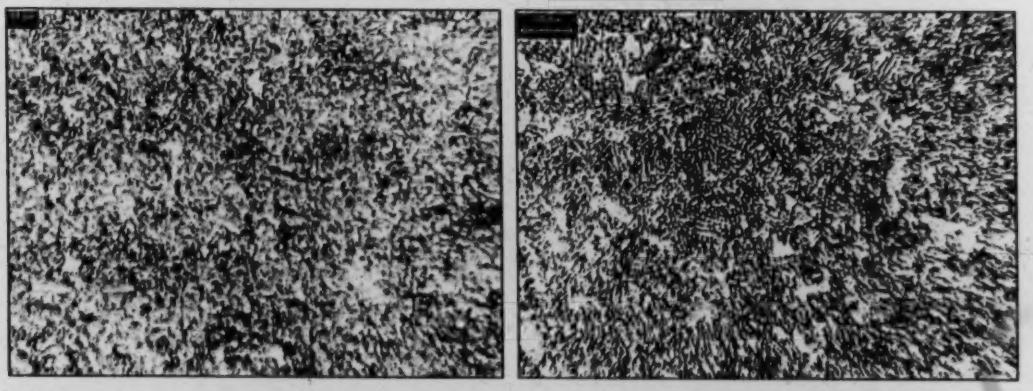

Fig. 4.8. –Microstructures of 1043 steel after Q&T heat treatment: T_A=860^{0}C/0.5 hr – T_T=500^{0}C/15.0 hrs (400x and 800x)

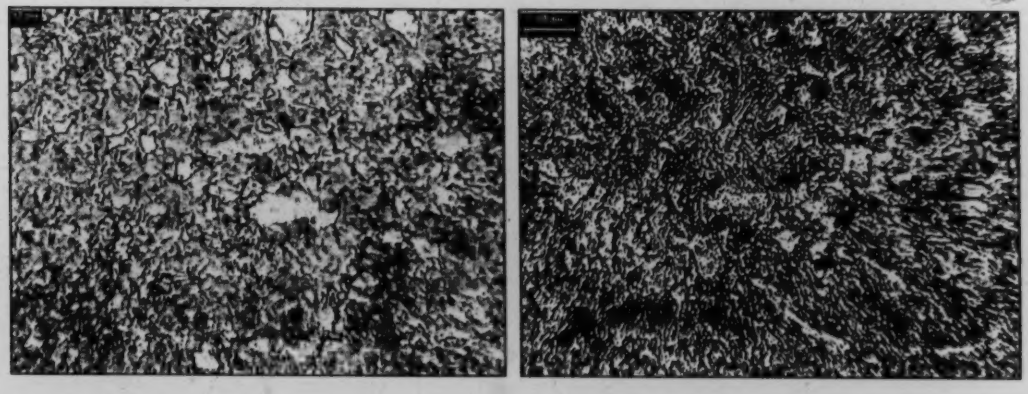

Fig. 4.9. – Microstructures of 1043 steel after Q&T treatment: T_A=860^{0}C/0.5 hr – T_T=500^{0}C/226 hrs (400x and 800x)

These Q&T heat treatments at 500^0C tempering temperature and holding times of 6.0, 15.0 and 226 hrs resulted in hardness values given in Table 4.5.

Tempering Parameters	Hardness HV 1043 steel	+/-	Avg
$T_T = 500^0$C/ 6.0 hrs	277 – 236 – 267 – 246 – 242 - 256	41	254
$T_T = 500^0$C/ 15.0 hrs	255 – 251 – 246 – 258 – 255 - 248	10	252
$T_T = 500^0$C/ 226.0 hrs	209 – 210 – 215 – 223 – 199 - 217	18	212

Table 4.5. – Hardness measurements after Q&T at 500^0C for different holding times

The extent and the rate of change of the microstructure and hardness values during tempering are not only temperature dependent, but also time dependent as well. Hardness values do not confirm the presence of very hard microstructure constituents even after tempering at the relatively low temperature of 500^0C. The resulting microstructures of tempered martensite are different in grain size, where the biggest grain size is associated with the longest tempering times of 226 hrs. This 226-hour holding time at 500^0C also produced an increased presence of ferrite, with consequent drop of hardness value to 212 HV. Regardless of the tempering temperature, both microstructure and hardness values do not confirm the presence of hard, brittle, just-quenched martensite which was still untempered.

The graphic presentation of hardness variations for all temperature-time tempering parameters is given in Fig. 4.10.

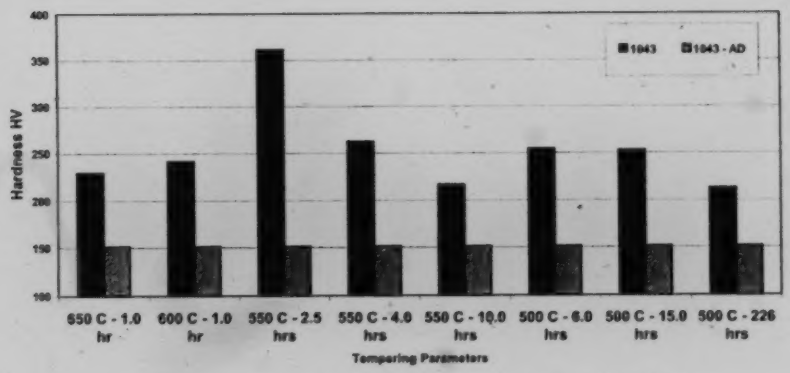

Fig. 4.10. - Hardness Profile of 1043 steel after different Q&T treatments

The hardness values of the 1043 steel samples are significantly different when the tempering temperature was 550^0C for 2.5 hrs (361 HV) and 10.0 hrs (216 HV). At 550^0C, the peak hardness is associated with the shortest tempering time, which did not allow the tempering process to be accomplished. Hardness values of other tempering treatments are relatively similar confirming that these lower hardness values are related to the ductile phases of ferrite and tempered martensite formed during tempering.

The most dominant factor in determining the acceptable hardness value is usually defined by the previous heat treatment hardness value (if any is done) or by the purchaser of the structure.

CHAPTER 5

Microstructure and Microhardness Examinations of 4140 steel

The same procedures and experiment were carried out for a low- alloy Cr-Mo 4140 steel as those performed for medium carbon 1043 steel as described in Chapter 4, namely an investigation of the effect of different tempering parameters after quenching on microstructure and microhardness values.

5.1. Low-alloy Cr-Mo 4140 steel

The microstructure of as-received 4140 steel is shown in Fig. 5.1.

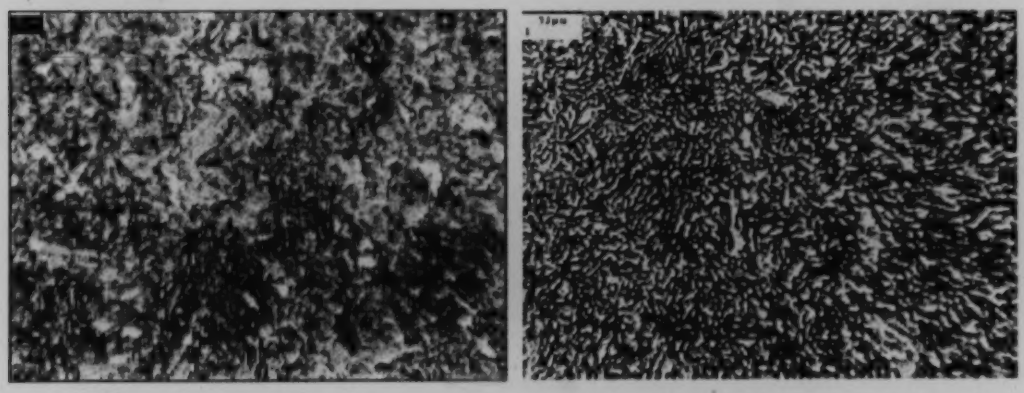

Fig. 5.1. – Microstructures of 4140 steel
As Received (left 400x – right 800x)

The results of hardness measurements of as-received 4140 steel are given in Table 5.1

	Hardness HV	+/-	Avg
	4140 steel		
As received	286 – 293 – 289 – 277 – 310 - 293	24	291

Table 5.1. – Hardness values of 4140 steel – as-received

The photographs of microstructure as well as the hardness value clearly show and indicate that as-received 4140 steel was already heat treated consisting the tempered martensite microstructure and a martensite-ferrite-carbide aggregate.

Quenching from T_A=860^{0}C in oil was carried out the same for all samples while tempering temperature T_T and holding time were varied according to the Table 3.7. The microstructure of 4140 steel after the first set of tempering parameters at 650^{0}C/1.0 hr is presented in Fig. 5.2.

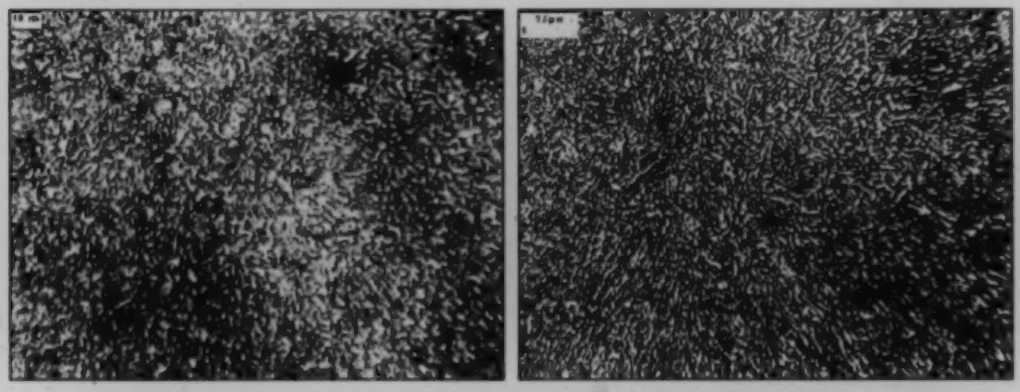

Fig. 5.2. – Microstructure of 4140 steel after Q&T treatment: T_A=860^{0}C/0.5 hr – T_T=650^{0}C/1.0 hr (400x and 800x)

The results of hardness measurements after this heat treatment are given in Table 5.2.

	Hardness HV 4140 steel	+/-	Avg
Q&Tcondition	268 – 277 – 298 – 278 – 284 - 273	30	281

Table 5.2. – Hardness values after Q&T at 860°C/650°C/1.0 hr

This microstructure consists predominantly of tempered martensite (dark) with very little ferrite (white). The hardness value of as-received 4140 steel of 291 HV is slightly higher than the 281 HV measured after tempering at 650°C/1.0 hr, which indicates that as-received 4140 steel was tempered at little lower temperature or shorter time.

The 600°C/1.0 tempering parameters produced the microstructure shown in Fig. 5.3. and hardness values given in Table 5.3.

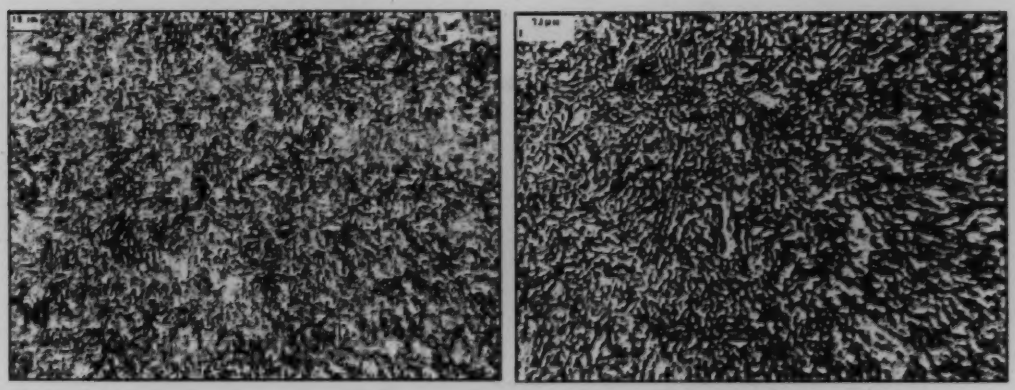

Fig. 5.3. – Microstructures of 4140 steel after Q&T heat treatment: T_A=860°C/0.5 hr – T_T=600°C/1.0 hr (400x and 800x)

	Hardness HV 4140 steel	+/-	Avg
Q&T Condition	317 – 318 – 312 – 321 – 307 - 303	18	313

Table 5.3. – Hardness values after Q&T at 860°C/600°C/1.0 hr

The main characteristic of all three microstructures above (as-received, tempered at 650^0C/1.0 hr and at 600^0C/1.0 hr) is that they consist of tempered martensite but with small particles of ferrite. Results of hardness measurements confirm that the hardness increases with decreasing the tempering temperature when the holding time is the same.

5.2. Q&T Heat Treatment Microstructures after the 550^0C Tempering Temperature for Different Holding Times

In Chapter 2, from Figure 2.8 it can be clearly seen how a tempering temperature influences all steel properties and how important this temperature is in optimization all these properties. Toughness, for example, significantly increases when the tempering temperature is above 550^0C but the tensile and yield strengths decrease with increasing the temperature.

Tempering at 550^0C affects changes in steel properties compared to tempering at 600^0C or 650^0C.
If tempering must be carried out at 550^0C, then the only way to optimize all mechanical properties would be by increasing the holding time at this temperature.

Quenching conditions were the same for all three samples ($T_A = 860^0$C/0.5 hr – oil) while the holding times at 550^0C were 2.5 hrs, 4.0 hrs and 10.0 hrs.
Microstructures resulted after tempering at 550^0C for different holding times are shown in Fig. 5.4., Fig. 5.5. and Fig. 5.6. while the results of hardness measurement are given in Table 5.4.

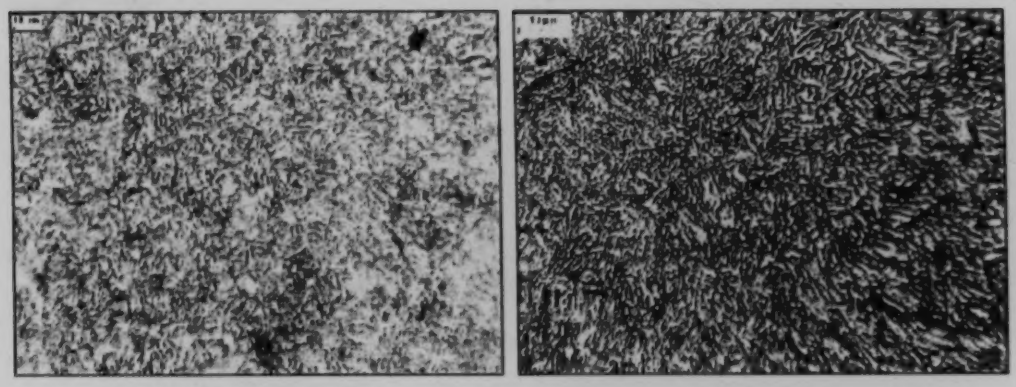

Fig. 5.4. – Microstructures of 4140 steel after Q&T heat treatment: T_A=860°C/0.5 hr – T_T=550°C/2.5 hrs (400x and 800x)

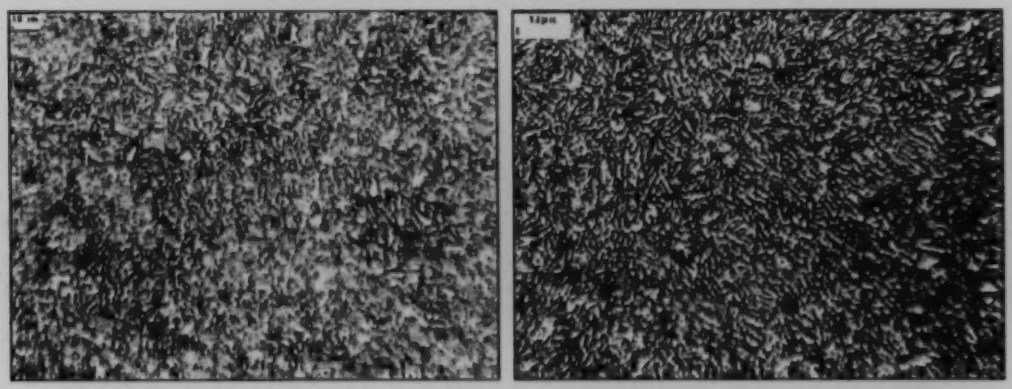

Fig. 5.5. – Microstructures of 4140 steel after Q&T heat treatment: T_A=860°C/0.5 hr – T_T=550°C/4.0 hrs (400x and 800x)

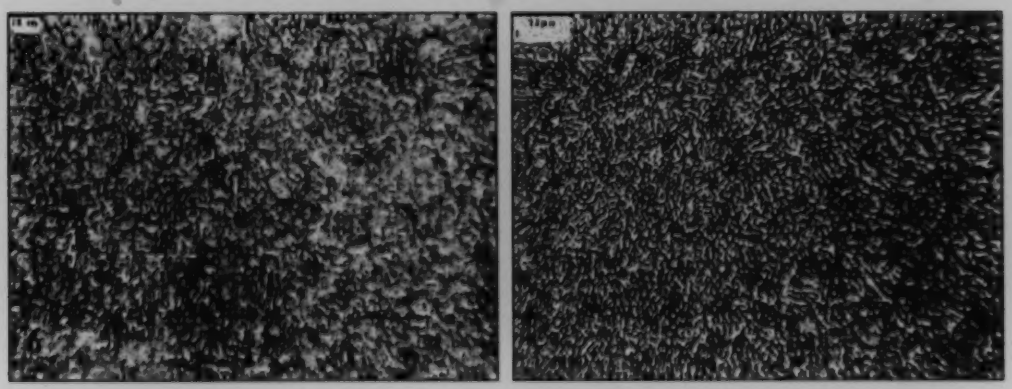

Fig. 5.6. – Microstructures of 4140 steel after Q&T heat treatment: T_A=860°C/0.5 hr – T_T=550°C/10.0 hrs (400x and 800x)

Tempering Parameters	Hardness HV 4140 steel	+/-	Avg
T_T=550^{0}C/2.5 hrs	346 – 333 – 329 – 330 – 329 - 334	17	334
T_T=550^{0}C/4.0 hrs	340 – 316 – 313 – 314 – 320 -317	24	320
T_T=550^{0}C/10.0 hrs	301 – 316 - 297 – 322 – 302 - 316	21	309

Table 5.4. – Hardness measurements after Q&T at 550^{0}C for different holding times

Although the tempering temperature of 550^{0}C was the same, the different holding times produced different results in hardness measurements showing the importance of the soaking time at lower temperature as well. The differences in hardness values from 309 HV to 334 HV or about 7.5% are not so drastic and neither are the corresponding microstructures. To summarize, the shortest holding time at the tempering temperature resulted in the highest hardness value which the microstructure consisting of a little more needle-like tempered martensite.

5.3. Q&T Heat Treatment Microstructures after the 500^{0}C Tempering Temperature for Different Holding Times

The microstructures resulting from tempering a just-quenched martensite at 500^{0}C for different holding times are shown in Fig. 5.7., Fig. 5.8., and Fig. 5.9. while the hardness values obtained after these treatments are given in Table 5.5.

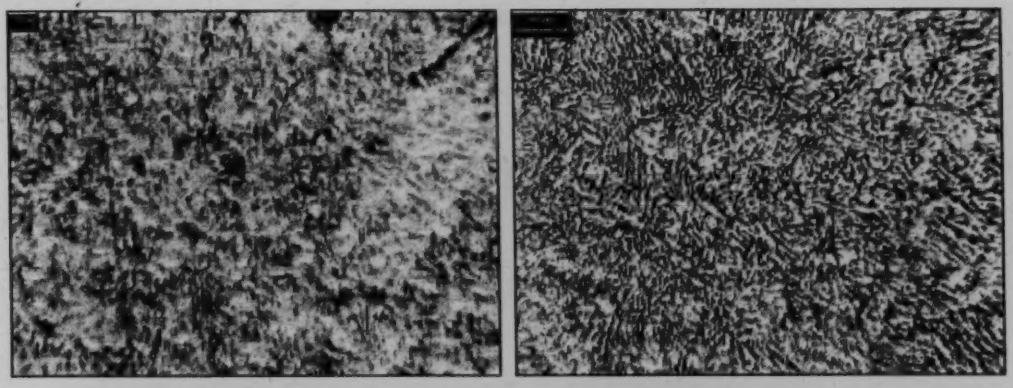

Fig. 5.7. – Microstructures of 4140 steel after Q&T heat treatment: T_A=860^{0}C/0.5 hr – T_T=500^{0}C/6.0 hrs (400x and 800x)

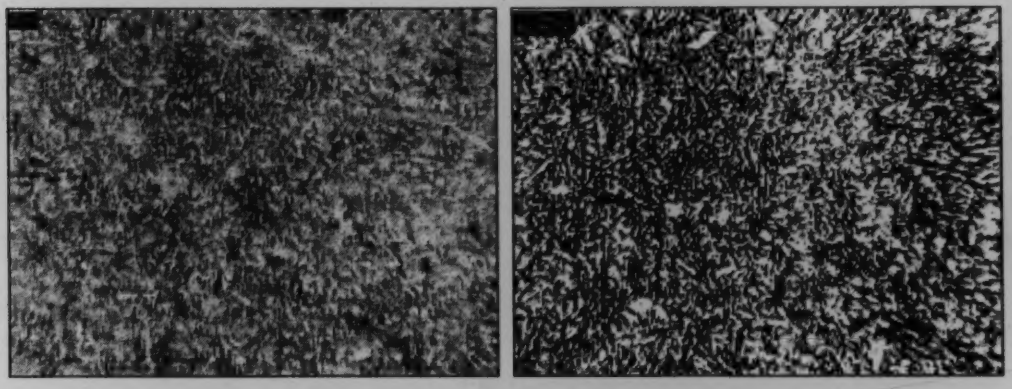

Fig. 5.8. – Microstructures of 4140 steel after Q&T heat treatment: T_A=860^{0}C/0.5 hr – T_T=500^{0}C/15.0 hrs (400x and 800x)

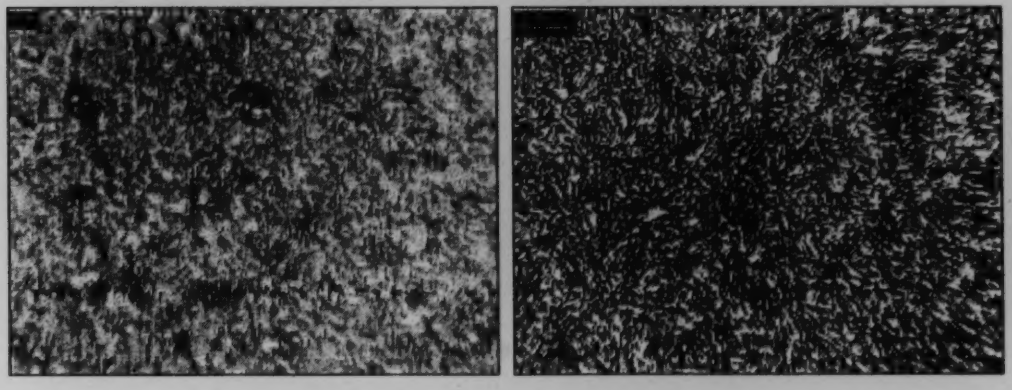

Fig. 5.9. – Microstructures of 4140 steel after Q&T heat treatment: T_A=860^{0}C/0.5 hr – T_T=500^{0}C/226 hrs (400x and 800x)

Tempering Parameters	Hardness HV 4140 steel	+/-	Avg
T_T=500^{0}C/6.0 hrs	376 – 361 – 374 – 356 – 363 – 369	20	367
T_T=500^{0}C/15.0 hrs	323 – 338 – 336 – 331 – 335 - 340	17	334
T_T=500^{0}C/226.0 hrs	307 – 323 – 311 – 304 – 322 - 323	19	315

Table 5.5 – Hardness measurements after Q&T at 500^{0}C for different holding times

The highest hardness value of 367 HV was obtained at the 500^{0}C for 6 hour holding time(comparing all other tempering parameters). Even the holding time of 226 hours resulted in the relatively high hardness level. The microstructure corresponding to the highest hardness value is close to the shape of a needle-like martensite (compared to the microstructures obtained at the same tempering temperature but for different tempering times). This clearly indicates that both a 500^{0}C tempering temperature and a 6-hour holding time are not sufficient enough to avoid formation of a hard and low toughness microstructure.

The following Fig.5.10. graphically illustrates the hardness changes compared to the as-received hardness of 4140 steel after different temperature – time parameters. Analyzing the curve of the hardness profile it can be concluded that the hardness values produced at the highest tempering temperatures of 650^{0}C and 600^{0}C (for just an hour holding time) gave the same hardness value of as-received 4140 steel. Since this steel was delivered in a Q&T condition, it may be assumed that the tempering temperature after a quenching was between 600^{0}C and 650^{0}C.

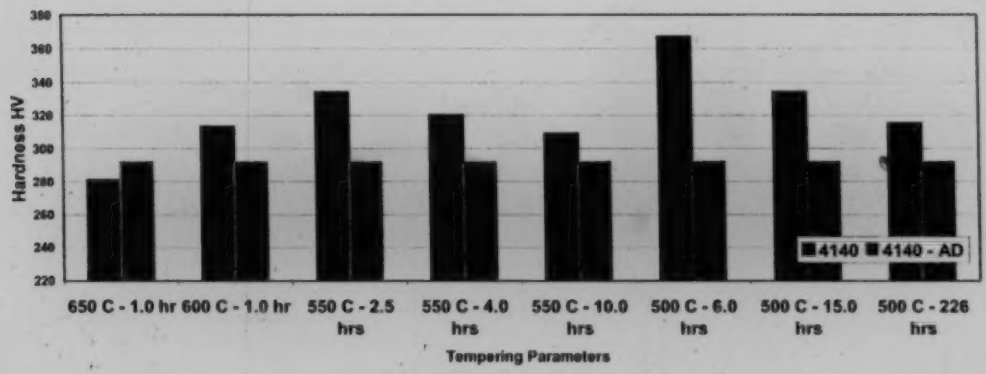

Fig. 5.10. - Hardness Profile of the 4140 steel after different Q&T treatments

Tempering temperatures bellow 650^0C and 600^0C such as 550^0C and 500^0C constantly produced higher hardness results with the shortest tempering times. It can be also seen that by applying some tempering parameters at lower tempering temperatures (550^0C/4.0 hrs and 500^0C/15.0 hrs) resulted in microstructures and hardness values similar to these obtained at the most common tempering temperatures of 650^0 and 600^0C.

CHAPTER 6

Microstructure and microhardness examinations of the 1043 weld zone after different PWHT's

The effect of different post-weld heat treatment (PWHT) parameters from the Table 3.6. in Chapter 3 on the microstructures and microhardness values of 1043 steel weld zone are examined and discussed in this chapter.

Both microstructures and microhardness results were taken from the each zone related to the welding process: the weld metal (WM), the heat-affected zone (HAZ) and the base metal (BM).

The welding procedures were the same for all eight samples of 1043 steel and PWHT's were performed immediately after welding where the heating and cooling rates were the same for all samples. Two PWHT's were carried out according to the most common code recommendations while 6 PWHT's were performed at lower temperatures.

6.1. Examinations of the 1043 weld zone after PWHT @ 650^{0}C – 1.0 hour

The results of microhardness measurement of all relevant weld zones are given in Table 6.1.

PWHT	Hardness HV	+/-	Avg
650^0C – 1.0 hr	1043 steel weld zones		
WM	195 – 182 – 190 – 184 – 169 – 184	25	184
HAZ – 1	188 - 212 - 194 – 170 – 165 - 159	42	181
HAZ – 2	178 – 204 – 212 – 224 – 183 – 168	56	195
HAZ – 3	187 – 195 – 191 – 176 – 172 – 163	32	181
BM	147 – 131 – 136 – 132 – 136 – 135	16	136

Table 6.1. – Hardness measurement results of 1043 weld zone after PWHT @ 650^0C/1.0 hr

The microstructures resulted after carrying out this PWHT parameters are presented in Fig. 6.1. The diagram of hardness profile of the HAZ of the weld zone is shown in Fig. 6.2.

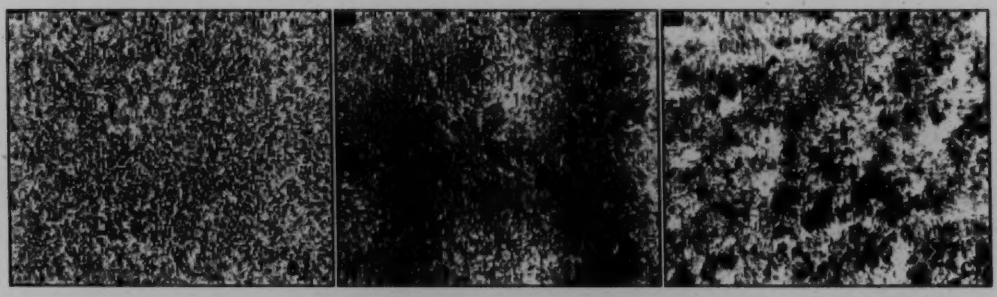

Fig. 6.1. – Microstructures of the 1043 weld zone after PWHT @ 650^0C – 1.0 hr (127x)
a) - WM
b) - HAZ
c) – BM

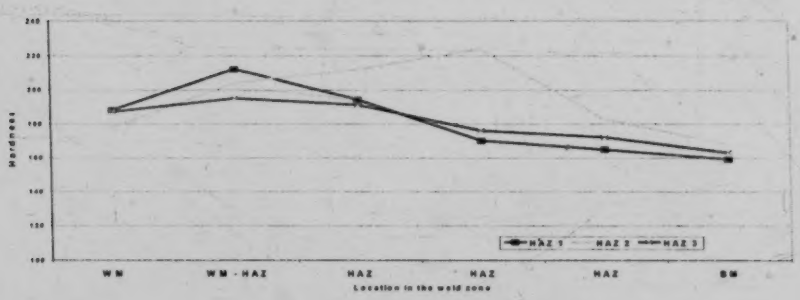

Fig. 6.2. - Hardness Profile of the 1043 HAZ after PWHT @ 650°C - 1.0 hr

The highest hardness value of 224 HV is measured in the HAZ while the lowest hardness values are taken from the BM, which is the "as received" HV 138. This indicates that this steel did not have any previous heat treatment.

The hardness of the WM of 184 HV is close to the hardness of normalized 1043 steel i.e. 211 HV (Table 3.2). The WM microstructure of 1043 steel welded with E 48010 electrode is directly influenced by the type of this electrode and is predominantly acicular ferrite. The HAZ microstructure indicates the transition zone between the acicular ferrite and coarse-grained heat affected zone CGHAZ as well as the presence of fine grained heat affected zone FGHAZ. Hardness measurements also confirm that the formation of martensite did not take the place in the HAZ and that the microstructure shows the presence of Widmansttäten ferrite, pearlite and polygonal ferrite. The BM microstructure consists of polygonal ferrite and pearlite.

6.2. Examinations of the 1043 weld zone after PWHT @ 600^{0}C – 1.0 hour

The microstructures formed after this PWHT are shown in the Fig. 6.3., the hardness profile of the weld zone in Fig. 6.4 and the hardness measurement results are given in Table 6.2.

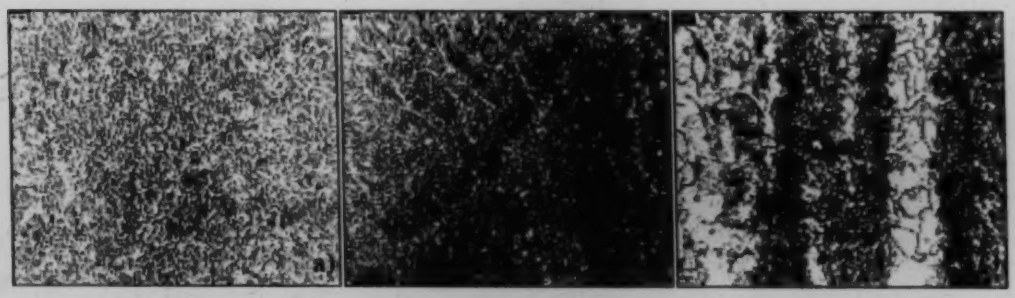

Fig. 6.3. – Microstructures of the 1043 weld zone after PWHT @ 600°C – 1.0 hr (127x)
a – WM b) – HAZ c) - BM

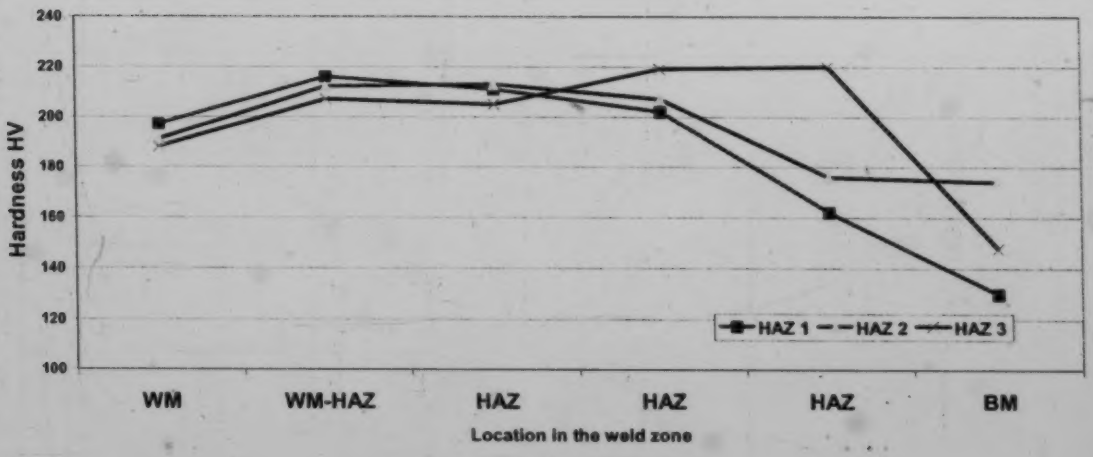

Fig. 6.4. - Hardness Profile of the 1043 HAZ after PWHT @ 600° C - 1.0 hr

PWHT 600^0C – 1.0 hr	Hardness HV 1043 steel weld zones	+/-	Avg
WM	188 – 185 – 196 – 178 – 173 – 194	21	186
HAZ – 1	197 – 216 – 211 – 202 – 162 – 130	86	186
HAZ – 2	191 – 212 – 213 – 207 – 176 – 174	38	196
HAZ – 3	188 – 207 – 205 – 219 – 220 – 149	71	198
BM	153 – 150 – 158 – 135 – 178 - 139	39	152

Table 6.2. – Hardness measurement results of 1043 weld zone after PWHT @ 600^0C/1.0 hr

Weld metal microstructure consists of acicular ferrite and grain boundary ferrite. The microstructure in the HAZ clearly shows regions of CGHAZ and FGHAZ. Also, the columnar grain growth occurred in the transition zone between the WM and HAZ. The microstructure constituents present in the HAZ are pearlite and Widmanstätten ferrite. Martensite does not seem to be present after this PWHT. The BM microstructure is composed of polygonal ferrite and pearlite.

The maximum hardness values in the welding zone are related to the HAZ but these values are only slightly higher than those of the WM. It is associated with the absence of as quenched martensite in the microstructure of the HAZ. The minimum hardness values are again measured for the BM.

6.3. Examinations of the 1043 weld zone after PWHT @ 550^{0}C – 2.5 hours

The microstructures of the WM, HAZ and WM formed after this PWHT are shown in Fig. 6.5. The hardness variations in the HAZ are given in Fig. 6.6. and hardness measurement results are given in Table 6.3.

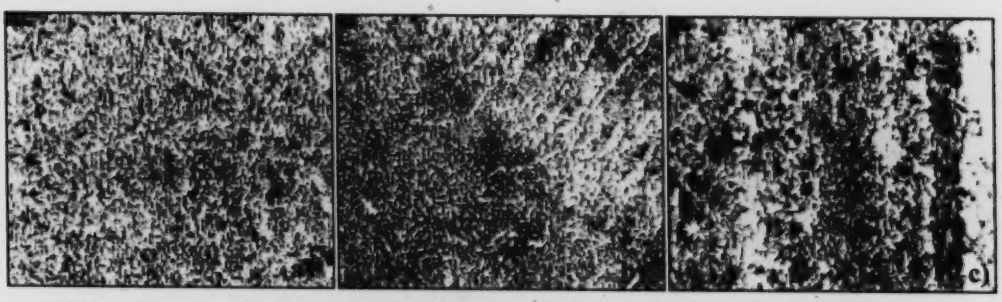

Fig. 6.5. – Microstructures of the 1043 weld zone after PWHT @ 550^{0}C – 2.5 hrs (127x)
a) – WM b) – HAZ c) – BM

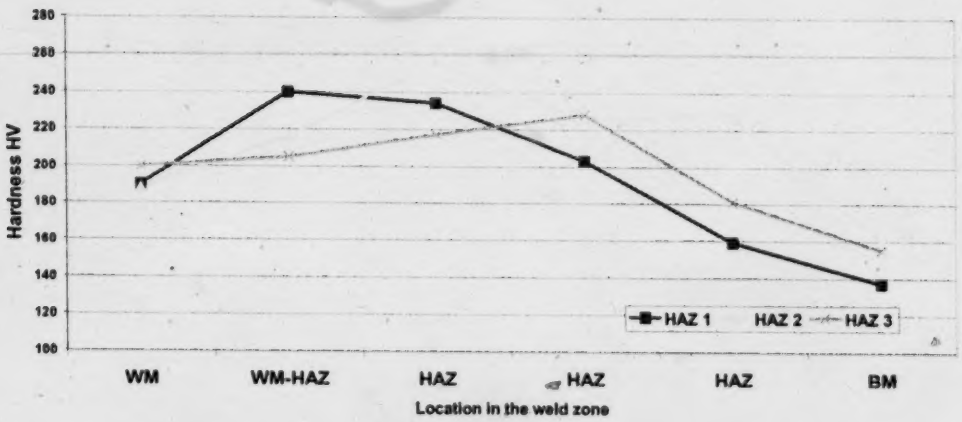

Fig. 6.6. - Hardness Profile of the 1043 HAZ after PWHT @ 550^0 C - 2.5 hrs

PWHT 550^{0}C – 2.5 hrs	Hardness HV 1043 steel weld zone	+/-	Avg
WM	196 – 193 – 166 – 193 – 193 – 207	41	191
HAZ – 1	190 – 240 – 234 – 203 – 160 – 137	90	194
IIAZ – 2	188 – 216 – 256 – 226 – 228 – 160	96	212
HAZ – 3	200 – 205 – 217 – 228 – 181 – 155	73	198
BM	144 – 149 – 178 – 165 – 180 - 149	56	161

Table 6.3. – Hardness measurement results of 1043 weld zone after PWHT @ 550^{0}C/ 2.5 hrs

The hardness values in the welding zone indicate the maximum hardness of 256 HV in the HAZ. This value is significantly higher than both WM and BM hardness. Although the increased hardness values in the HAZ, the HAZ microstructure does not reveal the presence of hard martensite microstructure. This microstructure shows CGHAZ and FGHAZ as well as the columnar grain growth in the HAZ adjacent to the fusion zone with the BM. The constituents of this microstructure are Widmansttäten ferrite and pearlite. The WM microstructure consists of acicular and polygonal ferrite while the BM microstructure consists polygonal ferrite and pearlite.

6.4 Examinations of the 1043 weld zone after PWHT @ 550^{0}C – 4.0 hours

The hardness measurements obtained after this PWHT are given in Table 6.4. The microstructures of the each region of the weld zone are shown in Fig.6.7 and the hardness variation across the HAZ is presented in Fig. 6.8.

PWHT 550^{0}C – 4.0 hrs	Hardness HV 1043 steel weld zone	+/-	Avg
WM	212 – 201 – 202 – 208 – 214 – 212	13	208
HAZ –1	209 – 220 – 219 – 208 – 218 - 160	60	206
HAZ – 2	180 – 207 – 211 – 174 – 152 – 140	71	177
HAZ – 3	206 – 205 – 216 – 218 – 215 – 186	30	208
BM	164 – 157 – 183 – 172 – 167 – 151	32	166

Table 6.4. – Hardness measurement results of 1043 weld zone after PWHT @ 550^{0}C/4.0 hrs

Fig. 6.7. – Microstructures of the 1043 weld zone after PWHT @ 550^{0}C – 4.0 hrs (127x)

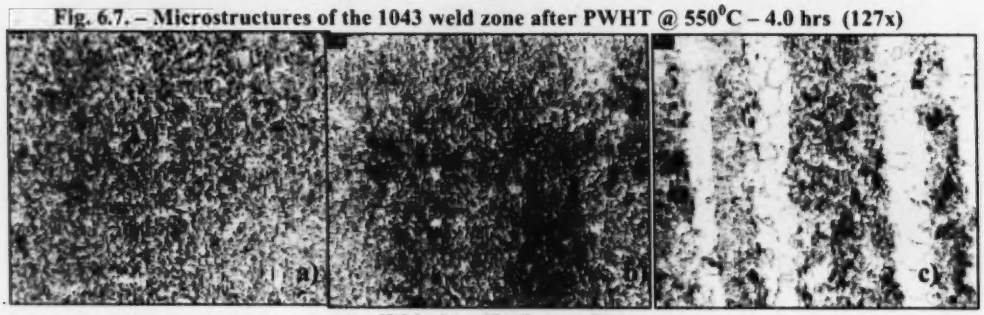

a) – WM b) – HAZ c) – BM

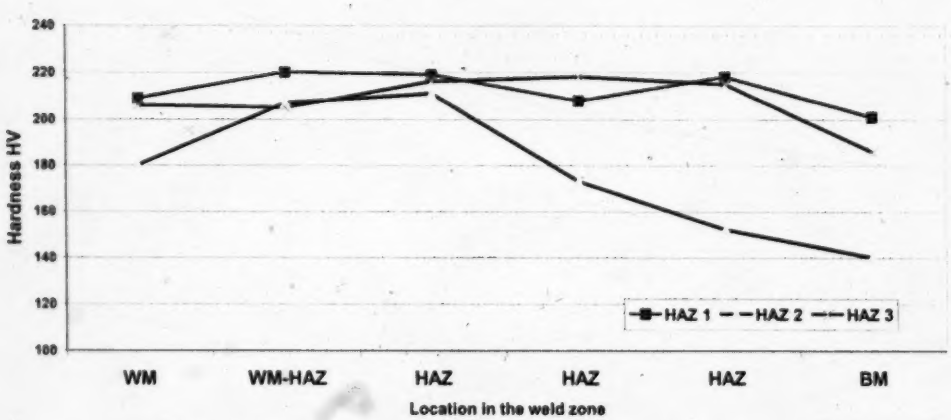

Fig. 6.8. - Hardness Profile of the 1043 HAZ after PWHT @ 550^{0}C - 4.0 hrs

The maximum hardness values are measured in the HAZ microstructure. The HAZ does not have any hard constituent and also there are not strictly emphasized the CGHAZ and FGHAZ regions. There are also very low hardness values in the HAZ, indicating very soft zones in regions close to the BM. The HAZ microstructure consists of pearlite, grain boundary ferrite and Widmansttäten ferrite; the WM microstructure consists of acicular and grain boundary ferrite while the BM is characterized with pearlite and polygonal ferrite. The micrograph of the BM shows the presence of the some form of spheroidized pearlite and polygonal ferrite.

6.5. Examinations of the 1043 weld zone after PWHT @ 550^{0}C – 10.0 hours

The hardness values measured after this PWHT are given in Table 6.5, micrographs of microstructure are shown in Fig. 6.9 while the hardness variation throughout the HAZ is given if Fig. 6.10.

PWHT 550^{0}C – 10.0 hrs	Hardness HV 1043 steel weld zone	+/-	Avg
WM	174 – 176 – 179 – 172 – 169 – 168	8	173
HAZ – 1	156 – 198 – 210 – 207 – 171 – 158	52	183
HAZ – 2	174 – 186 – 198 – 198 – 231 – 150	81	190
HAZ – 3	185 – 197 – 204 – 220 – 191 – 168	52	194
BM	159 – 114 – 145 – 132 – 131 – 132	45	136

Table 6.5. – Hardness measurement results of 1043 weld zone after PWHT @ 550^{0}C/10 hrs

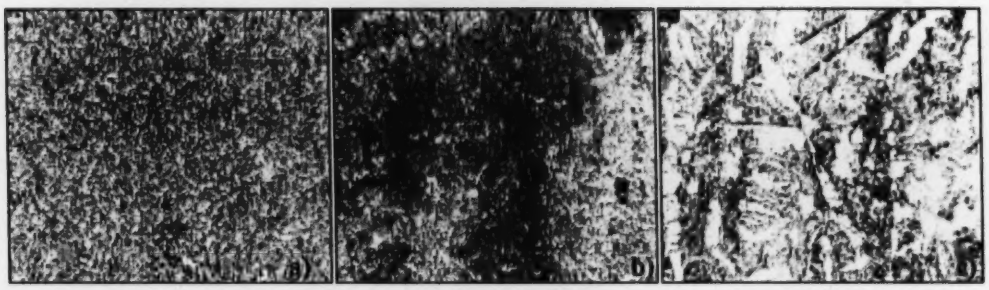

Fig. 6.9. – Microstructures of the 1043 weld zone after PWHT @ 550^{0}C – 10.0 hrs (127x)
a) – WM b) – HAZ c) – BM

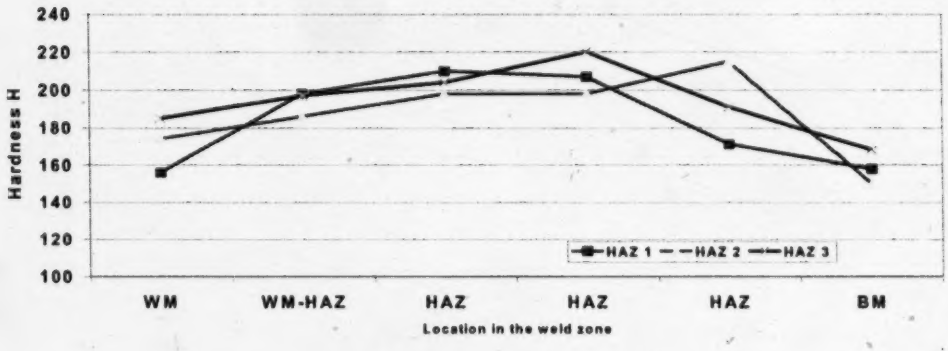

Fig. 6.10. - Hardness Profile of the1043 HAZ after PWHT @ 550^0 C - 10.0 hrs

The WM microstructure still consists of acicular ferrite even after this prolonged PWHT but also there are no visible hard constituents in the HAZ, which corresponds to results of lower hardness values in the HAZ that can be associated with the presence of pearlite and ferrite. The BM micrograph shows the

coarse-grained pearlite and polygonal ferrite and this microstructure is related to the lowest hardness values in the weld zone.

6.6. Examinations of the 1043 weld zone after PWHT @ 500^{0}C – 6.0 hours

The 500^{0}C was the lowest temperature at which three PWHT's were carried out with three different holding times.

The 500^{0}C – 6.0-hour set of parameters produced the hardness values presented in Table 6.6. Micrographs of the WM, HAZ and BM are shown in Fig. 6.11 and the hardness variation across the HAZ is illustrated in Fig. 6.12.

PWHT	Hardness HV	+/-	Avg
500^{0}C – 4.0 hrs	1043 steel weld zone		
WM	185 – 189 – 196 – 187 - 182 – 178	18	186
HAZ – 1	209 – 223 – 229 – 223 – 206 – 161	68	210
HAZ – 2	187 – 200 – 192 – 202 – 197 – 181	21	193
HAZ – 3	186 – 193 – 203 – 190 – 165 – 143	60	180
BM	141 – 164 – 120 – 129 – 166 – 137	46	143

Table 6.6. – Hardness measurement results of 1043 weld zone after PWHT @ 500^{0}C/6.0 hrs

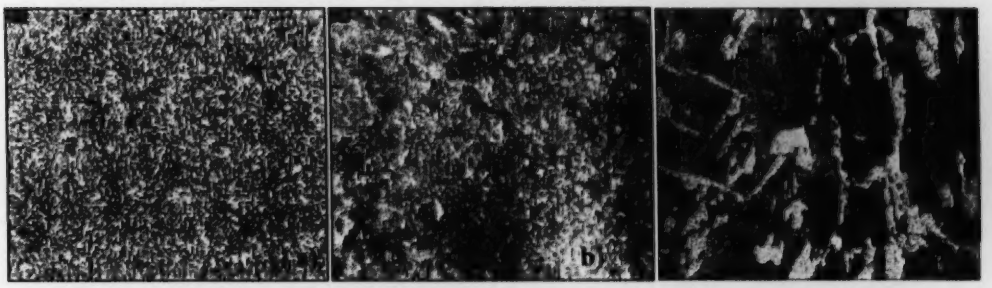

Fig. 6.11. – Microstructures of the 1043 weld zone after PWHT @ 500^{0}C – 6.0 hrs (127x)
a) – WM b) – HAZ c) - BM

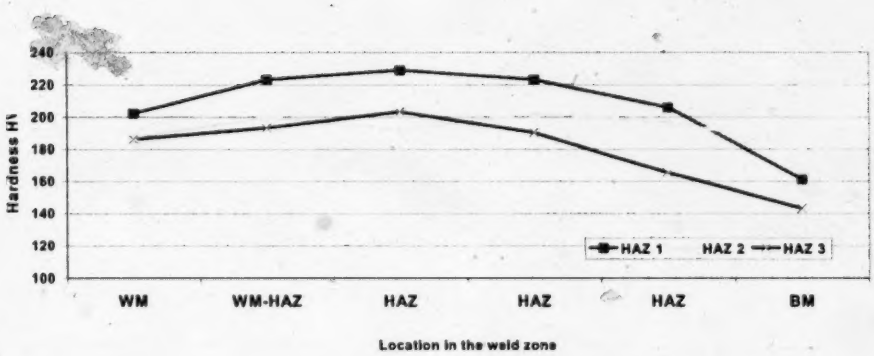

Fig. 6.12 - Hardness Profile of the 1043 HAZ after PWHT @ 500^0 C - 6.0 hrs

The shortest holding time of 6.0 hours at 500^{0}C produced the highest hardness value of 229 HV in the HAZ, which clearly shows both the CGHAZ and FGHAZ regions but without the formation of higher hardness constituents. The WM microstructure consists mostly of acicular ferrite and some polygonal ferrite.

The micrograph of the BM microstructure shows the coarsened pearlite and polygonal ferrite constituents.

6.7. Examinations of the 1043 weld zone after PWHT @ 500^{0}C – 15.0 hours

The microstructure constituents of WM, HAZ and WM are shown in Fig. 6.13, the hardness variation in the HAZ is present in Fig. 6.14. and the measured hardness levels are given in Table 6.7.

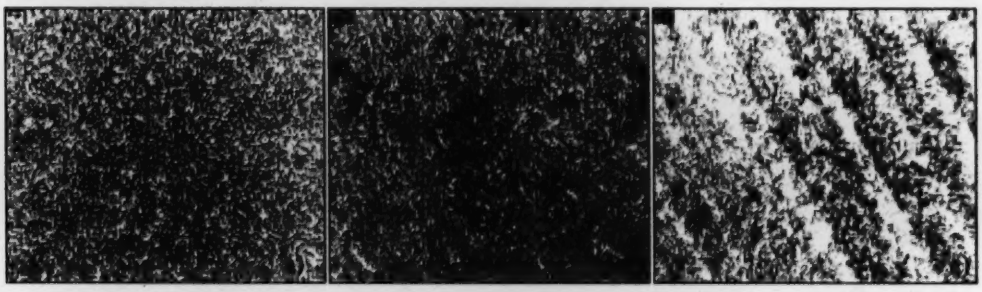

Fig. 6.13. – Microstructures of 1043 weld zone after PWHT @ 500^{0}C – 15.0 hrs (127x)
a) – WM b) – HAZ c) – BM

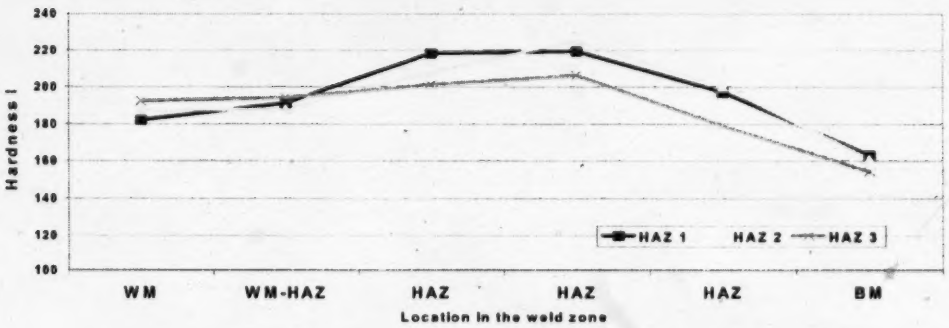

Fig. 6.14 - Hardness Profile of the 1043 HAZ after PWHT @ 500 C - 15.0 hrs

PWHT	Hardness HV	+/-	Avg
500^0C – 15.0 hrs	1043 steel weld zone		
WM	188 – 187 – 189 – 177 – 186 – 183	12	185
HAZ – 1	182 – 191 – 218 – 219 – 197 – 163	56	195
HAZ – 2	187 – 188 – 208 – 225 – 200 – 161	64	195
HAZ – 3	192 – 194 – 201 – 206 – 179 – 154	52	188
BM	178 – 161 – 176 – 154 – 144 – 172	34	164

Table 6.7. – Hardness measurement results of 1043 weld zone after PWHT @ 500^0C/15.0 hrs

The highest hardness value of 225 HV is measured in the HAZ and it confirms the absence of any hard constituents in the HAZ such as martensite or upper bainite. There is only a small difference in the grain size between CGHAZ and FGHAZ regions in the HAZ. The lowest hardness is produced in the BM, which is characterized by polygonal ferrite and pearlite microstructure constituents.

6.8. Examinations of the 1043 weld zone after PWHT @ 500^0C – 226.0 hours

This PWHT produced the hardness values in the weld zone given in Table 6.8. Micrographs of microstructure in the weld zone are shown in Fig. 6.15, and the hardness profile of the HAZ is presented in Fig. 6.16.

PWHT 500^{0}C – 226.0 hrs	Hardness HV 1043 steel weld zone	+/-	Avg
WM	172 – 177 – 171 – 188 – 182 – 175	17	176
HAZ – 1	187 – 197 – 217 – 216 – 178 – 140	77	189
HAZ – 2	174 – 169 – 184 – 187 – 165 – 147	40	171
HAZ – 3	169 – 174 – 184 – 187 – 165 – 147	40	171
BM	126 – 152 – 121 – 148 – 146 – 141	31	139

Table 6.8. – Hardness measurement results after PWHT @ 500^{0}C/226.0 hrs

Fig. 6.15. – Microstructures of the 1043 weld zone after PWHT @ 500^{0}C – 226.0 hrs (127x)
WM b) – HAZ c) – BM

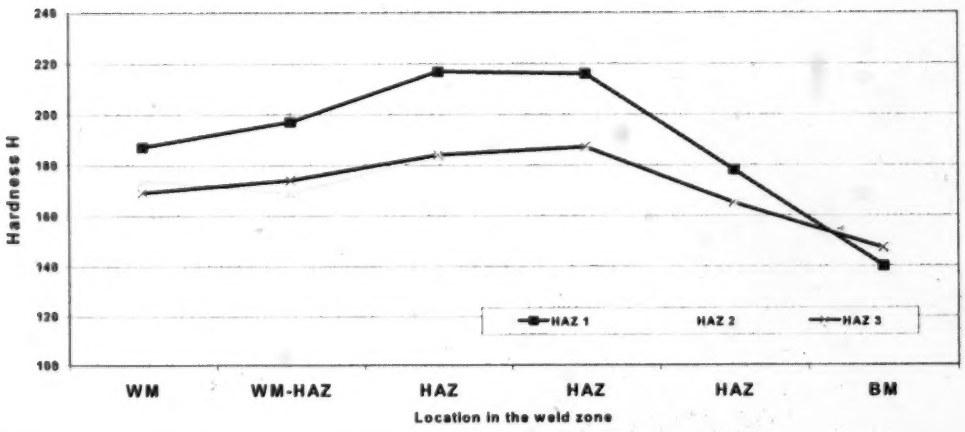

Fig. 6.16. - Hardness Profile of the 1043 HAZ after PWHT @ 500 C - 226 hrs

The hardness levels after this long holding time of post weld heat treatment produced a slight increase of the hardness level in the HAZ but with the maximum value of 218 HV. The HAZ microstructure consists of pearlite and polygonal ferrite while the BM microstructure is characterized with very large pearlite-ferrite grain size. The WM microstructure still consists fine-grained acicular ferrite.

6.9. Discussion of PWHT results of 1043 weldments

In order to compare the results of different PWHT parameters on microhardness results, Fig. 6.17, based on average hardness results, is plotted.

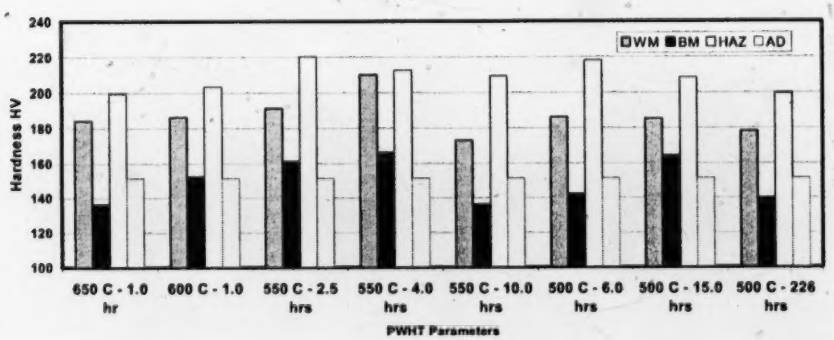

Fig. 6.17. - Hardness Profile of the 1043 weldments after different PWHTs

To analyze the results after different PWHT treatments, it is essential to establish the values of one PWHT, which is governed by most codes for C steels, and the PWHT @ 600^0C/1.0 hr is the most accepted one for further comparisons.

Both microhardness measurements and micrographs of the weld zone microstructures confirm the beneficial effects of performing this PWHT. It should be emphasized that the hardness measurement in the HAZ were taken at three different height levels to find out if any difference occurred among them. The maximum hardness value of 203 HV is measured in the HAZ and this value is very close to the hardness value of the WM of 186 HV with its acicular ferrite microstructure. After this PWHT, the formation of high or higher hardness constituents such as martensite or bainite is definitely avoided. The BM hardness value of 152 HV corresponds to the soft annealed pearlite-ferrite microstructure. If this 1043 steel were previously normalized, this hardness should be from 195 to 210 HV.

Overall hardness differences and variations throughout this 1043 weld zone from the WM, across the HAZ to the BM are very small and, generally, the smaller these hardness difference are, the more sound the welds are.

The second common PWHT set of parameters according to the codes of 650^0C/1.0 hr produced similar results to the PWHT @ 600^0C/1.0 hr. This tempering temperature is higher than 600^0C, and for the same holding times of one hour, it resulted in lower hardness values in all weld zone regions. Since the 650^0C temperature is close to A1 temperature, it produced the soft-annealed pearlite-ferrite microstructure of the BM with its hardness of only 136 HV, which is the lowest hardness value of the BM measured after all PWHT's. There is just a slight decrease in hardness values of both WM and HAZ of about 3-4 HV after this

PWHT, which is almost negligible. From the plotted diagrams of hardness profile in Fig. 6.2 and Fig. 6.4, it can be seen that there are some low hardness values in the HAZ after both PWHTs indicating the presence of soft zones in the intercritical HAZ. Also, there are slight differences between the hardness values among HAZ region itself with a trend of higher hardness results measured close to the weld surface. It is directly the result of multipass welding and its process of tempering by new weld of previously deposited weld.

These PWHTs at 650^0C and 600^0C for one hour confirm that the temperature is high enough and the hold time is long to produce beneficial metallurgical changes in the weld zone of 1043 steel.

The first lower temperature of PWHT, which is not regulated by any codes, was 550^0C with three different holding times: 2.5, 4.0 and 10.0 hours.

From the results of microstructural and microhardness examinations after the 550^0C/2.5 hour PWHT, it can be seen that the largest hardness value of 256 HV is measured in the HAZ region and also the average hardness level of 220 HV in the HAZ is the highest one measured after this PWHT. The hardness profile of the weld zone illustrates big differences and variation in hardness values throughout the weld zone. This PWHT also produced coarse-grained HAZ and it can be concluded that holding time of 2.5 hours is not long enough to accomplish all transformation processes in the weld zone.

The 550^0C/4.0 hour PWHT resulted in lower hardness values in all regions of the weld zone as well as the finer grain microstructures. The average HAZ hardness

value of 212 HV, the BM hardness of 166 HV and the WM hardness result of 210 HV are very close in values to the desirable PWHT @ 600^0C/1.0 hour. Also, the biggest difference between hardness values across the weld zone of 46 HV is little lower than that of 51 HV of the 600^0C/1.0 hour PWHT. The 550^0C temperature and a 4.0-hour holding – tempering time are parameters sufficient enough to achieve good microstructure results and hardness levels. Consequently, good mechanical properties of all weld zone regions are obtained.

The longest holding time of 10 hours at 550^0C also produced relatively low hardness value of the HAZ, but this long tempering time also produced the lowest WM and BM hardness values of all PWHTs making them very soft and ductile. This results in low strength properties of this weld zone. It can be concluded that the 10-hour holding time at 550^0C is definitely too long causing not only the decrease in hardness values, but also enlarged grain size of the BM what can be clearly seen from Fig. 6.9.c).

The PWHT temperature of 500^0C is certainly the lowest one for any metallurgical alterations in the weld zone and longer holding times of 6.0, 15.0 and 226 hours (based on Hollomon-Jaffe formula) are needed.

The 500^0C/6.0 hour PWHT produced the second highest hardness value of 229 HV in the HAZ comparing all others PWHT's. From the hardness results, it can be seen that the largest hardness variation among weld regions of 76 HV is present in the weld zone after this PWHT set of parameters. Neither is the tempering temperature high enough, nor is the holding time sufficiently long enough to

accomplish anticipated microstructural transformations and subsequent processes such as stress relaxation.

On the other hand, by extending the holding time to 15.0 hours at the same 500^0C, produced the hardness results that are almost identical to these of mostly recommended PWHT at 600^0C/1.0 hr or 650^0C/1.0 hour. The biggest hardness difference among the WM, HAZ and BM is 44 HV and it represents the most evenly distributed hardness values in the weld zone in comparison with other PWHTs. Also, microstructures of the weld regions show the smooth transitions from the WM microstructure to the HAZ microstructure and from the HAZ microstructure to the BM fine-grained microstructure.

Extending the holding time to 226 hours at 500^0C resulted in an expected low hardness value of the BM of 139 HV and low hardness value of WM of 178 HV. The HAZ hardness of 199 HV is identical to the HAZ hardness value of the 650^0C/1.0 hour PWHT. The low hardness value of the BM and its microstructure with very large grain size indicates poor strength properties of the weld zone overall. Decarburization was likely to take place considering this extremely long holding time.

The measurement results of hardness values of all samples, regardless on the PWHT parameters being used, generally show the highest hardness values in the HAZ in all samples, then in the WM and the lowest hardness values are measured in the BM. Although these highest hardness values measured in the HAZ usually indicate the presence of the formation of higher hardness constituent, the

occurrence of martensite or upper bainite is not visible. The HAZ microstructures differ from coarse-grained to fine grained with presence of soft microstructures in the intercritical region of the HAZ adjacent to the BM. These differences in the HAZ are more pronounced at lower temperatures and shorter holding times of PWHTs, particularly for 550^0C/2.5 hours and 500^0C/6.0 hours PWHTs. By extending the holding time even at lower temperatures, good results can be obtained with the results of recommended PWHTs. The most similar results to these of recommended PWHTs at 650^0C/1.0 hour and 600^0C/1.0 hour are achieved by performing PWHTs at 550^0C/4.0 hours and at 500^0C/15.0 hours.

6.10. Analysis and comparison of 1043 weld zone microstructures after different PWHTs

To emphasize effects of different PWHT parameters on formed microstructures, the following Fig. 6.18 shows all WM microstructures of the 1043 steel weld zone, Fig. 6.19 shows obtained HAZ microstructures and Fig. 6.20 illustrates BM microstructures formed after eight different PWHT processes.

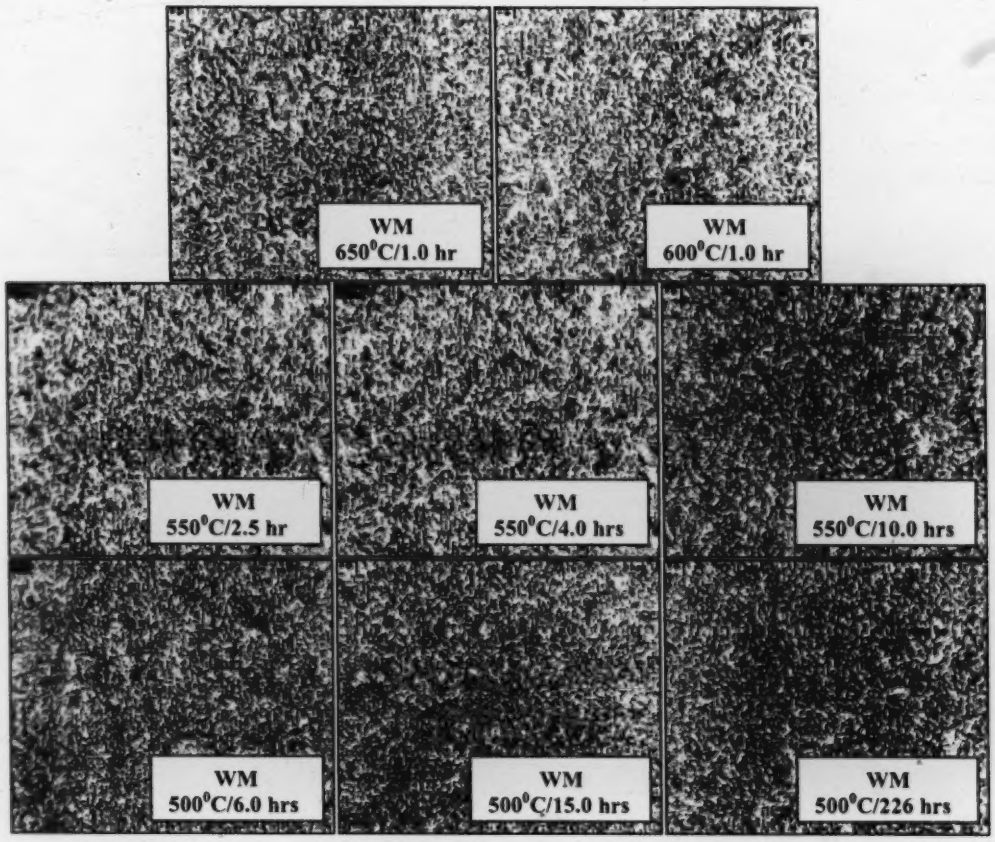

Fig. 6.18. – Microstructures of the WM of 1043 weld zone after different PWHTs (127x)

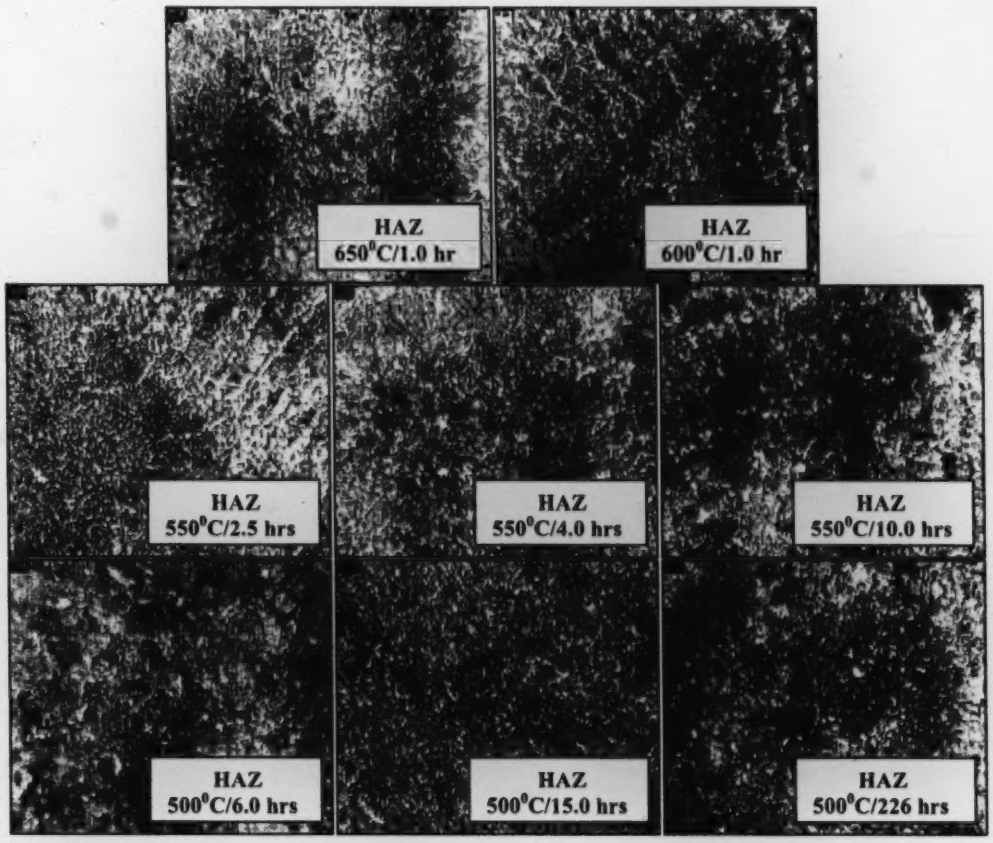

Fig. 6.19. – Microstructures of the HAZ of 1043 weld zone after different PWHTs (127x)

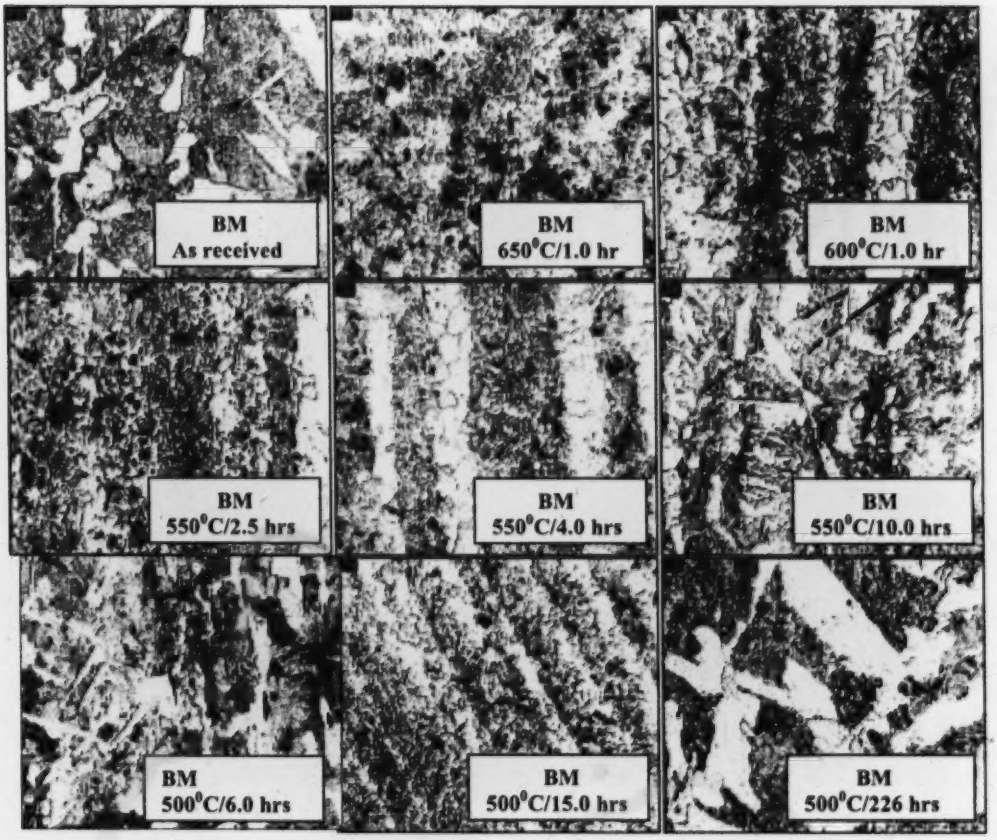

Fig. 6.20. – Microstructures of BM of 1043 weld zone after different PWHTs (127x)

From Fig. 6.18, where all obtained WM microstructures of 1043 steel after eight different PWHTs are shown, it can be concluded that the WM microstructures mainly contain acicular ferrite which is characterized with good strength and optimum toughness due to its small grain size and the way in which the plates of ferrite are dispersed in the microstructure. Consequently, it causes the plane of a cleavage crack to be frequently deflected. In contrast, the presence of allotriomorphic ferrite, parallel formation of Widmanstätten ferrite plates, or grain boundary nucleated sheaves of bainite is considered to be detrimental to the toughness of the weld, because these constituents allow cracks to propagate without much deflection. The problem is, in fact, more complicated, since it appears that there are instances when large amounts of acicular ferrite do not lead to the best toughness [Sugden, 1989]. Whatever the optimum microstructure, it is clear that a better understanding of the phases involved would permit more detailed investigation of the relationship with mechanical properties [Sugden, 1989].

All WM microstructures have regions of polygonal ferrite in a matrix of acicular ferrite. The amount of this ferrite can vary considerably, but in this case these differences are not so significant. Hardness testings, used to help characterized microstructures, just confirm that hardness values of the WM do not significantly oscillate, in fact, six of eight results are almost identical.

It can be also noted that the acicular ferrite is somewhat coarser after PWHTs performed at higher temperatures of 650^0C and 600^0C. It is well established that

acicular ferrite nucleates at nonmetallic inclusions, which occur frequently in arc-weld deposits, but its mechanism of growth has not been clear and still has been the cause of much research.

The HAZ microstructures of the medium-carbon 1043 steel, shown in Fig. 6.19, are all characterized with a coarse grained HAZ between the fusion zone and fine-grained HAZ. The HAZ microstructures in this type of steel are governed by the steel chemistry ant the thermal cycle experienced. The thermal cycle at any point in the HAZ is highly dependent on the heat input and the distance from the fusion boundary. As this distance increases, the peak temperature and cooling rate through the transformation range are reduced, giving progressively softer microstructures. The additional PWHT can only contribute the formation of these softer microstructural constituents.

Martensite, which is hard and usually of poor toughness and can give rise to HAZ hydrogen cracking, is not found in any of eight HAZ microstructures.

The principal microstructural constituent is intragranular Widmanstätten ferrite, which resembles acicular ferrite commonly found in weld metal. Widmanstätten ferrite forms at higher transformation temperatures, and is favored by the slower cooling rates associated with high heat input. Ferrite with martensite/austenite/carbides (M-A-C) is generally the dominant microstructural constituent and this ferrite with M-A-C can have an aligned AC, or non-aligned FN appearance, but this variation is probably largely a sectioning effect and is beyond the scope of this current project. The HAZ microstructures obtained at shorter

holding times at considered temperatures (550^0C/2.5 hours and 500^0C/6.0 hours) are coarser and hardness test results of the HAZ are in agreement and higher after these PWHTs. Also, the longest holding time of 226 hours produced the HAZ microstructure with a high proportion of coarse rextallized ferrite and pearlite. The BM microstructures are affected after performed PWHT's, although the maximum temperature in this part of the weld zone is less than Ac_1. As-received pearlite-ferrite microstructure of the BM was altered in a way that spherodization of pearlite took place as well as changes in the grain size having the largest ones resulted after the longest holding times.

Considering the weld zone as the assembly of the WM, HAZ and BM, and obtained microstructures and hardness values, it is evident that PWHT at lower temperatures of 550^0C and 500^0C can be satisfactorily undertaken. The good results are achieved after the PWHT @ 550^0C-4.0 hours and 500^0C-15.0 hours stating that good relationships between the tempering temperature and holding times are obtained. The PWHTs based on the Hollomon-Jaffe parameter, characterized with the longest holding times, resulted in lower hardness values and usually in lower strength properties of the weld zone as a whole. Also, the formed microstructures of each part of the weld zone after these PWHTs can only assume that the toughness is poorer than that resulted after other PWHTs.

CHAPTER 7

Microstructure and microhardness examinations of the 4140 weld zone after different PWHTs

The 4140 welded species were post weld heat treated at eight different temperature-time parameters. Microstructure and microhardness examinations of the weld zone as well as a discussion of the results are presented in this Chapter. Micrographs and hardness measurements were taken from the zones most interesting in welding: the WM, HAZ and BM.

The welding of 4140 steel samples was done with the same welding procedure according to the Table 3.4. while PWHT's were carried out immediately after welding. PWHT's were performed at the temperatures recommended by the most codes and at lower temperatures than these of recommended, but at extended times.

7.1 Examinations of the 4140 weld zone after PWHT @ 650^{0}C – 1.0 hour

The values of microhardness measurements of all regions in the weld zone after this PWHT are presented in Table 7.1. Resulting weld zone microstructures are shown in Fig. 7.1 while hardness variations of the HAZ are plotted in Fig. 7.2.

PWHT 650^0C – 1.0 hr	Hardness HV 4140 steel weld zones	+/-	Avg
WM	278 – 275 – 278 – 288 – 278 – 281	13	280
HAZ – 1	264 – 294 – 302 – 281 – 271 – 243	59	276
HAZ – 2	275 – 268 – 283 – 298 – 264 – 223	72	269
HAZ – 3	268 – 291 – 280 – 316 – 264 – 233	83	275
BM	291 – 250 – 240 – 230 – 288 - 233	58	255

Table 7.1. – Hardness measurement results of 4140 weld zone after PWHT @ 650^0C/1.0 hr

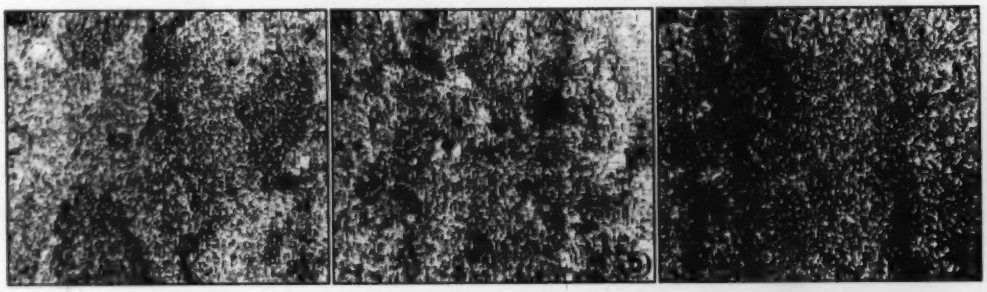

Fig. 7.1. – Microstructures of 4140 weld zone after PWHT @ 650^0C/1.0 hr (127x)
a) – WM b) – HAZ c) – BM

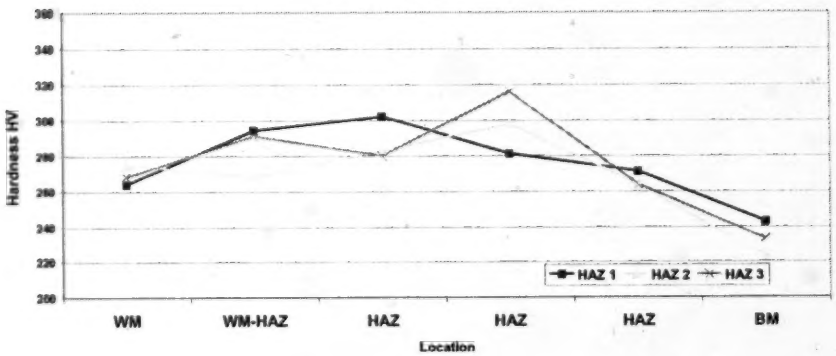

Fig. 7.2. - Hardness Profile of the 4140 HAZ after PWHT @ 650 C - 1.0 hr

It can be seen from the Table 7.1 and Fig. 7.2 that the highest hardness value of 316 HV is measured in the HAZ, but this hardness result is only slightly higher than the hardness value of as-received heat treated 4140 steel of 291 HV. The BM hardness of 255 HV is lower due to the fact that tempering was carried out at 650^0C on the previously quenched and tempered BM. The WM hardness value of 280 HV is higher than the BM hardness and this hardness, as well as the microstructure, is directly related to the composition of the filler material used for welding. The hardness profile also indicates the soft zone in the HAZ adjacent to the BM.

The WM microstructure consists of ultrafine acicular ferrite. The HAZ macrograph shows both CGHAZ and FGHAZ confirming that the HAZ was undergoing a range of temperatures that affects microstructure from reaustenitization, transformation or tempering. The HAZ microstructure is composed of bainite plus ferrite at the prior austenite grain boundaries with the maximum hardness value of 312 HV.

The BM microstructure consists of tempered martensite. It should be emphasized that this microstructure is, in fact, the result of double tempering process knowing that the BM was previously quenched and tempered, then welded and then again tempered at 650^0C/1.0 hour. This resulted in lower hardness values of the BM of 255 HV.

7.2. Examinations of the 4140 weld zone after PWHT @ 600^{0}C – 1.0 hour

This PWHT resulted in hardness values given in Table 7.2, microstructures shown in Fig. 7.3 and hardness profile plotted in Fig. 7.4.

PWHT 600^{0}C – 1.0 hour	Hardness HV 4140 steel weld zones	+/-	Avg
WM	328 – 314 – 314 – 325 – 283 – 313	45	313
HAZ – 1	327 – 333 – 353 – 349 – 297 – 267	86	321
HAZ – 2	307 – 323 – 323 – 305 – 296 – 282	31	306
HAZ – 3	302 – 305 – 295 – 291 – 336 – 257	79	298
BM	256 – 250 – 257 – 259 – 269 - 263	19	259

Table 7.2. – Hardness measurement results of 4140 weld zone after PWHT @ 600^{0}C/1.0 hr

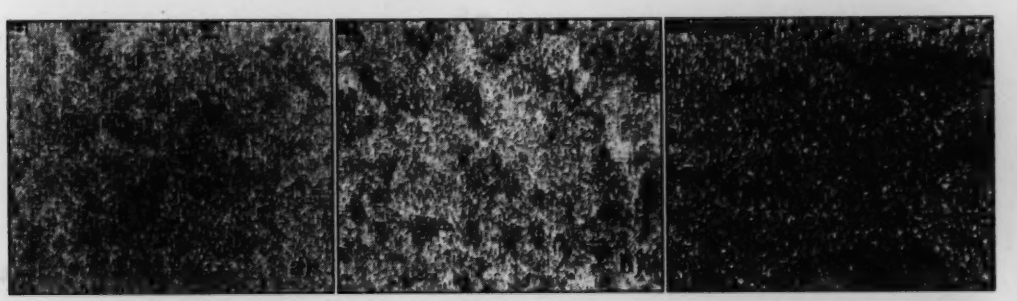

Fig. 7.3. – Microstructures of 4140 weld zone after PWHT @ 600^{0}C/1.0 hr (127x)
a) – WM b) – HAZ c) – BM

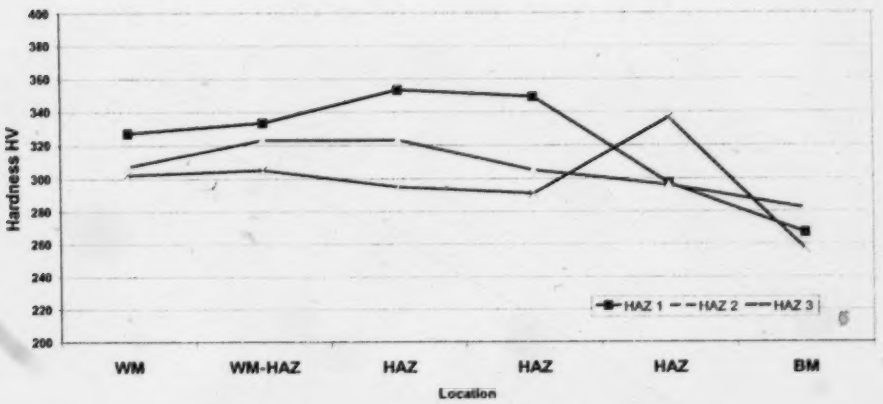

Fig. 7.4. - Hardness Profile of the 4140 HAZ after PWHT @ 600 C - 1.0 hr

From three height levels in the HAZ where hardness measurements were taken, it is evident that the hardness values in the HAZ close to the top of the weld has increased hardness in comparison to the HAZ hardness in the middle and at the bottom of the weld. Basically, these hardness values are close or even lower than those of the WM hardness values, which can only confirm the absence of hard and brittle microstructure constituents. The WM microstructure is composed of acicular ferrite. The CGHAZ and FGHAZ are visible on the HAZ micrograph but no martensite is present. TheCGHAZ, adjacent to the fusion zone, is characterized with columnar region due to epitaxial grain growth effect, while fine-grained zone is partially transformed zone in the HAZ region. The main constituents in the HAZ region are coarse and fine bainite and Widmanstätten ferrite while the BM microstructure consists of tempered martensite.

7.3. Examinations of the 4140 weld zone after PWHT @ 550^{0}C – 2.5 hours

Hardness values obtained after this PWHT are present in Table 7.3, microstructures of the weld zone are shown in Fig. 7.5 and hardness variations of the HAZ are illustrated in Fig. 7.6.

PWHT 550^{0}C – 2.5 hours	Hardness HV 4140 steel weld zones	+/-	Avg
WM	267 – 308 – 300 – 291 – 303 – 300	41	295
HAZ – 1	307 – 350 – 377 – 331 – 391 – 385	70	357
HAZ –2	302 – 304 – 356 – 336 – 356 – 328	54	330
HAZ – 3	299 – 278 – 318 – 315 – 289 – 257	61	293
BM	271 – 318 – 241 – 272 – 282 – 268	47	275

Table 7.3. – Hardness measurement results of 4140 weld zone after PWHT @ 550^{0}C/2.5 hrs

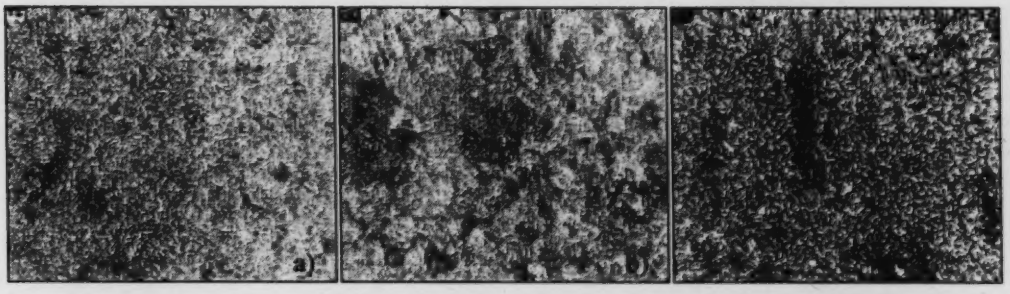

Fig. 7.5. – Microstructures of 4140 weld zone after PWHT @ 550^{0}C/2.5 hrs (127x)
a) – WM b) – HAZ c) – BM

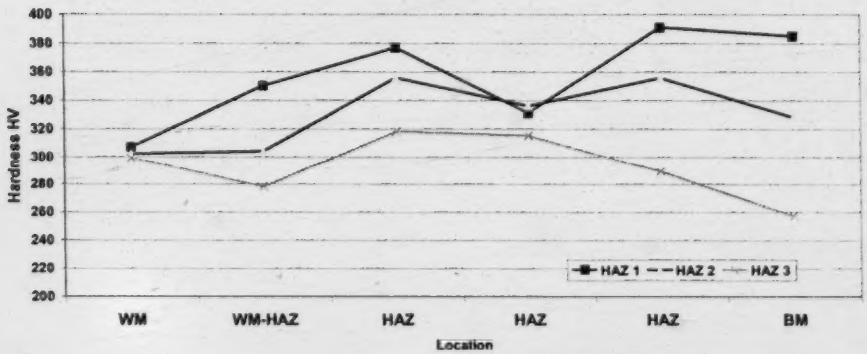

Fig. 7.6. - Hardness Profile of the 4140 HAZ after PWHT @ 550 C - 2.5 hrs

The largest hardness value of 391 HV is measured in the upper HAZ, but also hardness values of the medium and lower HAZ are higher than the hardness values of the BM of 275 HV and WM of 295 HV. The hardness profile across the weld zone indicates also unevenly distribution of hardness value with steep increase and decrease of these values. The higher hardness of the HAZ is still even in the transition zone between the HAZ and the BM. The microstructure of the HAZ is comprised of very coarse grains of upper adjacent to the fusion zone and grains are finer toward the BM. The main structure constituents are upper and lower bainite, pearlite and some islands of ferrite. The WM microstructure consists of acicular ferrite and the BM consists tempered martensite.

7.4. Examinations of the 4140 weld zone after PWHT @ 550^{0}C – 4.0 hours

The hardness results obtained after this PWHT are given in Table 7.4, the microstructures of the weld zone are shown in Fig. 7.7 and the hardness variations throughout the HAZ zone is illustrated in Fig. 7.8.

PWHT 550^{0}C – 4.0 hours	Hardness HV 4140 steel weld zones	+/-	Avg
WM	270 – 266 – 276 – 273 – 279 – 271	13	273
HAZ – 1	291 – 306 – 328 – 313 – 319 – 270	58	305
HAZ – 2	285 – 265 – 336 – 328 – 281 – 247	78	290
HAZ – 3	279 – 286 – 287 – 284 – 302 – 249	53	281
BM	304 – 244 – 296 – 262 – 300 - 235	50	274

Table 7.4. – Hardness measurement result of 4140 weld zone after PWHT @ 550^{0}C/4.0 hrs

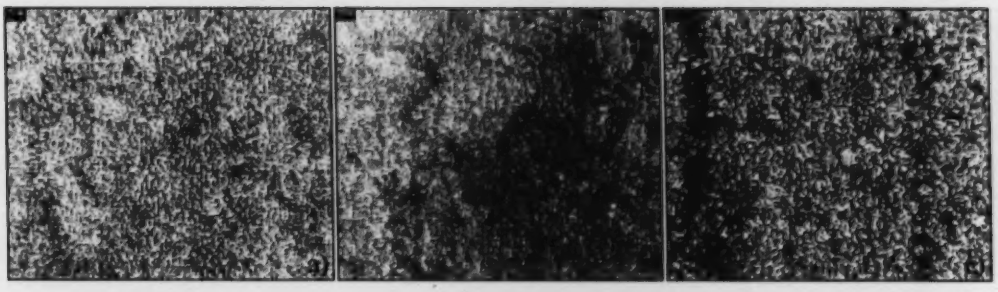

Fig. 7.7. – Microstructures of 4140 weld zone after PWHT @ 550^{0}C/4.0 hrs (127x)
a) – WM b) – HAZ c) – BM

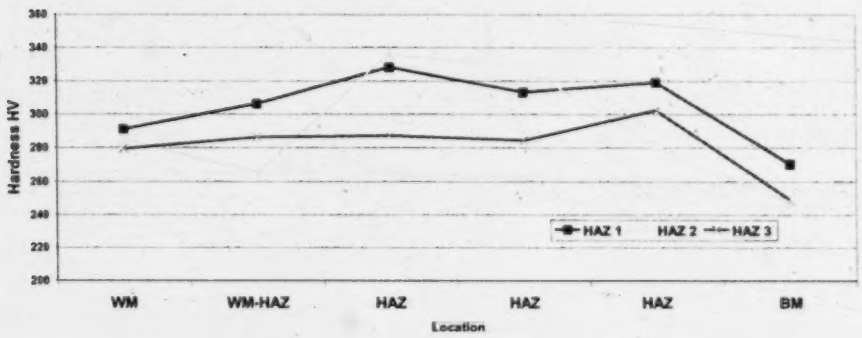

Fig. 7.8. - Hardness Profile of the 4140 HAZ after PWHT @ 550 C - 4.0 hrs

The highest hardness value of 336 HV is again associated with the HAZ but this value does not indicate a presence of hard microstructures. The most interesting fact is that the hardnesses of both WM and BM are almost identical at 273 HV and 274 HV, respectively, although the WM microstructure is comprised of acicular ferrite while the BM microstructure consists of tempered martensite and ferrite. There are visible coarser and finer grains in the HAZ but they are not significantly

different as well as theirs hardness values. The formed HAZ microstructure is a mix of bainite and pearlite.

7.5. Examinations of the 4140 weld zone after PWHT @ 550^{0}C – 10.0 hours

The hardness values measured after this PWHT are given in Table 7.5, micrographs of microstructures of the weld zone are shown in Fig. 7.9 and the hardness variation is presented in Fig.7.10.

PWHT	Hardness HV	+/-	Avg
550^{0}C – 10.0 hours	4140 steel weld zones		
WM	293 – 286 – 278 – 267 – 295 – 275	33	282
HAZ –1	289 – 290 – 304 – 320 – 323 – 279	44	285
HAZ – 2	274 – 290 – 325 – 299 – 259 – 247	66	282
HAZ – 3	300 – 302 – 305 – 320 – 334 – 263	57	304
BM	233 – 229 – 236 – 229 – 236 - 237	8	233

Table 7.5. – Hardness measurement results of 4140 weld zone after PWHT @ 550^{0}C/10.0 hrs

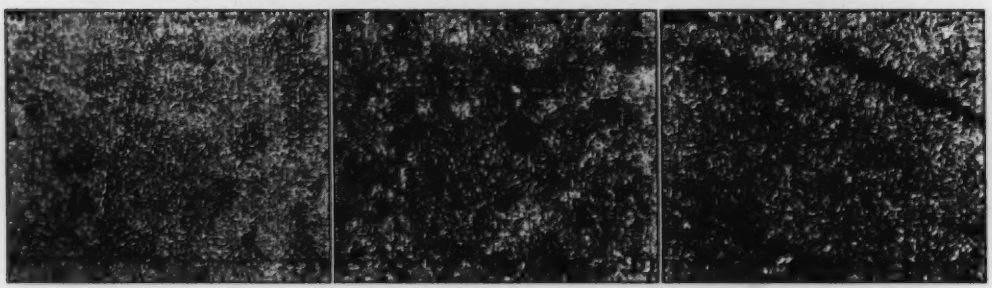

Fig. 7.9. – Microstructures of 4140 weld zone after PWHT @ 550^{0}C/10.0 hrs (127x)
a) – WM b) – HAZ c) – BM

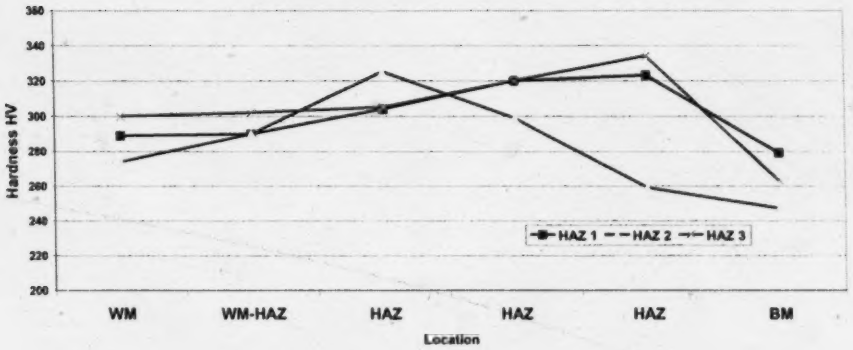

Fig. 7.10. - Hardness Profile of the 4140 HAZ after PWHT @ 550 C - 10.0 hrs

This PWHT, with its longest holding time of 10.0 hours at 550^0C, resulted in lowering the hardness value of the BM to 233 HV and the maximum hardness value of 334 HV measured in the HAZ. The hardness levels of the upper, middle and bottom HAZ are higher than the hardness of the BM even after this extended holding time. All hardness measurements could not indicate hard microstructure constituents in the weld zone. The WM microstructure consists of acicular ferrite, the HAZ still has coarse and fine grained regions with a mix of bainite and pearlite. The BM is comprised of tempered martensite with a small presence of pearlite and ferrite.

7.6. Examinations of the 4140 weld zone after PWHT @ 500^0C – 6.0 hours

The shortest holding time of 6.0 hours at the lowest PWHT temperature of 500^0C produced the hardness levels of the weld zone presented in Table 7.6. The resulting

microstructures of the weld zone are shown in Fig. 7.11, and the hardness profile of the HAZ is plotted in Fig. 7.12.

PWHT 500^{0}C – 6.0 hours	Hardness HV 4140 steel weld zones	+/-	Avg
WM	322 – 315 – 308 – 293 – 302 – 316	29	309
HAZ – 1	330 – 344 – 369 – 384 – 365 – 320	64	352
HAZ – 2	313 – 325 – 330 – 344 – 354 – 299	55	322
HAZ – 3	309 – 335 – 341 – 339 – 326 – 286	43	320
BM	259 – 262 – 237 – 253 – 260 – 267	30	256

Table 7.6. – Hardness measurement results of 4140 weld zone after PWHT @ 500^{0}C/6.0 hrs

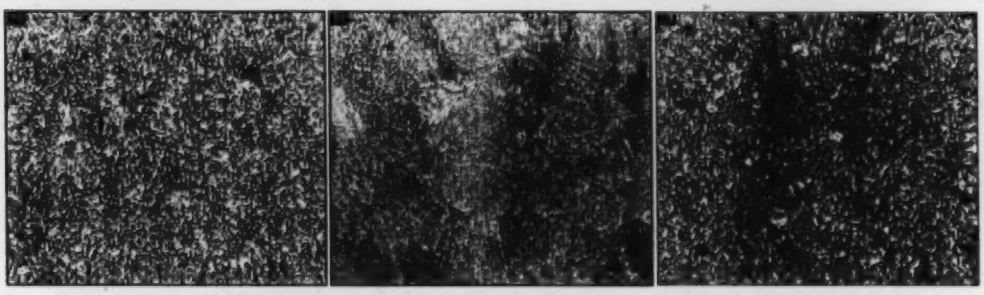

Fig. 7.11. – Microstructures of 4140 weld zone after PWHT @ 500^{0}C/6.0 hrs (127x)
a) – WM b) – HAZ c) – BM

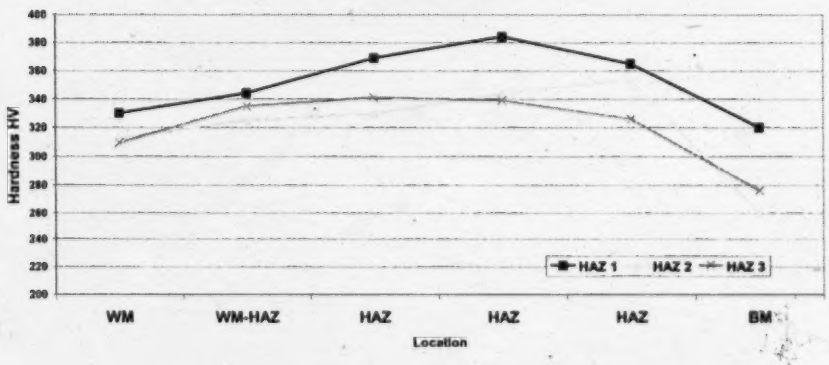

Fig. 7.12. - Hardness Profile of the 4140 HAZ after PWHT @ 500 C - 6.0 hrs

The highest hardness level of 384 HV in the HAZ is the highest level measured from all PWHTs carried out. The hardness values of the upper, middle and bottom HAZ are all higher than the hardness of the WM of 309 HV and this increased hardness can be associated with coarse ferritic structure and it is likely due to secondary carbide precipitation, possibly from Mo. This microstructure contains tempered bainite with cementite precipitates. The WM microstructure is comprised of acicular ferrite and the BM microstructure consists tempered martensite and ferrite.

7.7. Examinations of the 4140 weld zone after PWHT @ 500^{0}C – 15.0 hours

This PWHT resulted in hardness values given in Table 7.7, obtained microstructures are shown in Fig. 7.13 and the hardness profile across the HAZ is illustrated in Fig. 7.14.

PWHT 500^{0}C – 15.0 hours	Hardness HV 4140 steel weld zones	+/-	Avg
WM	291 – 301 – 300 – 293 – 312 – 314	23	302
HAZ – 1	315 – 326 – 339 – 340 – 332 – 297	43	325
HAZ – 2	307 – 287 – 299 – 333 – 322 – 283	46	305
HAZ – 3	296 – 309 – 307 – 303 – 281 – 273	26	295
BM	264 – 305 – 290 – 266 – 318 - 255	50	283

Table 7.7. – Hardness measurement results of 4140 weld zone after PWHT @ 500^{0}C/15.0 hrs

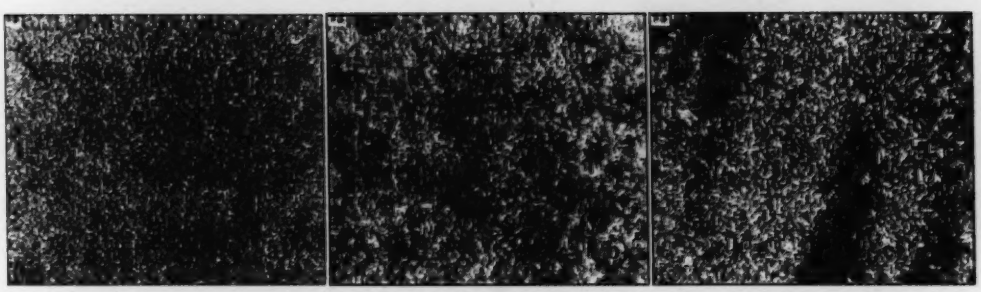

Fig. 7.13. – Microstructures of 4140 weld zone after PWHT @ 500^{0}C/15.0 hrs (127x)
a) – WM b) – HAZ c) – BM

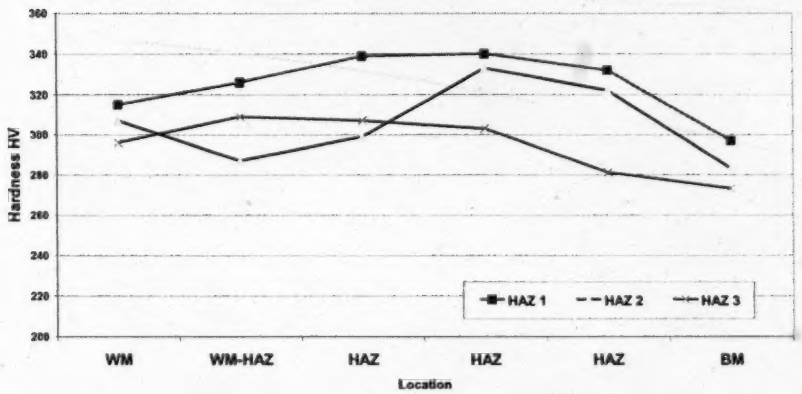

Fig. 7.14. - Hardness Profile of the 4140 HAZ after PWHT @ 500 C - 15.0 hrs

The hardness variation among these weld zones indicates the highest hardness levels in the upper HAZ while the medium and lower HAZ have hardness levels that are very close to the hardness values of both WM and BM. The maximum hardness value of 339 HV in the upper HAZ also is not too high to cause a big

concern regarding a presence of unfavorable HAZ microconstituents. The BM hardness measurement of 283 HV is almost identical to the as-received BM hardness value of 291 HV. The developed microstructure of the WM is acicular ferrite, the tempered bainite is formed in the HAZ while the BM microstructure is a composite structure of tempered martensite and ferrite.

7.8. Examinations of the 4140 weld zone after PWHT @ 500^{0}C – 226.0 hours

The hardness values through the cross section of the weld zone are given in Table 7.8, micrographs of each region are shown in Fig. 7.15. and the hardness distribution in Fig. 7.16.

PWHT 500^{0}C – 226.0 hours	Hardness HV 4140 steel weld zones	+/-	Avg
WM	280 – 287 – 290 – 286 – 283 – 288	10	286
HAZ – 1	280 – 305 – 336 – 331 – 281 – 267	64	300
HAZ – 2	293 – 309 – 309 – 296 – 311 – 299	18	303
HAZ – 3	281 – 289 – 297 – 304 – 317 – 255	49	291
BM	242 – 235 – 248 – 236 – 249 - 246	14	243

Table 7.8. – Hardness measurement results of 4140 weld zone after PWHT @ 500^{0}C/226.0 hrs

Fig. 7.15. – Microstructures of 4140 weld zone after PWHT @ 500^{0}C/226 hrs (127x)
a) – WM b) – HAZ c) – BM

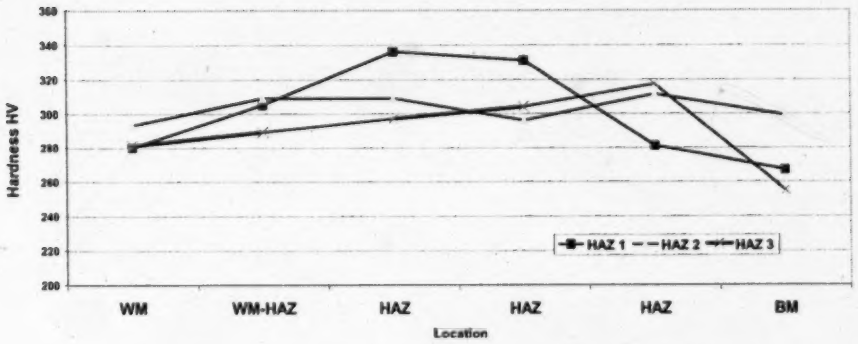

Fig. 7.16. - Hardness Profile of the 4140 HAZafter PWHT @ 500 C - 226 hrs

The highest hardness values were measured in the upper HAZ and even after this extremely long holding time of 226 hours resulted in the HAZ hardness values higher than the WM hardness of 286 HV. The BM hardness result of 243 HV is the second lowest hardness obtained after this PWHT. The microstructure of the WM consists of fine acicular ferrite; the HAZ microstructure is composed of reheated

bainite while the BM microstructure is comprised of reheated tempered martensite and ferrite.

7.9. Discussion of PWHT results of 4140 weldments

The graphic distribution of the hardness values through the cross weld zone of 4140 steel after eight different PWHT, based on average values, is illustrated in Fig. 7.17.

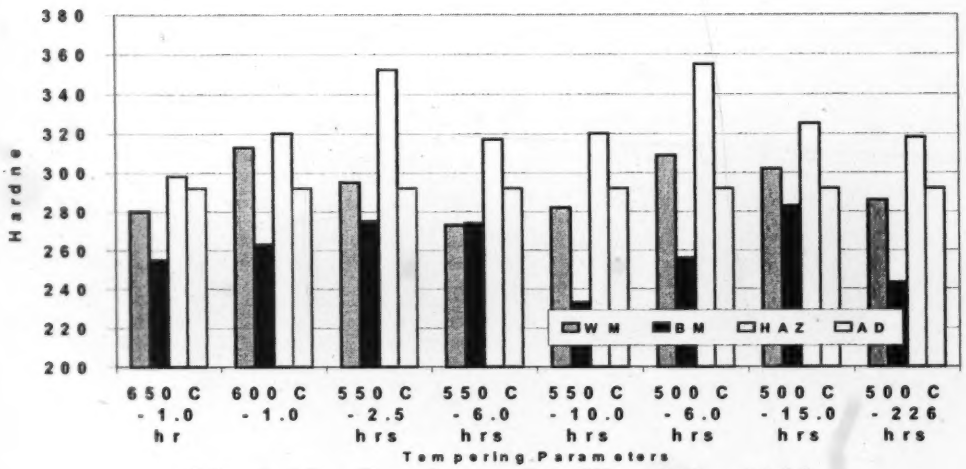

Fig. 7.17 - Hardness Profile of the 4140 weldments after different PWHTs

The comparison of results after these PWHTs can be based on results obtained by the code recommendations, but also there can be specific requirements from the mechanical properties of the steel being welded. The PWHTs @ 650^0C/1.0 hr and

@ 600^0C/1.0 are the closest ones to most code requirements. It is evident that PWHT @ 650^0C/1.0 hr resulted with the lowest hardness value of the HAZ after all PWHTs of 298 HV. This tempering temperature and tempering time also resulted in lower hardness value of the BM of 255 HV in comparison with as-received hardness value of 4140 steel of 292 HV.

It is important to point out that the as-received hardness value of 292 HV of 4140 steel indicates that this steel was previously Q&T heat treated where the tempering temperature was about 580^0C-600^0C. Due to this, the PWHT of this steel should not be ever carried out at higher temperatures than these because of deterioration of the strength properties. Even if the PWHT is carried out at the same temperature as the tempering temperature during the common Q&T heat treatment, it will result in lower hardness value of the BM due to the process of tempering previously tempered microstructure or the double tempering of the BM.

The highest hardness value of the HAZ of 384 HV is associated with the lowest tempering temperature of 500^0C and the shortest holding time at this temperature of 6.0 hours. The HAZ hardness values obtained after different PWHTs are characterized with biggest differences among them of 57 HV (from 355 HV to 298 HV) while the hardness values within the BM and WM do not have such a big difference. In fact, the maximum hardness value difference among the BM hardness results after all PWHTs is 39 HV, while the maximum difference among the WM hardness values is 40 HV. The PWHT that produced the biggest hardness

discrepancy within the weld zone of 87 HV is again related to the lowest temperature – shortest time parameters of 500^0C/6.0 hours.

Generally, PWHTs at 600^0C and 650^0C (according to the most codes) are almost always beneficial since both hardness measurement results and produced microstructures do not indicate the presence of hard microconstituents that could cause concerns. These temperatures are high enough to promote structural alterations as well as the relaxation of residual stresses. The most appropriate tempering temperature should be adjusted to the tempering temperature of the Q&T process if it is known. For example, if the tempering temperature after quenching is 600^0C, then the tempering temperature of PWHT should be about 580^0C.

The PWHTs carried out at lower temperature of 550^0C and three different holding times of 2.5, 4.0 and 10.0 hours, also induced changes in the weld zone of 4140 steel. The shortest holding time of 2.5 hours at this temperature resulted in second highest hardness value of the HAZ of 352 HV. Also, the second maximum hardness variation throughout the cross section of the weld zone of 77 HV resulted after this PWHT. The longest holding time at this temperature of 10.0 hours, based on Hollomon-Jaffe parameter, resulted in a low hardness value of the BM of 233 HV, which is significantly lower than as-received hardness of 292 HV. This PWHT resulted in close hardness values of the WM and HAZ of 282 HV and 320 HV respectively. The lowest hardness discrepancy across the weld zone of 4140 steel of 44 HV is achieved after PWHT @ 550^0C/4.0 hours. It is evident that, based

on hardness values of the weld zone and resulting microstructures, this temperature is high enough to accomplish some transformation processes and that a satisfactory relationship between the tempering temperature and holding time can be established.

The further lowering of PWHT temperature to 500^0C had to inevitably extend the holding times to 6.0, 15.0 and, based of Hollomon-Jaffe parameter formula for this temperature, to 226.0 hours.

The 500^0C/6.0 hour PWHT, characterized with the lowest tempering temperature and the shortest tempering time, accordingly resulted in the highest hardness value of the HAZ and the biggest hardness value difference within the weld zone of 87 HV. These results can just confirm that a satisfactory relationship between the temperature and time is not achieved with this PWHT.

Although the 500^0C is considered as very low temperature for both metallurgical and stress relief processes, the prolonged holding time from 6.0 hours to 15.0 hours produced the results very similar to the results obtained after PWHTs recommended by most codes. The hardness value discrepancy among the WM, HAZ and BM is maximum of 42 HV, which is the lowest values considering results obtained after other PWHTs. It indicates that, based on the hardness results, the mechanical properties of different regions of the weld zone are similar and uniform.

The further extension of holding time at this lowest tempering temperature to 226.0 hours resulted in low hardness value of the BM of 243 HB in comparison with as-

received 4140 hardness level of 292 HV. The hardness values of the WM of 286 HV and the HAZ of 318 HV are in a relatively good agreement, but due to the low BM hardness result, the overall hardness difference in this weld zone is pretty high of 75 HV.

It will be stressed again that all performed PWHTs with eight different time-temperature parameters were done on welded 4140 steel samples, which were previously Q&T treated obtaining the average hardness value of 292 HV and having the microstructure of tempered martensite. The effect of each PWHT on the BM properties was done by comparing the results obtained in Chapter 5 (Q&T processes for 4140 steel where tempering temperatures after quenching were the same as the PWHT temperatures) and the results of BM after performed PWHTs on this 4140 Q&T and welded steel. Since the PWHTs were carried out on previously Q&T 4140 steel, this double tempering process resulted in the BM hardness values illustrated in Fig. 7.17.

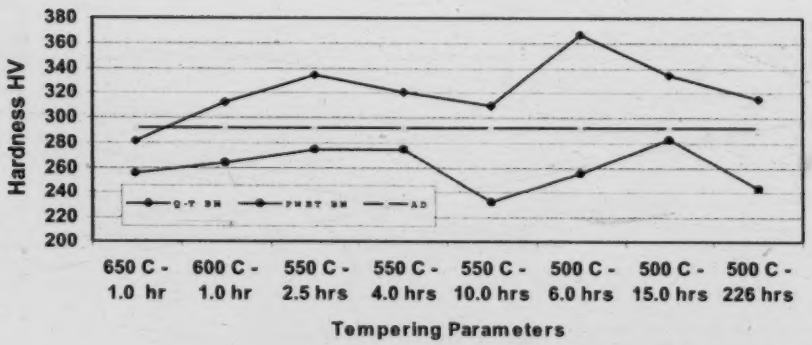

Fig. 7.18 - Hardness Profile of the 4140 BM after different Q&T and PWHTs

From the Fig. 7.17 it is evident that the 4140 Q&T steel hardness value decreases when exposed to PWHT temperatures due to the effect of tempering and exposing of previously tempered martensite to one more thermal cycle. When tempered martensite of as-received 4140 steel was again exposed to the different PWHT processes, the tempered martensite became softer and more ductile, but also with lower strength properties, what is confirmed with lower measured hardness values. From PWHTs carried out at lower temperatures of 550^0C and 500^0C, the 550^0C/4.0 hour and the 500^0C/15.0 hour PWHT produced very similar results to the results of PWHT's recommended by codes at 600^0C and 650^0C.

The PWHTs performed by applying Hollomon-Jaffe parameter are characterized with significantly longer holding times and obtained results after the PWHT @ 550^0C/10.0 hours and 500^0C/226 hours are almost identical. Both PWHT's resulted in very low hardness values of the 4140 base metal.

On the contrary, the shortest holding times of 2.5 hours and 6.0 hours at the same temperatures of 550^0C and 500^0C resulted in the highest hardness values, particularly in the HAZ indicating that these tempering times are not sufficient enough for the PWHT to be successfully accomplished.

7.10. Analysis and comparison of 4140 weld zone microstructures after different PWHTs

In order to recognize any significant difference among obtained WM microstructures after different PWHT's, the following Fig. 7.19 is plotted. Fig. 7.20 and Fig. 7.21. show all HAZ and BM microstructures produced after eight different PWHT processes.

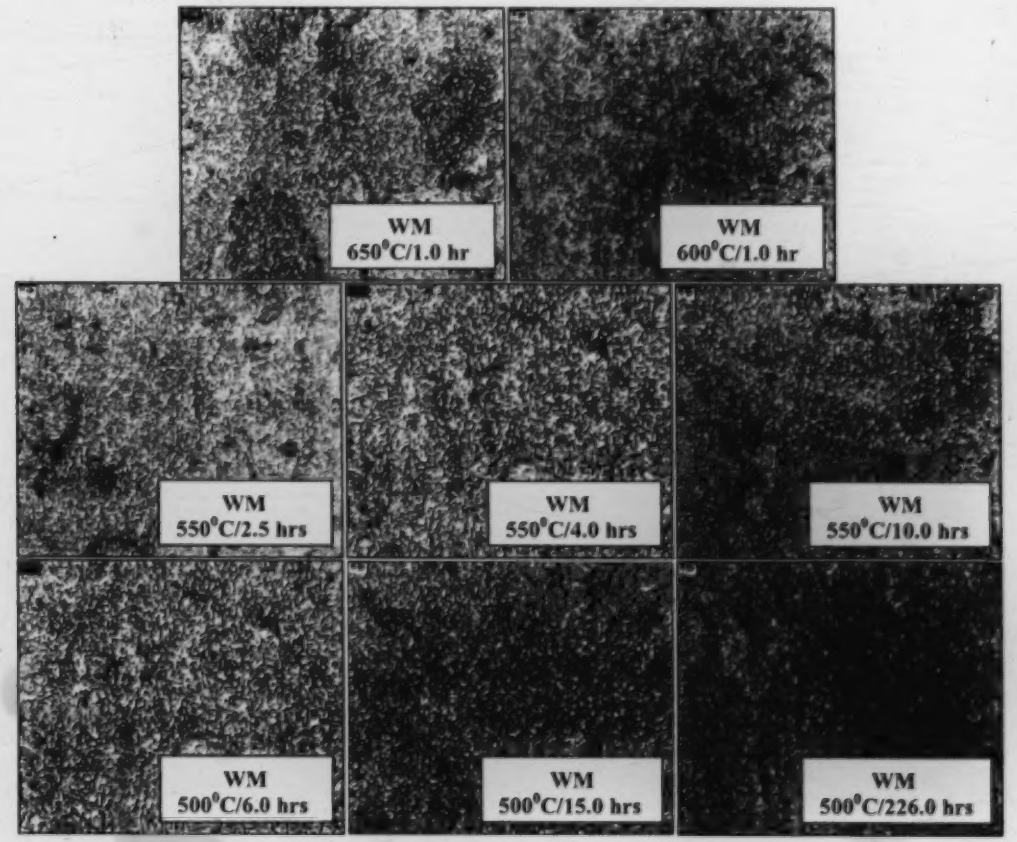

Fig. 7.19. Microstructures of theWM of 4140 weld zone after different PWHTs (127x)

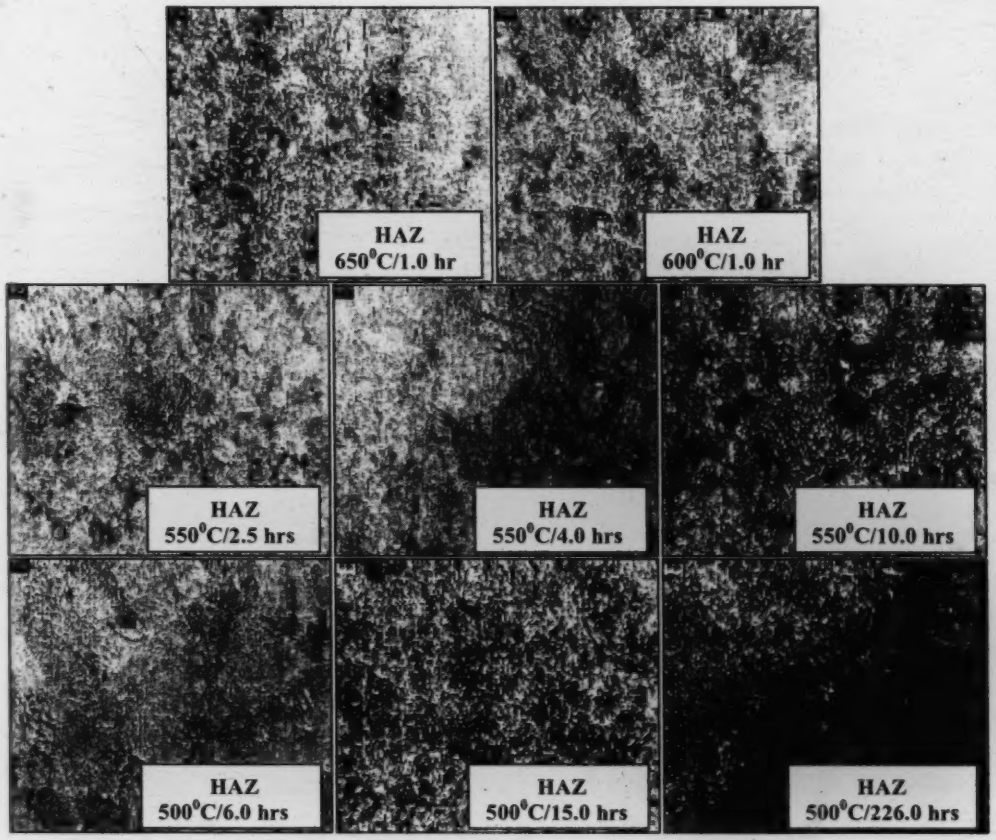

Fig. 7.20. – Microstructures of the HAZ of 4140 weld zone after different PWHTs (127x)

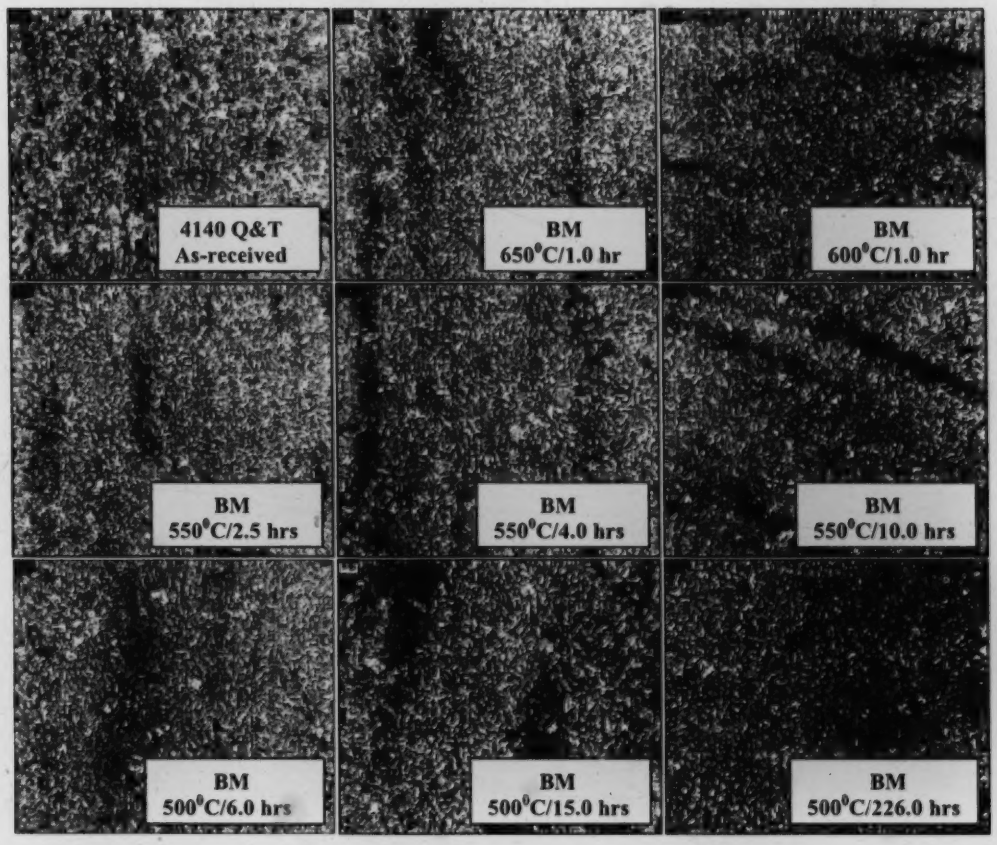

Fig. 7.21. – Microstructures of the BM of 4140 weld zone after different PWHTs (127x)

The weld metal microstructures are essentially dictated by the weld metal chemistry, which in this case was the electrode E 11018 – M, with very low carbon content and Ni and Mo additions. The microstructures formed comprise a mixed transformation product of ultrafine acicular ferrite. In these weld deposits, some other morphologies of ferrite are present such as proeutectoid ferrite or grain-boundrary polygonal ferrite particularly after the PWHT @ 550^0C/6.0 hours. This volume fraction is not significant, but this WM microstructure is characterized with the lowest hardness value of 273 HV. It also can be reasonable assumed that some form of bainitic ferrite is formed since some investigations have confirmed that the transformation mechanisms for bainitic ferrite and acicular ferrite are similar. [Babu, 1990] This study emphasizes the fact that reactions taking place in the γ/γ grain boundaries can be crucial in determining the microstructures that develop in the weld metal. The ratio of the grain boundary and intragranular nucleation site densities can be modified to obtain the desired microstructure in transformation from austenite. The ability of inclusions to induce intragranular acicular ferrite is now a well-established concept, although the nature and mechanism are not clear. Removal of inclusions clearly causes an acicular ferrite microstructure to change to one that contains bainite.

The coarsening of acicular ferrite is not visible since some investigators have considered it as a cause of poor toughness.

The microstructures of the HAZ are largely affected by chemical composition of the steel and weld thermal cycle. Since the preheating was applied to the weld

zone, the critical cooling rate from $800^0C \rightarrow 500^0C$ prevented the formation of almost always undesirable hard martensitic constituents. This is in an agreement with the hardness testing results, where the maximum HAZ hardness value measured was 355 HV, which is even the result of the lowest tempering temperature and the shortest holding time of PWHT at 500^0C/6.0 hours. It should be certainly stressed that hardness values of the HAZ are partly due to the fact that this steel was previously quenched and tempered, having the tempered martensite as the initial microstructure. The HAZ, which is adjacent to the weld, was exposed to a variety of temperatures that modify microstructure throughout reaustenization, transformation and tempering. The produced HAZ microstructures after all PWHTs are a mix of several microstructures in combinations such as bainite, pearlite, polygonal ferrite and Widmanstätten ferrite. The coarse grains in the HAZ are related to the low tempering temperature-short holding time PWHTs at 550^0C/2.5 hours and 500^0C/6.0 hours.

The BM microstructures obtained after eight different PWHTs were undergone to further tempering or double tempering of the BM since the initial base metal microstructure was the tempered martensite. The PWHTs resulted in predominantly tempered martensite microstructures with polygonal ferrite and their hardness variations shown in Fig. 7.17 clearly show the lower hardness values of the BM after PWHTs than the hardness values obtained after Q&T processes.

Further metallographic examination at higher magnification was done to find out the relationship between the highest hardness value of the HAZ and produced microstructure after particular PWHTs. From Fig. 7.16, significantly higher hardnesses of the HAZ of ~350 HV were obtained after PWHTs at 550^0C/2.5 hours and 500^0C/6.0 hours and produced HAZ microstructures after these PWHTs are very similar and they are shown in Fig. 7.22.

Fig. 7.22 – HAZ microstructures with highest hardness values (800x)

It is also evident from Fig. 7.16 that the highest hardness value of ~ 280 HVof the BM of 4140 steel is obtained after PWHT at 500^0C/15.0 hours. The micrographs of this microstructure under higher magnifications in comparison with other microstructures are presented in Fig. 7.23.

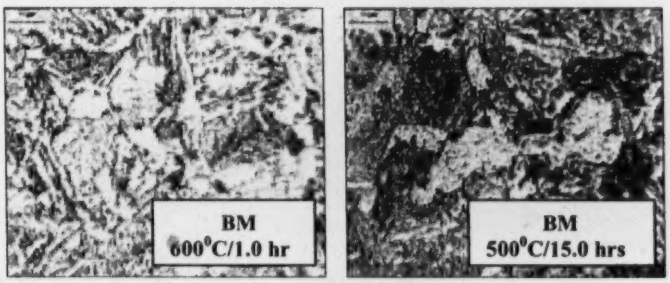

Fig. 7.23 – BM microstructures of 4140 steel with increased hardness values (800x)

Two PWHTs that produced the hardness value close to the Q&T hardness value were performed at 550°C/4.0 hours and 500°C/15.0 hours. Increased hardness value particularly after the PWHT at 500°C for a relatively long holding time of 15.0 hours can be associated with the secondary hardening due to Mo and Cr carbides precipitation in Cr-Mo steels.

7.11. PWHT – Diffusion Coefficients

The phenomena that occur during a heat treatment almost always involve atomic diffusion. Often an enhancement of diffusion rate is desired [Callister, 1999]. The magnitude of the diffusion coefficient D is indicative of the rate at which atoms diffuse. Solid state diffusion is a means of mass transport within solid materials. The term "self-diffusion" refers to the migration of host atoms; for impurity atoms, the term "interdiffusion" is used. Two mechanisms are possible: vacancy and interstitial [Callister, 1999]. Coefficients, both self- and

interdiffusion, for several metallic systems are listed in Table 13.4 [Brandes, 1992].

Temperature has a most profound influence on the coefficients D and diffusion rates. The temperature dependence of diffusion coefficient is related to temperature according to:

$$D = D_0 \exp\left(-\frac{Q_d}{RT}\right)$$

where:

Do = a temperature-independent preexponential (m^2/sec)

Qd = the activation energy for diffusion (J/mol, cal/mol, or eV/atom)

R = the gas constant, 8.31 J/mol-K, 1.987 cal/mol-K, or 8.62×10^{-5} eV/atom-K

T = absolute temperature (K)

The diffusion coefficient D can be used to determine the approximate time at a lower temperature that will produce the same diffusion result as at higher temperature.

In this case, by knowing the diffusion coefficient for Cr - D_{Cr} – of 4140 Cr-Mo steel at 600^0C and 500^0C, the approximate time at 500^0C that will produce the same diffusion result as a 1.0-hour heat treatment at 600^0C, can be calculated as:

D_{Cr} at 600^0C can be calculated by using the equation:

$$D = D_0 \exp\left(-\frac{Q_d}{RT}\right)$$

$$D_{0\,(Cr)} = 2.33 \times 10^{-4}\ m^2/sec$$

$$Q_d = 238.8 \text{ kJ/mol}$$

$$R = 8.31 \text{ J/mol}$$

$$D_{Cr\,(600^0C)} = 2.33\text{x}10^{-4} \exp(-238800/8.31\text{x}873)$$

$$D_{Cr\,(600^0C)} = 1.1795\text{x}10^{-18} \text{ (m}^2\text{/sec)}$$

$$D_{Cr\,(500^0C)} = 1.6686\text{x}10^{-20} \text{ (m}^2\text{/sec)}$$

$$(D\,x\,t)_{500^0C} = (D\,x\,t)_{600^0C} = \text{constant}$$

$$t_{500} = \frac{(Dt)_{600}}{D_{500}}$$

$$t_{500^0C} = 1.1795\text{x}10^{-18} \text{ x } 1.0 \text{ hr}/1.6686\text{x}10^{-20}$$

$$t_{500^0C} = 70.688 \text{ hours}$$

For the 4140 steel, the diffusion coefficient of Mo, D_{Mo}, can also be analyzed to calculate the approximate time at lower temperature of 500^0C that produces the same diffusion result as the post-weld-heat-treatment at the common PWHT temperature of 600^0C.

$$D_{0\,(Mo)} = 0.663\text{x}10^{-4} \text{ (m}^2\text{/s)}$$

$$Qd = 224.2\text{x}10^3 \text{ (J/mol)}$$

$$R = 8.31 \text{ (J/mol)}$$

$$T = 773 \text{ (K)}, 873 \text{ (K)}$$

$$D_{Mo\,(500^0C)} = 0.663\text{x}10^{-4} \exp(-224200/8.31\text{x}773)$$

$$D_{Mo\,(500^0C)} = 4.6\text{x}10^{-20} \text{ (m}^2\text{/s)}$$

$$D_{Mo\,(600^0C)} = 2.51x10^{-18}\ (m^2/s)$$

$$(D\,x\,t)_{500^0C} = (D\,x\,t)_{600^0C} = \text{constant}$$

$$t_{500} = \frac{(Dt)_{600}}{D_{500}} = 2.51x10^{-18}x1.0/4.6x10^{-20}$$

$$t_{500^0C} = 54.57 \text{ hours}$$

The same procedure is applied in the case of the diffusion coefficient of C, D_C, for 500^0C and 600^0C. The results are shown below:

$$D_{0\,(C)} = 6.2x10^{-7}\ (m^2/s)$$

$$Qd = 80\ (kJ/mol)$$

$$D_{C\,(500^0C)} = 2.4x10^{-12}\ (m^2/s)$$

$$D_{C\,(600^0C)} = 6.2x10^{-7} \exp(-80000/8.31x873)$$

$$D_{C\,(600^0C)} = 1.00x10^{-11}\ (m^2/s)$$

$$(D\,x\,t)_{500^0C} = (D\,x\,t)_{600^0C} = \text{constant}$$

$$t_{500} = \frac{(Dt)_{600}}{D_{500}} = 1.00x10^{-11}x1.0/2.4x10^{-12}$$

$$t_{500^0C} = 4.197 \text{ hours}$$

Due to the fact that PWHTs were performed not only at 600^0C and 500^0C, but also at 550^0C, the same analysis of the approximate diffusion times at this temperature is done and results are shown below:

-For the diffusion coefficient of Cr:

$$D = D_0 \exp\left(-\frac{Q_d}{RT}\right)$$

$$D_{Cr\,(550^0C)} = 2.33\text{x}10^{-4} \exp\,(-238800/8.31\text{x}823)$$

$$D_{Cr\,(550^0C)} = 1.5966\text{x}10^{-19}\ (m^2/s)$$

$$D_{Cr\,(600^0C)} = 1.1795\text{x}10^{-18}\ (m^2/sec)$$

$$(D\,x\,t)_{550^0C} = (D\,x\,t)_{600^0C} = \text{constant}$$

$$t_{550^0C} = 1.1795\text{x}10^{-18}\text{x}1.0/1.5966\text{x}10^{-19}$$

$$t_{550^0C} = 7.387 \text{ hours}$$

Diffusion time at 550^0C considering the diffusion coefficient of Mo, D_{Mo}, is calculated as follow:

$$D_{Mo\,(550^0C)} = 0.663\text{x}10\text{-}4 \exp\,(-224200/8.31\text{x}823)$$

$$D_{Mo\,(550^0C)} = 3.84\text{x}10^{-19}\ (m^2/s)$$

$$D_{Mo\,(600^0C)} = 2.51\text{x}10^{-18}\ (m^2/s)$$

$$t_{550^0C} = 6.54 \text{ hours}$$

The diffusion time of C at 550^0C in comparison with the temperature at 600^0C is presented below:

$$D_{C\,(550^0C)} = 6.2\text{x}10^{-7} \exp(-80000/8.31\text{x}823)$$

$$D_{C\,(550^0C)} = 5.15\text{x}10^{-12}\ (m^2/sec)$$

$$D_{C\,(600^0C)} = 1.00\text{x}10^{-11}\ (m^2/s)$$

$$t_{550^0C} = 1.94\ \text{hours}$$

The calculations of the approximate diffusion times of Cr, Mo and C at lower temperatures of 500^0C and 550^0C that will produce the same diffusion rate as the diffusion rate at 600^0C may indicate the following:

There are significant differences in the diffusion rates-times at 500^0C and 550^0C between the carbon diffusion time and both chromium and molybdenum diffusion times:

$t_{600^0C\,(C)} = 1.0$ hour	$t_{600^0C\,(Cr)} = 1.0$ hour	$t_{600^0C\,(Mo)} = 1.0$ hour
$t_{500^0C\,(C)} = 4.197$ hours	$t_{500^0C\,(Cr)} = 70.688$ hours	$t_{500^0C\,(Mo)} = 54.57$ hours
$t_{550^0C\,(C)} = 1.94$ hours	$t_{550^0C\,(Cr)} = 7.387$ hours	$t_{550^0C\,(Mo)} = 6.54$ hours

Based on this data, it can be concluded that PWHT of the carbon steel and low alloy steel can be performed at significantly different temperature-time relationships. Basically, the more alloyed the steel, the longer the diffusion-holding time at the lower temperatures. This is particularly important when PWHT is

required after welding those types of steels such as medium carbon 1043 steel and low alloy 4140 Cr-Mo steel.

The following chart shown in Fig. 7.24 graphically illustrates how significant differences in tempering parameters are,based on different approach of calculating these principal variables such as the tempering temperature and tempering time.

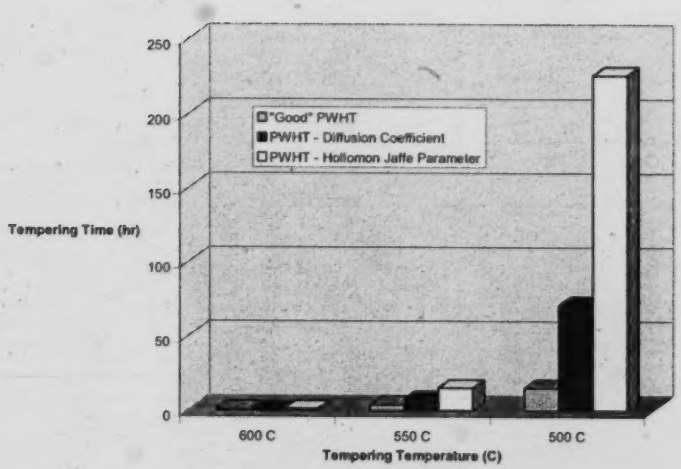

Fig. 7.24 - Relationship among Tempering Parameters

It can be concluded that both PWHT parameters (based on diffusion coefficient and Hollomon-Jaffe parameter) are conservative, and even the longest diffusion time of Cr of approximately 71 hours at 500^0C is significantly shorter then the holding time based on Hollomon-Jaffe parameter of 226.0 hours at 500^0C.

The diffusion times of Cr and Mo at 500^0C and 550^0C are relatively similar with slightly longer diffusion times for Cr due to the little higher activation energy of Cr due to the fact that a large activation energy results in a relatively small diffusion coefficient (Qd_{Cr} = 238.8 kJ/mol, Qd_{Mo} = 224.2 kJ/mol). More fundamental investigation of diffusion mechanisms that occurs in temperature range from 500^0C to 600^0C in both alloy systems of 1043 and 4140 steels could be further investigated and it is beyond the scope of this project.

CHAPTER 8

Conclusions and Recommendations

8.1 Conclusions

Two PWHTs were performed according to the recommendations found in most codes at 650^{0}C and 600^{0}C, while six PWHTs were carried out where the principal parameters such as the tempering temperature and holding time were lower and have not been prescribed by any codes for the medium-carbon 1043 and low-alloy 4140 Cr-Mo steel. These investigations on finding the most suitable PWHT procedure by applying different PWHT parameters have led to the following conclusions:

1. The tempering temperature has the most dominant role of all PWHT parameters. The tempering temperature below 600^{0}C requires longer holding times.

2. The PWHTs carried out at 550^{0}C/4.0 hours and 500^{0}C/15.0 hours resulted in both microstructures and hardness values similar to those of the required PWHTs by the codes.

3. The PWHTs performed by applying the Hollomon-Jaffe parameter for the determination of the holding time of 10.0 hours at 550^{0}C and 226.0 hours at

500^0C are very long. The microstructures of the weld zone of both 1043 and 4140 steels are characterized by low hardness values for both the WM and the BM. Also, the microstructure of the BM after these PWHTs is characterized with a very coarse grain size, particularly the BM microstructure of the 1043 steel. Hardness results as well as the produced microstructures after these two PWHTs are similar, thus confirming the linear relationship between the temperature and log time at lower temperature proposed by Hollomon and Jaffe.

4. The WM microstructures of both 1043 and 4140 steels do not differ significantly among each other regardless on the PWHT temperature-time parameters being used. The lowest hardness values of the WM are obtained after the longest holding time PWHTs.

5. The HAZ microstructures of 1043 steel have higher hardness values than those of the WM and BM. These higher hardness values in the HAZ are measured after the shortest holding time of PWHTs performed.

6. The HAZ microstructures of 4140 steel demonstrate the same pattern as the HAZ microstructures of 1043 in terms of having the highest hardness values after the shortest PWHTs, but these differences are more pronounced for 4140

steel. It might be associated with the more complex chemical composition of this steel with its Mo content and its inclinations to the secondary hardening.

7. The BM of 1043 steel was changed significantly in both metallurgical and mechanical terms after all PWHTs. It is expected due to the fact that this steel did not have any previous heat treating process. Almost all PWHTs caused the spheroidization of initial ferrite-pearlite microstructure to some degree. Only two longest time PWHTs resulted in very coarse grain size of the 1043 BM.

8. The HAZ hardness is slightly higher in the upper levels close to the top of the weld zone (HAZ-1). This indicates that the upper HAZ was not completely tempered by the previous deposited weld and that the heat input in this part of the weld zone should have been higher. It can be associated with the fact that the welding was done only with the electrode with 3.2 mm in diameter and that this heat input is not sufficient enough. Due to this, the welding procedure with higher heat input should be applied to the weld zone by welding with the electrode with 4.0 mm or 5.0 mm in diameter after the root weld and a couple following welds were done.

9. The PWHT of welded 4140 steel, which was previously Q&T, decreased the hardness values of the base metal regardless of the temperature-time

parameters being used. This double tempering effect of the PWHT of Q&T 4140 steel lowered the hardness for approximately 15% of the Q&T hardness values.

10. A linear relationship between the tempering temperature – holding time could not be found in performing PWHTs at lower temperatures based on the Code requirements

11. . PWHT parameters based on the diffusion coefficient or Hollomon Jaffe parameters are very conservative, requiring long tempering times at lower tempering temperatures.

12. The temperature-time relationship for PWHT at lower temperatures can be established for a particular welded structure. The suitable PWHT temperature-time parameters will depend on the specifications and required and desired properties that have to be achieved from that welded structure.

8.2. Recommendations

This investigation has just confirmed how difficult it is to relate tempering time-tempering temperature at lower temperature to obtain the same result to equivalent PWHT results at common tempering temperatures. The following are recommendations for further study of establishing the most suitable PWHT at lower temperatures for a specific welding application:

1. Measurement of amount of residual stresses after each set of performing PWHT parameters. This is required due to the fact that one of the PWHT's main goal is reduction of amount of residual stresses, although the relationship between the hardness values and the yield strength properties are established for low alloy and C-Mn steels, which can give us some rough information about it. More importantly, the relationship between produced microstructures in the weld zone and the corresponding amount of residual stresses could be analyzed.

2. Further microstructure observations and mechanical testings of each weld zone need to be done since every microstructure shown in this project can be subjected to more and deeper investigations. The investigation of the tempering effect of PWHT on acicular ferrite microstructure of the WM can be of particular interest since there have not been many investigations done on it.

3. The PWHT performed at temperatures even lower then 500^0C may be done to find out the temperature-time limits in obtaining satisfactory results.
4. PWHTs based on the diffusion coefficient calculations can be further investigated.

References

ASM, 1977, *Atlas of Isothermal Transformation and Cooling Transformation Diagrams,* American Society for Metals

Babu, S.S., Bhadeshia, H.K.D.H., 1990, "Transition from bainite to acicular ferrite in reheated Fe-Cr-C weld deposits," Materials Science and Technology, Vol.6, October, 1990

Benson, L.E., Watson, S.J., 1955, "Effect of Preheating on Residual Stresses in Mild-Steel Welds," *British Welding Journal,* September, 1955

Bjorhovde, R., Brozzetti, J., Alpsten, G.A., Tall, L., 1972, "Residual Stresses in Thick Welded Plates," *Welding Research Supplement*, August, 1972

Boyd, G.M, 1961, "Metallurgical Concomitants of Residual Stresses," *Welding Technology, British Welding Journal* July, 1961.

Brandes, E.A., Brook, G.B., 1992, "*Smithells Metal Reference Book*," Seventh Edition, Butterworth-Heinemann

Bratt, J.F., Berme, N., 1966, "Residual stresses and strain energy in butt welds;" British Welding Journal, December, 1966 Butterworths & Co., London

Callister, Jr. William, 1999, "*Materials Science and Engineering-An Introduction*," Fifth Edition, John Wiley & Sons, Inc.

Datsko Joseph, Hartwig Laura, McClory Brian., 2001, "On the Tensile Strength and Hardness Relation for Metals," *Journal of Materials Engineering and Performance*, Volume 10(6) December, 2001

Dolby, R.E., 1983. *Metals Technology*, 10, 349-362

Easterling, K., 1983, *Introduction to the Physical Metallurgy of Welding* Butterworths & Co., London

Fidler, R., Hepworth, J.K., 1984, "Residual Stresses in CrMoV—2CrMo Pipe Welds,' *Metal Construction*, Volume 16, no. 9, pp. 540-545

Honeycombe, R., Bhadeshia, H.K.D.H., 1995, *Steels Microstructures and Properties*,

Hrivnak, I., 1985, " A Review of the Metallurgy of Heat Treatment of Welded Joints," *Int..J. Pressure Vessels Piping*, Volume 20, no. 3, pp. 223-237

Huang, C.c., Pan, Y.C., Chuang, T.H., 1997, "Effects of Post-Weld Heat Treatments on the Residual Stress and Mechanical Properties of Electron Beam Welded SAE 4130 Steel Plates," *Journal of Materials Engineering and Performance*, Vol. 6(1) February 1997 – 61

IIW, 1987, "Stress Relieving Heat Treatments of Welded Steel Constructions," *Proceedings of the International Conference held in Sofia, Bulgaria, 6-7 July 1987 under auspices of the International Institute of Welding*

Impurity Diffusion in Iron., 2003 http://inaba.nims.go.jp/diff/DIF_Oikawa/Table.html

Lancaster, J, F., 1993. *Metallurgy of Welding*, Fifth Edition – Chapman&Hallb

Liscic, B., 1997, "Steel Heat Treatment," *Steel Heat Treatment Handbook/* [edited by] George E. Totten, Maurice A.H. Howes, 1997

Mabelly, Ph., Bourges, G., 2001, "Effect of metallurgical transformation on weld residual stresses – application to E690 steel grade," *Marine Structures 14* (2001) 553-567

Material Web, www.matweb.com/search/SpecificMaterial.asp?bassnum=M414AO., 2003

Mochizuki, M., Toyoda, M., 2001, "Numerical Analysis of Residual Stress in Welded Structures Using Inherent Strain," *Department of Manufacturing Science, Graduate School of Engineering, Osaka University, Suita, Osaka 565-0871, Japan*

Murakawa, H., 1997, "Theoretical prediction of residual stress in welded structures," *Welding International* 1997, Volume 11 Number 8

Murray, J.D., 1967, "Stress-relief Cracking in Carbon and Low Alloy Steels," *British Welding Journal* August 1967

Nawrocki, J, N., DuPont, J.N., Marder, A.R., 1998, "The Weldability of a Modified 2.25 Cr – Mo Steel (HCM2S);" *Materials Solutions 98. Joining of Advanced and Specialty Materials*, Rosemont, IL, USA, 12-15 Oct. 1998

Olabi, A.G., Hashmi, M.S.J., 1996, "Stress Relief Procedures for Low Carbon Steel (1020) Welded Components," *Journal of Materials Processing Technology*, Vol.56, No.1-4, pp.552-562

Patchett, B., 2000, *The Metals Blue Book: Welding Filler Metals*. Second Edition, Casti Publishing.

Shiga, C., 1990, "Effects of Steelmaking, Alloying and Rolling Variables on the HAZ Structures and Properties in Microalloyed Plate and Linepipe," *The Metallurgy, Welding, and Qualification of Microalloyed (HSLA) Steel Weldments*, Texas, pp. 327-350.

Shiga, C., Gotoh, A., Kojima, T., Horii, Y., Fukada, Y., Iketi, K., Matuda, F., 1996, "State of the art review on the effect of PWHT on properties of steel weld metal," *Welding in the World*, Vol. 37, No.4, pp.17-30

Smith, D.J., Garwood, S.J., 1992, "Influence of Post Weld Heat Treatment on the Variation of Residual Stresses in 50 mm Thick Welded Ferritic Steel Plates," *International Journal of Pressure Vessels and Piping*, Vol.51, No.2, pp. 241-256, 1992

Still, J.R., 1997, "Welding of AISI 4130 and 4140 Steels for Drilling Systems," *Welding Journal*, June 1997

Sudha, C., Terrance, A.L.E., Albert, S.K., Vijayalakshmi, M., 2002, "Systematic study of formation of soft and hard zones in the dissimilar weldments of Cr – Mo steels," *Journal of Nuclear Materials*, 302 (2002) 193-205

Sugden, A.A.B., Bhadeshia, H.K.D.H., 1989, "Lower acicular ferrite," *Metallurgical Transactions A*, Volume 20A, pp. 1811-1818

Szilvassy, C.C., Gergely, M., Reti, T., 1995, "Computer Simulation of Heat Treatment Transformation Processes," *Macau Study* No.3 Nov 1995

Tamaki, K., Kawakami, H., Suzuki, J., 1999, "Temper Embrittlement in HAZ of Cr-Mo Steels," *Welding in the World*, March/April, Volume 43, No.2, 1999

Watkins, B., Wood, D.S., Nichols, R.W., 1963, "Effects of Prolonged Stress Relieving Treatments on the Mechanical Properties of Reactor Pressure Vessel Steels," *British Welding Journal*, February, 1963

Withers, P.J., Bhadeshia, H.K.D.H., 2001, "Residual stresses Part 2 – Nature and origins," *Materials Science and Technology*, Vol.17, April, 2001